The use of otolith microchemistry to investigate natal origins and movement of lacustrine wild rainbow trout (*Oncorhynchus mykiss*) and common smelt (*Retropinna retropinna*)

Matthew Sean Riceman

A thesis
submitted in partial fulfilment
of the requirements for the Degree
of
Master of Science in Biological Sciences
at
The University of Waikato
Hamilton
New Zealand

February
2008

The University of Waikato
Te Whare Wānanga o Waikato

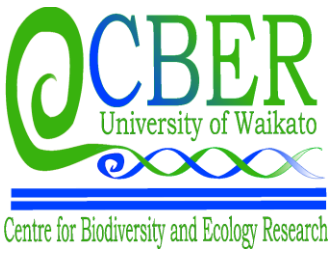

Abstract

Otolith microchemistry can be used to determine the natal origins of fish. Solution-based inductively coupled plasma mass spectrometry (ICP-MS) analysis of water samples from tributary streams and beach locations around Lake Rotorua and Lake Rotoiti, Rotorua lakes district, New Zealand, indicate different and unique water isotopic chemistries at sample locations The concentrations of ^{24}Mg, ^{43}Ca, ^{55}Mn, ^{85}Rb, ^{88}Sr and ^{137}Ba differed significantly between tributary streams. The concentrations of ^{43}Ca, ^{85}Rb and ^{88}Sr differed significantly between beaches. Discriminant function analysis (DFA) was used to classify the stream water samples from six tributary streams around Lake Rotorua and Lake Rotoiti with 100% accuracy. Beach water samples from seven sample locations around Lake Rotorua and Lake Rotoiti were classified with 64% accuracy. When grouped by lake, the water samples could be classified with 93% accuracy. The ambient water chemistry is a major influence on the otolith chemical composition. The water results indicate unique water chemistries and suggest using the microchemistry of otoliths to determine natal origins.

Laser ablation inductively coupled plasma mass spectrometry (LA-ICP-MS) was used for single spot analysis of otoliths of rainbow trout (*Oncorhynchus mykiss*) and common smelt (*Retropinna retropinna*) to determine concentrations of Mn, Zn, Rb, Sr and Ba. Juvenile trout otoliths from six spawning tributaries around Lake Rotorua and Lake Rotoiti could be classified to lake of origin with 98% accuracy overall. Using the DFA of 43 juvenile trout from spawning tributaries as the training set, classification coefficients were applied to analyses of elemental concentrations in the otolith nucleus of 92 adult wild rainbow of unknown natal origin captured in lakes

Rotoiti and Rotorua and the Ohau Channel. Classification results suggest that the tributary streams of Lake Rotorua contribute the majority of individuals to the wild populations of adult rainbow trout of both lakes, comprising 88% of Lake Rotorua fish, 86% of Lake Rotoiti fish, and 100% of Ohau Channel fish.

LA-ICP-MS spot analysis of common smelt otolith at the nuclei and edges provided information related to the movements between different chemical habitats across the fishes life. The concentrations of Mn, Zn, Rb, Sr and Ba differed significantly between the nucleus and edge spots in the smelt samples suggesting movement for some individuals. The scores from lake DFA classification functions showed two classes of smelt. Approximately 70% of smelt were lake residents and approximately 30% of smelt had migrated between the lakes. The nucleus results were compared with the known smelt capture location and the results are similar to the otolith analyses.

The results of this investigation can be used to determine fish migration and assist with fisheries management decisions. Otolith microchemistry suggests that the construction of the wall diverting Lake Rotorua water into the Okere Arm of Lake Rotoiti is likely to impede migrations of wild rainbow trout from Lake Rotorua into Lake Rotoiti. Disruption of common smelt, migrations is likely to be less severe than for trout, but the prediction of smelt migration is less reliable because of the lower accuracy of classification.

Preface & Acknowledgements

This work was carried out using funding from Environment Bay of Plenty and without which could not have gone ahead. I am extremely grateful to everybody who helped out with the gathering of fish samples, especially Rob Pitkethley and the rangers of Eastern Region Fish and Game Concil, Alex Ring, Technician at the University of Waikato and Ray Tana who assisted in the field.

I would also like to thank Steve Cameron, manager of the ICP suite at The University of Waikato who has gone out of his way to facilitate the large amount of LA-ICP-MS time I have needed. I would also like to thank Gavin Robinson, Amber Whittaker and Simon Jackson who provided valuable technical assistance for LA-ICP-MS work. I offer special thanks to Ray and Jen who sat through numerous hours of analysis for my samples providing much needed assistance and companionship.

This work would not have taken place without the expert assistance of my supervisor Associate Professor Brendan Hicks who has provided me with guidance and support along the journey of this Masters thesis. His knowledge has been critical and helped immensely.

Finally I would like to thank my family and my loving partner Cherie whom have supported me through this Masters research.

Table of Contents

List of Figures

List of Tables

Chapter 1

1. Otoliths

1.1. Otolith introduction

Otoliths (ear stones) are small calcium carbonate structures located in the inner ear of all teleost fish (Campana, 1999). Three different pairs of otoliths are located within three vestibules in the inner ear (Popper et al., 2005). The utriculus vestibule, in which the lapillar otolith is located, occupies the ventral portion of the inner ear. The saculus and lagena vestibules, in which the sagittal and astersci otoliths are located respectively, occupy the dorsal portion of the inner ear (Chen and Yan 2002). The three pairs of otoliths differ in sizes; the largest pair is the sagittae which have been used extensively for research. The lapillar and astersci otoliths are listed in descending size and are less frequently used for research (Secor et al., 1991).

Otoliths are relatively pure structures composed predominantly of aragonite (Campana, 1999; Swearer et al., 2003; Tomas and Geffen, 2003), one of the three morphs of calcium carbonate. The composition of the aragonite portion of the otolith is estimated to be between 96-99% (Payan et al., 2002). A small proportion, approximately 3-4% (Campana 1999) of the otolith is composed of protein. The protein plays an important role in otolith formation, providing the framework for aragonite deposition (Borelli et al., 2003). Trace elements comprise <1% of otolith composition and may be incorporated into the otolith matrix (Campana, 1999). Trace elements inclusions are in three different locations in the otolith. An element may substitute for Ca in the aragonite matrix, e.g. Ba (Lucas and Baras, 2000), Mn (Miller et al., 2006) and Sr (Arai and Hirata, 2006). Trace elements that substitute for Ca in

the matrix typically have similar chemical structure to Ca, e.g., Sr and Ba which are both divalent cations and have similar ionic radii (Campana, 1999). Trace elements may also be included in the interstitial spaces of the otolith, or associated with the otolith protein matrix, e.g., Cu and Zn (Miller et al., 2006). The chemical composition of the otolith is dependant on the endolymph fluid which bathes the otolith in each vestibule. The endolymph provides the precursors for otolith material, ultimately influencing the otolith chemical composition (Borelli et al., 2003).

Otolith growth occurs continuously through a fishes life (Borelli et al., 2001; Campana and Thorrold, 2001; Swearer et al., 2003). Calcium carbonate is deposited in discrete daily increments onto the growing surface of the otolith (Campana and Neilson, 1985; Brophy et al., 2004; Ruttenberg et al., 2005). The nucleus region provides the initial point for the subsequent calcium carbonate deposition (Campana and Neilson, 1985; Brophy et al., 2004). Otolith growth is unique because it occurs in the acellular environment, and is dependant on the endolymph fluid. Acellular formation of the otolith in the endolymph negates the potential for otolith material to be reworked metabolically. The otolith is a permanent record of trace metals incorporated into the matrix at discrete time scales (Campana and Thorrold, 2001). Otolith growth is continuous through the fish's life irrespective of external conditions. This growth is unique as the external environment often influences fish growth conditions (Campana and Thorrold, 2001).

The locations of the otoliths in the inner ear indicate the main function of the otoliths is to assist the fish in hearing and maintaining balance (Campana, 1999; Borelli et al., 2001; Swearer et al., 2003; Tomas and Geffen, 2003; Begg et al., 2005). The natural tag or data logging properties of the otolith are purely coincidental and are a by product of otolith formation.

The otolith is considered a natural tag because of two properties. The otolith material is laid down in daily increments sequentially from the otolith nucleus providing chronological information in each daily increment (Borelli et al., 2001; Begg et al., 2005). Each daily increment is identified as a permanent, discrete record of age and chemical information relevant to environmental variables. The progression of otolith research has led to the development of a range of analytical techniques that assess the microchemical composition of an otolith which has been used as a proxy for the assessment of environmental variables (Borelli et al., 2001; Begg et al., 2005; Miller et al., 2006).

1.2. Otolith chemistry influences

Elucidating fish life histories from the chemistry of an otolith assumes a link between environmental variables and otolith composition. Different exogenous and endogenous variables influence the microchemistry of the otolith (Payan et al., 1999)

The ambient water chemistry is regarded as the greatest influence on otolith microchemistry. Fish assimilate dissolved ions through branchial uptake, occurring as water passes over gill epithelia. Ions and oxygen are assimilated into the bloodstream and are distributed around the body through cellular transport by the blood. Blood chemical composition influences the composition of endolymph fluid, which changes the chemical composition of the material crystallising onto the otolith surface. (Campana, 1999; Elsdon and Gillanders, 2002).

The influence of water chemistry is illustrated in a range of studies. The Sr:Ca and Ba:Ca ratios in *Leiostomus xanthurus* otoliths were deposited relative to concentrations in the ambient water (Bath et al., 2000). Linear relationships were

identified between otolith and scale chemistry of one year old westlope cutthroat trout (*Oncorhynchus clarki lewisi*) with water ratios of Mg, Sr and Ca (Wells et al., 2003). A positive proportional relationship was observed for the Sr:Ca ratios of water sample and the otoliths of white perch (*Morane Americana*) when salinity levels in the water were altered (Kraus and Secor, 2004). Freshwater systems have been observed to have a higher Ba:Ca ratio in the otolith. A strong positive effect of Ba levels in the water was observed in the otoliths Ba of (*Acanthopaygrus butcheri).* The Sr:Ca ratios in the water reflected Sr:Ca in the otolith consistently also (Elsdon and Gillanders, 2004).

Diet is another potential influence on otolith chemistry. The minor and trace elements associated with food are absorbed at the gut epithelia of fishes. Elements are then assimilated into the blood and potentially into the endolymph, a similar process to that of dissolved ions from the ambient water (Campana, 1999). The influence of diet on otolith chemical composition is not known conclusively. American shad (*Alosa sapidissima*) (Limburg, 1995) and *Girella elevate* (Gallahar and Kingsford, 1996), were fed Sr enriched diets which increased the Sr:Ca ratio of the otoliths of some individuals. Trophic transfer of Sr and Ba in prey items to otolith was demonstrated by elevated levels of trace elements in the otoliths of juvenile trumpeters (*Pelates sexlineatus*). (Sanchez-Jerez et al., 2002).

In contrast, the levels of a range of trace elements in the diet of young red-drum (*Scianeops ocellatus*) had no observed influence on sagittal otolith concentrations (Hoff and Fuiman, 1995). Radioisotopes illustrated the diet of Nile tilapia (*Oreochromis niloticus*) contributed a minor proportion of Sr to the otolith composition when compared with the external water concentration (Farrell and Campana, 1996). Juvenile barramundi (*Lates calcirfer*) otoliths showed no

significant concentration change when fed a diet enriched in levels of Cu, Sr and Pb (Milton and Chenery, 2001). Buckel et al., 2004, reported mixed effects for dietary influence on otolith chemical composition. Two of seven elements showed a significant increase in otolith chemistry relative to enhanced dietary items when the sagittal otoliths of bluefish (*Potomatus salatrix*) were analysed using solution based ICP-MS.

Dietary items are likely to have a minor influence on the chemical composition of the otolith. Elemental concentrations appear to remain stable when fish prey upon organisms with normal levels of trace elements in the environment. The otolith is influenced by abnormal levels of trace elements.

Ambient temperature potentially influences the chemical composition of an otolith. Otoliths show a seasonal relationship with temperature which results in the formation of seasonal growth rings which reflect seasonal protein deposition rates at different temperatures. A significant relationship between temperature and Sr:Ca ratios were observed for larval spot (*Leiostomus xanthurus*) otoliths. Sr substitution into the otolith is suggested to be a function of the partition coefficient between otolith aragonite and endolymph from which Sr and Ca precipitate (Bath Martin et al., 2004). Kalish 1989, conversely reports no clear relationship between otolith Sr:Ca ratio and temperature. This relationship is also observed by Clarke and Friedland, 2004, who kept Atlantic salmon (*Salmo salar*) in cages in the natural environment. Distinct Sr:Ca ratio peaks were observed in the otoliths, unrelated to environmental temperature or the growth of the fish. Temperature and salinity effects on the composition of black bream (*Acanthopagrus butcheri*) otoliths are suggested to be dominated by the influence of ambient water chemistry (Elsdon and Gillanders, 2005a).

The influence of salinity on otolith composition has been investigated in a range of different studies. The focus of my research is investigating otolith microchemistry within a freshwater system, therefore, no further investigation is required into salinity effects, other than to recognise the potential for salinity effects for marine species.

Physiology and ontogeny have been hypothesised as potential influences on otolith microchemistry. Elevated levels of trace elements at the nuclei of otoliths relative to external otolith concentrations have been observed. Elevated trace element concentrations can potentially identify specific regions of the otolith microstructure chemically as well as visibly (Brophy et al., 2004; Ruttenberg et al., 2005). Life history events may potentially influence the composition of the endolymph concurrently influencing otolith chemistry. This may allow greater substitution rates of minor elements in the absence of major elements such as a decrease in free Ca but constant Ba levels could potentially lead to a concomitant rise in otolith Ba composition (Kalish, 1989). When investigating migration the nucleus is compared with the external concentration of the otolith. This assumes minimal ontogenetic effect in the otolith although spots proximal to the otolith nucleus suggest the potential for ontogenetic effects.

2. Microchemical techniques

A range of techniques are available to assess the microchemical composition of otoliths. Electron probe microanalysis (EPMA) x-ray analysis has been widely used to investigate the microchemistry of otoliths (Arai et al., 2006). EPMA allows the researcher to point sample using a probe. This technique is good at detecting the

ratios of elements that are largely abundant in the otolith matrix. The ability to sample specific locations provides information relative to the life history of a fish. The challenge associated with this analytical technique is the limited number of elements routinely quantified, with only six major and minor elements regularly investigated (Thorrold et al., 1997). This technique is typically used to investigate life history events such as migration which is often inferred by different Sr:Ca ratios relative to marine and freshwater occupancy (Lamson et al., 2006; Shiao et al., 2006).

Proton induced x-ray emission (PIXE) analysis has also been used to investigate the microchemistry of otoliths. The ratios from PIXE analysis have also been shown to correlate with elemental counts obtained from LA-ICP-MS analysis (Crook et al., 2006, Morris Jr et al., 2003).

Solution based ICP-MS is another technique for the analysis of otoliths. This technique utilises the low detection limits available from ICP-MS sampling. The advantages of solution based ICP-MS analysis are the accurate quantification of minor and trace elements with low detection limits at resolution greater than LA-ICP-MS (Sanborn and Telmer, 2003). The suite of isotopes for quantification in the otoliths is also increased. The challenge of this analytical technique is the inability to sample specific loci on the otolith. The entire otolith is dissolved to allow liquid introduction to the ICP-MS. The samples may be prone to contamination and also be limited by sample sizes (Sanborn and Telmer, 2003). This technique has been used for a range of different otolith studies, investigating stock discrimination (Guido et al., 2004; Secor et al., 2001; Lo-Yat et al., 2005), inferring migration (Swearer et al., 2003). Solution based ICP-MS is the preferred option for bulk analysis (Sanborn and Telmer, 2003).

Laser ablation (LA) ICP-MS is a technique that combines the ability to sample specific loci on solid samples with the low detection limits offered by ICP-MS analysis. This allows the chemical composition of different areas on the otoliths over small gradients. The in situ analysis of otoliths occurs when the laser beam is focussed onto a specific location on the otolith. The otolith material is mobilised by the laser and transported to the ICP-MS by a continual flow of carrier gas, generally, argon, helium or a mix of the two. The ICP torch vaporises and ionises the sample and the subsequent isotopic masses are counted in the ICP-MS. The counts from LA-ICP-MS analysis correlate with other analytical techniques (Arai and Hirata, 2006). The challenges of this technique are, inter elemental fractionation, variable ablation yield and the influence of polyatomic interferences in the otolith. The influence of elemental fractionation is reduced by using an optimisation protocol; fractionation is tolerated in LA-ICP-MS (Chen, 1999). Laser performance and ablation yield has the potential to vary between samples. This is corrected for using an internal standard, commonly a minor isotope of a major element in the sample matrix this is often ^{43}Ca for otolith analyses. The formation of oxides and other polyatomic compounds during LA-ICP-MS potential influences the results by giving differential counts of elements not actually present. To remove these influences a background of carrier gas is quantified prior to analysis so gas influence can be removed and the elements selected are investigated for polyatomic interferences (May and Wiedmeyer, 1998).

LA-ICP-MS has been used to investigate fish migration (Clarke et al., 2007; Gemperline et al., 2002), investigate the spatial differences in geographically different populations (Brophy et al., 2003, Hamer et al., 2006, Chittaro et al., 2006, Chittaro et al., 2004), Thorrold et al., 1997), investigate ontogenetic differences in otolith composition (Chittaro et al., 2006) and to classify the nursery origin of fish

(Veinott and Porter, 2005, Milton et al., 1997). The retention of elements in the otolith matrix and continuous growth enable the investigation into the natural 'fingerprint' at the otolith. At the nucleus, the first material deposited, a signature of the original nursery locations may be present.

3. Framework and objectives

The aim of this research was to investigate the natal origin of wild adult rainbow trout and common smelt migration in Lake Rotorua and Lake Rotoiti, Rotorua lakes district, North Island, New Zealand, using otolith microchemistry. The initial objective was to investigate the water chemistry to see if the chemical compositions vary spatially, and that the analysis of otolith microchemistry is a feasible option for determining movement of trout and smelt between the lakes. Juvenile rainbow trout otoliths from tributary streams were analysed to develop a spatial map of otolith chemical signatures. Wild adult rainbow trout of unknown nursery origin were then classified, if possible, to a natal stream on the basis of the chemical signature present at the otolith nucleus.

The reason for investigating the natal origin of the trout is that Lake Rotorua is assumed to contribute the greatest percentage of juvenile fish to Lake Rotoiti wild trout population. This assumption is based on the relative tributary stream size differences between the lakes. Lake Rotoiti tributary streams are comparatively small, and the wild trout population of Lake Rotoiti is suggested to originate as recruits from Lake Rotorua spawning tributaries, by migrating through the Ohau

Channel which connects the lakes. Natal origin is of particular concern because of management of nutrient flow from Lake Rotorua to Lake Rotoiti.

To manage nutrient flow, a diversion wall, which Environment Bay of Plenty (EBOP) began constructing in June 2007 is being built at the downstream end of the Ohau Channel. Lake Rotoiti receives approximately 70% of inflowing nutrients from Lake Rotorua water which flows out through the Ohau Channel (Burns et al., 2005). A concern of fishery managers is that the wall may block a migration route for populations of rainbow trout in both lakes Rotorua and Rotoiti.

The aim of the smelt otolith analysis is to investigate migration occurring between the lakes by comparing the otolith nucleus chemical composition which represents the spawning location, with an otolith edge spot, that represents the chemical composition of the capture location. This will investigate whether the common smelt populations are resident in each lake or are migrating between the two lakes through the Ohau channel.

The overall objective for this research is to utilise otolith microchemistry techniques to assist in fisheries management investigations and decision making, relative to the potential influence of the Ohau Channel diversion wall.

Chapter 2. Trout investigation

1. Trout introduction

1.1. Species introduction

Rainbow trout, (*Oncorhynchus mykiss*) is an introduced, widespread species of trout that has important value in New Zealand, particularly as a game fish. Rainbow trout are present in a range of areas in New Zealand, particularly the large North Island lakes of the Bay of Plenty region, including Lake Rotorua and Lake Rotoiti (McDowall, 1978). New Zealand's rainbow trout populations are predominantly lake residents and are the main species caught by recreational anglers in the Rotorua lakes district. Wild and hatchery reared populations of rainbow trout are present in the lakes of the Rotorua district. Lake Rotorua is not stocked with hatchery reared fish as the large tributary streams provide ample habitat to support spawning that sustains the fishery. Lake Rotoiti is routinely stocked with hatchery reared fish to supplement the population of wild rainbow trout that spawn in the comparatively smaller tributaries of Lake Rotoiti and also any trout that are migrating from Lake Rotorua through the Ohau Channel which connects the two lakes.

Rainbow trout are widespread, partially due to the adaptability of this species. Rainbow trout can tolerate temperatures ranging from 0-25^{o}C (Gall and Crandell, 1992); the only factors that limit the distribution of rainbow trout are the need for year round water and the water temperature to remain constantly below 13^{o}C for a period of time allowing the trout to spawn (Scott and Poynter, 1999).

Juvenile rainbow trout usually occupy the natal tributary stream for approximately one year, before migrating downstream to the main body of the lake where the fish grow to adult size. Once sexual maturity is reached the trout migrates to a gravel-bedded spawning tributary. Rainbow trout generally demonstrate natal homing and high spawning site fidelity, often returning to their natal stream (McDowall, 1978).

Tributary streams provide spawning habitat for lake resident trout. Trout require the stream substrate to be composed of coarse uncompacted gravel, which allows the trout to dig a redd for egg deposition. The stream water requirements are cool, clear, rapidly flowing water that provides oxygen for buried eggs and alevins developing in the gravel redd (McDowall, 1978; McDowall, 1984).

Rainbow trout diet consists of a range of organisms, predominantly the most abundant species available in the habitat they occupy. Common dietary items are surface invertebrates and surface living fish like common smelt (McDowall, 1978). Common smelt (*Retropinna retropinna*) comprise a considerable amount of lake resident rainbow trout diet, (Watson, 1959; Ward et al., 2005) observed as much as 50-80% of rainbow trout diet (Smith, 1959).

The aim of this study is to investigate where the rainbow trout populations in each of the two lakes are spawning. To investigate migration, the elemental composition of the otolith nucleus from unknown adult rainbow trout samples was compared with a known set of juvenile. The results will assist fishery management decisions regarding rainbow trout populations of Lake Rotorua and Lake Rotoiti, particularly in the context of the diversion wall construction which may interrupt fish movement between the lakes.

2. Methods

2.1. Water samples

To assess the spatial variability of spawning stream water chemistry, water samples were collected from six spawning tributaries on 19-5-2007, 20-7-2007, 16-10-2007, and 17-11-2007. Water samples were collected in 15 ml sterile plastic tubes, previously filled with deionised Milli-Q water to leach metals (Elsdon and Gillanders, 2006). In the field the Milli-Q water was emptied, the tube was then submerged in the river and filled. The samples were stored on ice and transported back to the laboratory for sample preparation.

Water samples were filtered through a disposable 0.45 µm membrane Millipore filter. 9.8 ml of the filtered sample was transferred to a sterile 15 ml falcon tube by micropipette and was then acidified with 0.2 ml of concentrated HNO_3 prior to solution analysis.

Water samples were analysed for a suite of 26 isotopes using solution based inductively coupled plasma mass spectrometry (ICP-MS) on a Perkin Elmer Elan SCIEX DRC II mass spectrometer. The water samples were analysed at the ICP suite at the University of Waikato.

2.2. Sample locations

Juvenile rainbow trout were collected from six tributary streams (Figure 1) of Lake Rotorua and Lake Rotoiti. Adult wild rainbow trout were collected randomly from the main basin of each lake and at the Ohau Channel.

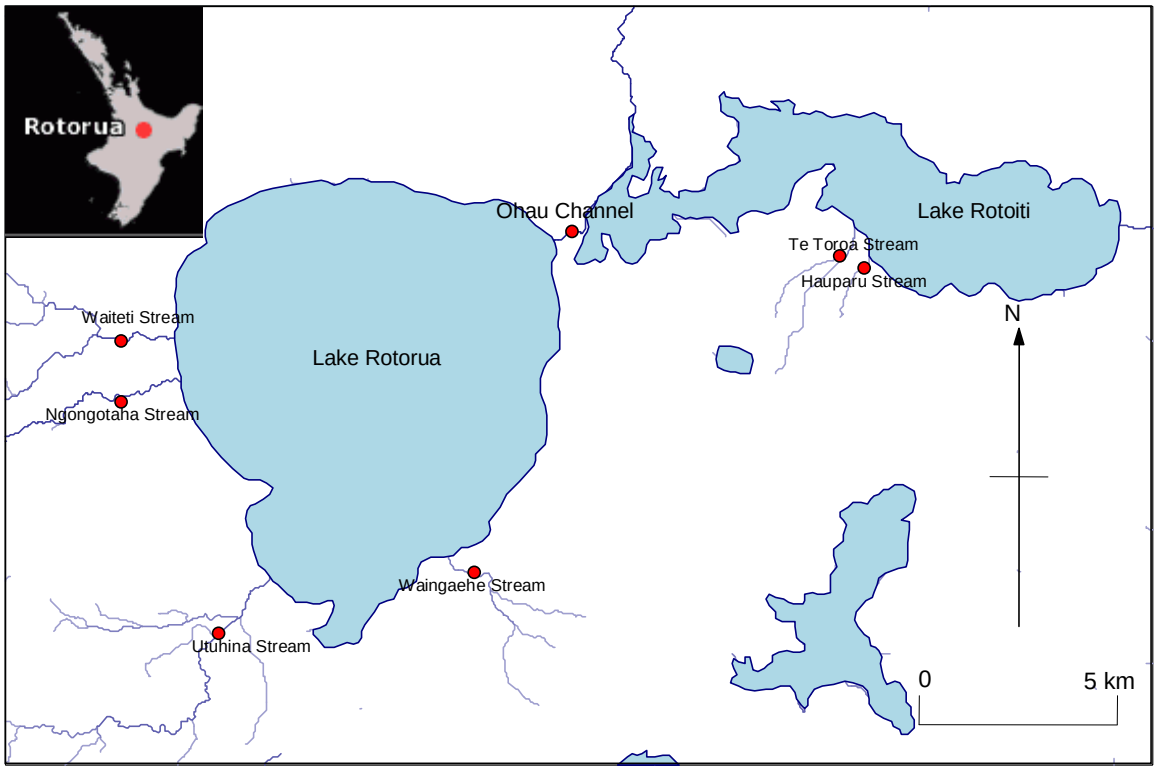

Figure 2.1: Juvenile rainbow trout tributary streams and adult rainbow trout collection sites from around Lake Rotorua and Lake Rotoiti. Map constructed with Freshwater Fish Database Assistant (Ian Jowett, National Institute of Water and Atmospheric Research, 2007).

Juvenile rainbow trout were collected from six tributary streams (Ngongotaha, Waiteti, Utuhina and Waingaehe tributary streams of Lake Rotorua, and Hauparu and Te Toroa tributary streams of Lake Rotoiti) (Figure 2.1). A seventh tributary stream (Waiiti Stream, Lake Rotoiti) was sampled, but no trout were caught. Each tributary stream has unique physical characteristics (Table 2.1).

Table 2.1: Summary of the physical characteristics of the juvenile rainbow trout spawning tributaries around Lake Rotorua and Lake Rotoiti. Data source, River Environment Classification data from Freshwater Fish Database, (Ian Jowett, NIWA).

Location	Stream order	Mean flow (m^3/s)	Catchment area (km^2)
Lake Rotorua			
Ngongotaha Stream	5	2.02	77.07
Waiteti Stream	5	3.00	60.47
Utuhina Stream	4	2.02	61.67
Waingaehe Stream	3	0.25	11.46
Lake Rotoiti			
Te Toroa Stream	3	0.27	7.40
Hauparu Stream	2	0.14	3.75

2.3. Sample collection

Juvenile rainbow trout were collected between 21-12-2005 and 6-3-2007, prior to the Ohau Channel diversion wall construction which began in June 2007. The trout were collected using a backpack electrofisher, dip net and stream net. Between 10 and 20 individuals were collected from each location. Juvenile trout from Waiteti Stream (fork length (FL) range 29 mm-63 mm), Hauparu Stream (23 mm -98 mm FL) and Te Toroa Stream (45 mm-49 mm FL) were collected on 21-12-2005. Juvenile trout from Utuhina Stream (28 mm-85 mm FL) were collected on 13-2-2006. Juvenile trout from Ngongotaha Stream (45 mm-96 mm FL), Waiteti Stream (39 mm-64 mm FL) and Waingaehe Stream (29 mm-54 mm FL) were collected on 6-3-2007. Waiiti Stream: Rotoiti was sampled 6-3-2007 unsuccessfully.

The juvenile trout were sacrificed in the field by immersion in an overdose of the anesthetic benzocaine, as outlined in the University of Waikato's Standard Operating Procedure for fish euthanasia. The fork length of the juvenile trout was measured to the nearest millimetre then the fish was preserved in 95% ethanol in a 500 ml container and transported to the laboratory.

The heads of wild adult rainbow trout were collected with the help of Eastern Region Fish and Game Council (ERFGC) rangers at Lake Rotoiti on season opening day (1-10-2005) *N* = 27. Additional trout heads from Lake Rotoiti were collected at the 'International' fishing competition (*N = 28*) held on 19-11-2005 and 20-11-2005. Adult rainbow trout heads (*N = 43*) from Lake Rotorua were collected at a local fishing competition on 28-1-2007, 11-2-2007 and 25-2-2007. Adult trout heads were collected from the Ohau Channel (*N = 13)* in early October 2005 in conjunction with a creel survey. The fork length, species/sex data and approximate capture location of each fish was recorded. The trout head was then removed below the operculum and placed in an individual plastic bag with the relevant data. Fish heads were kept in ice and transported to the laboratory.

Wild adult rainbow trout were identified by a visual observation of pelvic and adipose fins. Ngongotaha hatchery reared fish that are released to supplement wild trout populations have either the pelvic or adipose fins clipped to tag the individuals (pers comm. ERFGC). If the fins were intact the fish was assumed to be wild and the head was removed, any doubt in fin condition meant the fish head was excluded from collection.

2.4. Otolith extraction

The sagittal otoliths of juvenile trout were extracted using an adaptation of the 'open the hatch' method of Secor et al., 1991. The removal process involved sectioning along the midline of the dorsal surface through the skull (from the mouth to the back of the head). The left and right cranial cavities were separated and the brain tissue exposed. The brain was subsequently removed using forceps. This

exposed the sagittal otoliths in the semicircular canals of the inner ear, which were removed using fine forceps. Organic tissue adhering to the otolith was rinsed off using Milli-Q deionised water (18Ω) then the otolith was stored dry or in ethanol in 1.5 ml Eppendorf tubes until mounting.

Adult rainbow trout otoliths were removed using a variation of the previous process. The removed head was placed operculum down, thin sections were then sliced from snout to the operculum, dorsally behind the eyes. This exposed the brain which was extracted with forceps. Removal of the brain left the sagittal otoliths exposed. The otoliths were removed with fine forceps; any adhering organic tissue was rinsed off using Milli-Q deionised water. The otoliths were dried and stored in ethanol or dry in 1.5 mL sterile Eppendorf tubes until otolith preparation

2.5. Otolith preparation

Extracted otoliths were rinsed with Milli-Q deionised water then allowed to dry prior to mounting. One dry otolith from each pair (the left otolith where possible) was mounted sulcus side up, transversely along a glass microscope slide in Crystalbond®, a thermoplastic cement.

Otolith sections were achieved by hand grinding the mounted otoliths using wet or dry sand paper at a range of grits. Juvenile trout otolith nuclei were exposed and prepared using a series of 1200, 2000 and 4000 grit wet or dry sandpaper, moistened with Milli-Q deionised water. The larger adult rainbow trout otoliths were hand ground and polished using a series of 400, 800, 1200 grit sandpaper to expose the nucleus then 2000 and 4000 grit sandpaper to polish the otolith surface. The sandpaper was moistened with Milli-Q deionised water.

Otoliths were ground and polished in a circular motion to remove a uniform amount of material. A compound microscope was used during the grinding process to check the progression of the grinding. After the nucleus was exposed the otolith and slide were rinsed with Milli-Q water and stored dry awaiting preparation.

Composite slides of otoliths were prepared for LA-ICP-MS analysis. The individually mounted otoliths were cut from slides using a glass scribe, which allowed the mounted otoliths to be transferred to a Ward's petrographic slide (46 by 27 by 1.2 mm). The otoliths were mounted on the composite slide using double sided tape. The number of otoliths per slide ranged from 8-11 otoliths. The production of composite slides minimised the opening and closing of the laser ablation (LA) chamber. This reduced the influence of external gases entering the airtight gas chamber and potentially influencing the ICP-MS counts. The slides were stored until LA analysis. To minimise contamination, disposable latex gloves were worn during the otolith preparation process.

2.6. LA-ICPMS protocol

Laser ablation analysis was conducted at the University of Waikato's ICP suite using a Perkin Elmer Elan SCIEX DRC II ICP-MS with a New Wave Research Nd: YAG 213-nm wave-length laser. The carrier gas used to transport ablated material from the sample chamber to the ICP-MS was a mix of argon and helium.

Single-spot analysis was used on each of the otoliths; this was focussed on the nucleus of each otolith. The otolith nucleus is defined as the area within the first visible increment (Secor et al., 1991). Laser operating conditions were the same for juvenile and adult otolith analysis; the laser operating conditions differed slightly for external standard NIST 612 analysis (Table 2.2).

Table 2.2: The parameters for trout otolith and NIST612 standard materials analysis by LA-ICPMS.

Sample	Spot diameter (µm)	Laser output (%)	Laser dwell time (s)	Repetition rate (hz)
Juvenile rainbow trout	60	55	40	5
Adult rainbow trout	60	55	40	5
NIST 612 external reference	60	60	60	10

Prior to otolith analysis the laser was warmed up for approximately half an hour at analysis conditions, which allowed the laser energy to stabilise. The ICP-MS was optimised for LA data collection using NIST 612 SRM as a reference material. A line set at 5 Hz repetition rate, 70% power and 50 µm laser spot diameter was set across the NIST 612. ICP-MS optimisation was based on ICP-MS counts of Th^+, U^+ and ThO^+. The ICP was considered optimised when Th^+ and U^+ counts were >20,000 and the Th^+/U^+ ratio was ≈ 1 which indicates desirable ICP sensitivity. The ThO^+/Th^+ ratio was measured and the ICP was considered optimised when the ratio was <1%, which indicated negligible oxide formation. Gas flow rates and lens positions were manually altered at the ICP-MS to satisfy optimisation requirements.

After optimisation, an LA analysis method was set up, which comprised a suite of 13 isotopes (^{10}B, ^{25}Mg, ^{27}Al, ^{42}Ca, ^{43}Ca, ^{55}Mn, ^{60}Ni, ^{62}Ni, ^{65}Cu, ^{66}Zn, ^{85}Rb, ^{88}Sr and ^{137}Ba) which were analysed in each of the otoliths. This suite of isotopes was selected because the isotopes had minimal isobaric interference with the carrier gas Ar and have been used before in otolith analysis. The ICP-MS was set to analyse each isotope every 10 ms with 5 sweeps per second. This minimised the time between counting for each isotope, and resulted in a time resolved signal during the LA-ICP-MS data acquisition.

To quantify background interference and calculate limits of detection, counts were made of the carrier gas for 60 s without the laser firing, before each laser

ablation analysis. NIST 612 was ablated twice as an external standard prior to otolith analysis, after every 10 otolith analyses, and at the completion of each composite otolith slide. The NIST 612 spots differed from the otolith analysis and were used to correct for instrumental drift during the laser ablation period as well as providing a reference sample from which otolith chemical composition was calculated.

The concentrations of elements (ppm), in the otolith matrix were calculated in GLITTER Laser Ablation ICP/MS data reduction software (Version 4.4.1, Macquarie Research Limited © 1991-2000) software. The concentration conversion used published concentrations of NIST 612 SRM (Pearce et al, 1997), the ablation values obtained during the NIST 612 analysis and the Calcium Oxide (CaO) composition of the otolith to calculate elemental corrected values. The value used for CaO concentration in the otolith was 56.03%, based on the otolith Calcium Carbonate being made up of aragonite (http://webmineral.com/data/Aragonite.shtml).

2.7. Statistical analysis

Statistical analysis was conducted using parametric statistical tests with the exception of Spearman's rank order correlation with Statistica 7. Seven (^{24}Mg, ^{43}Ca, ^{55}Mn, ^{66}Zn, ^{85}Rb, ^{88}Sr, ^{137}Ba) of the 26 isotopes analysed by solution based ICP-MS were used to investigate the water samples. Five isotopic (^{55}Mn, ^{66}Zn, ^{85}Rb, ^{88}Sr, ^{137}Ba) counts were converted to elemental concentrations in GLITTER software and the elemental concentrations were used for trout otolith analysis.

Water sample isotopic concentrations satisfied the assumptions of data normality (Shapiro-Wilks W = 0.511-0.951) and homogeneity of variances (HOV) (Brown & Forsythe test of HOV P = 0.355-0.675) except for the ^{24}Mg isotope

concentration which was log transformed to satisfy HOV assumptions. To investigate stream specific differences one way analysis of variance (ANOVA) was used, then the differences between sample locations were investigated using Tukey honest significant difference (HSD) post-hoc test. Multivariate discriminant function analysis (DFA) was used to investigate the water samples; one linear DFA was calculated for the water samples to investigate separation between tributary streams.

Otolith elemental concentrations within two standard deviations of the mean for each location were included in statistical analysis; values outside two standard deviations were considered outliers and were excluded from analysis. Juvenile trout otolith data was normally distributed (Shapiro-Wilks W = 0.925-0.980) and had homogenous variances (Brown & Forsythe test, P = 0.207-0.681). Elemental concentrations in adult trout otolith nuclei were normally distributed (Shapiro Wilks W = 0.839-0.991) and the Rb, Sr and Ba elemental concentrations had homogenous variances (Brown & Forsythe test P = 0.475-0.841). The concentration of Mn (Brown & Forsythe test P = 0.032) and Zn (Brown & Forsythe test P = 0.026) did not have homogenous variances. All trout otolith elemental concentrations were square-root transformed to achieve normality.

Regression analysis was used to investigate the influence of fork length on otolith element composition. The values of Mn (P = 0.002) and Zn (P = 0.004) were influenced by fork length in the juvenile rainbow trout otoliths. One-factor analysis of covariance (ANCOVA), using fork length as a covariate was used to investigate differences in elemental Mn and Zn otolith composition between streams. The other elements were analysed using one-way ANOVA, followed by Tukey unequal N HSD post-hoc test to determine significant differences in otolith composition between tributary streams.

DFA was used to investigate the separation of juvenile rainbow trout from different streams on the basis of the elemental composition of the otolith nuclei. Two DFA analyses were computed, one that grouped juvenile trout by the lake the tributary streamed flowed into, and a second DFA that grouped juveniles by the tributary stream of capture. The classification functions for lake and stream from each DFA were used to determine the nursery origin of the known fish. The natal origin of the adult rainbow trout was subsequently investigated using the juvenile trout classification functions and the elemental concentrations from the nucleus of the adult rainbow trout otoliths Classification to natal lake and natal tributary stream was inferred from the highest classification score from the classification function equations. The unstandardised coefficients from the DFA grouping juvenile trout to lake were used to calculate the canonical score for juvenile trout to investigate separation between the lakes. The unstandardised canonical score was calculated for the stream DFA to investigate the spatial differences between spawning streams.

Nonparametric Spearman's rank order correlation matrices were computed for stream water samples, juvenile otolith samples and adult trout otolith samples to investigate the relationships between isotope concentrations in the water samples and the elemental concentrations in the otolith samples.

3. Results

3.1. Water samples

A summary table of the elemental corrected mean concentrations of the tributary stream water samples from the respective sample collection locations is presented in Table 2.3. The isotope concentrations were divided by the natural abundance of each isotope to infer elemental concentration. Waingaehe (high Mg, Mn, and Rb) and Te Toroa (high Ca and Sr, low Zn and Rb) streams stand out from the other streams. The negative value for ^{55}Mn log in the Hauparu Stream sample reflects the low values of ^{55}Mn in the water samples collected.

Table 2.3: Mean elemental corrected concentrations of the water samples collected from tributary streams around Lake Rotorua and Lake Rotoiti. Water samples were analysed by solution ICP-MS.

Location	Sample N	Mg (ppb)	Ca (ppb)	Mn log (ppb)	Zn (ppb)	Rb (ppb)	Sr (ppb)	Ba (ppb)
Lake Rotorua								
Ngongotaha Stream	4	1550	1356861	0.25	84.28	15.45	25.37	341.85
Utuhina Stream	4	1347	1110549	0.21	29.21	11.11	17.43	157.83
Waiteti Stream	4	1844	1589266	0.11	76.92	12.82	27.37	366.26
Waingaehe Stream	4	3783	2178903	0.53	31.42	17.05	25.86	306.64
Means summary	4	2131	1558895	0.28	55.46	14.10	24.01	293.15
Lake Rotoiti								
Te Toroa Stream	4	3312	3128351	0.50	16.57	9.64	42.98	158.28
Hauparu Stream	4	1991	2473334	-0.25	23.98	10.39	21.62	66.99
Means summary	4	2651	2800843	0.13	20.27	10.01	32.30	112.63

The concentration of six isotopes differed significantly between tributary streams, ^{24}Mg ($P < 0.001$), ^{43}Ca ($P < 0.001$), ^{55}Mn log ($P = 0.006$), ^{85}Rb ($P = 0.012$), ^{88}Sr ($P < 0.001$) and ^{137}Ba ($P < 0.001$). Table 2.4 illustrates the differences in stream water isotopic composition.

Table 2.4: Differences in the tributary stream water isotope composition illustrated by post hoc testing using Tukey HSD test. Values in bold and italicised are significant at $P < 0.05$

	Ngongotaha	Utuhina	Waiteti	Waingaehe	Te Toroa	Hauparu
^{24}Mg						
Ngongotaha Stream		0.988	0.943	***<0.001***	***0.001***	0.759
Utuhina Stream	0.988		0.661	***<0.001***	***<0.001***	0.401
Waiteti Stream	0.943	0.661		***<0.001***	***0.003***	0.997
Waingaehe Stream	***<0.001***	***<0.001***	***<0.001***		0.706	***0.001***
Te Toroa Stream	***0.001***	***<0.001***	***0.003***	0.706		***0.009***
Hauparu Stream	0.759	0.401	0.997	***0.001***	***0.009***	
^{43}Ca						
Ngongotaha Stream		0.942	0.954	0.072	***<0.001***	***0.008***
Utuhina Stream	0.942		0.523	***0.012***	***<0.001***	***0.001***
Waiteti Stream	0.954	0.523		0.308	***<0.001***	***0.046***
Waingaehe Stream	0.072	***0.012***	0.308		***0.029***	0.886
Te Toroa Stream	***<0.001***	***<0.001***	***<0.001***	***0.029***		0.213
Hauparu Stream	***0.008***	***0.001***	***0.046***	0.886	0.213	
^{55}Mn log						
Ngongotaha Stream		1.000	0.970	0.671	0.755	0.119
Utuhina Stream	1.000		0.995	0.523	0.610	0.184
Waiteti Stream	0.970	0.995		0.260	0.323	0.402
Waingaehe Stream	0.671	0.523	0.260		1.000	***0.006***
Te Toroa Stream	0.755	0.610	0.323	1.000		***0.008***
Hauparu Stream	0.119	0.184	0.402	***0.006***	***0.008***	
^{85}Rb						
Ngongotaha Stream		0.333	0.797	0.969	0.102	0.194
Utuhina Stream	0.333		0.959	0.091	0.978	0.999
Waiteti Stream	0.797	0.959		0.359	0.649	0.844
Waingaehe Stream	0.969	0.091	0.359		***0.022***	***0.047***
Te Toroa Stream	0.102	0.978	0.649	***0.022***		0.999
Hauparu Stream	0.194	0.999	0.844	***0.047***	0.999	
^{88}Sr						
Ngongotaha Stream		0.464	0.997	1.000	***0.008***	0.949
Utuhina Stream	0.464		0.240	0.401	***<0.001***	0.920
Waiteti Stream	0.997	0.240		0.999	***0.020***	0.762
Waingaehe Stream	1.000	0.401	0.999		***0.010***	0.917
Te Toroa Stream	***0.008***	***<0.001***	***0.020***	***0.010***		***0.001***
Hauparu Stream	0.949	0.920	0.762	0.917	***0.001***	
^{137}Ba						
Ngongotaha Stream		***0.009***	0.994	0.969	***0.009***	***<0.001***
Utuhina Stream	***0.009***		***0.003***	***0.043***	1.000	0.385
Waiteti Stream	0.994	***0.003***		0.778	***0.003***	***<0.001***
Waingaehe Stream	0.969	***0.043***	0.778		***0.043***	***0.001***
Te Toroa Stream	***0.009***	1.000	***0.003***	***0.043***		0.380
Hauparu Stream	***<0.001***	0.385	***<0.001***	***0.001***	0.380	

Significant positive correaltions were observed between a range of different isotopes in the stream water samples (Table 2.5). This suggests that the isotopes increase proportionally in concentration in the water samples.

Table 2.5: Spearman rank-order correlation matrix computed for the isotopic composition of tributary stream water from tributaries around Lake Rotorua and Lake Rotoiti. Values in bold and italicised are significant correlations at $P < 0.05$

	^{24}Mg	^{43}Ca	^{55}Mn	^{66}Zn	^{85}Rb	^{88}Sr	^{137}Ba
^{24}Mg	1.00	***0.79***	***0.43***	-0.17	0.04	***0.67***	0.20
^{43}Ca	***0.79***	1.00	0.13	-0.27	-0.20	***0.55***	-0.23
^{55}Mn	***0.43***	0.13	1.00	-0.37	0.34	***0.46***	0.40
^{66}Zn	-0.17	-0.27	-0.37	1.00	0.09	-0.21	0.33
^{85}Rb	0.04	-0.20	0.34	0.09	1.00	-0.04	***0.51***
^{88}Sr	***0.67***	***0.55***	***0.46***	-0.21	-0.04	1.00	***0.50***
^{137}Ba	0.20	-0.23	0.40	0.33	***0.51***	***0.50***	1.00

The linear DFA correctly classified 100% of the tributary stream water samples using the concentrations of six isotopes (^{43}Ca, ^{55}Mn log, ^{66}Zn, ^{85}Rb, ^{88}Sr and ^{137}Ba) as predictor variables (Table 2.6). The spatial separation of the water samples is illustrated in the scatterplot of the canonical scores (Figure 2.2), calculated from the unstandardised canonical coefficients (Equation 2.1) of the stream water DFA

Equation 2,1: The unstandardised coefficients from the stream water DFA grouping samples using the concentration of six isotopes (^{43}Ca, ^{55}Mn, ^{66}Zn, ^{85}Rb, ^{88}Sr, ^{137}Ba).

$$\textit{Unstandardised root 1 canonical score} = -1.890 - (0.006 \times {}^{43}Ca) + (1.199 \times {}^{55}Mn\ log) + (0.020 \times {}^{66}Zn) + (0.752 \times {}^{85}Rb) + (0.399 \times {}^{88}Sr) + (0.021 \times {}^{137}Ba)$$

$$\textit{Unstandardised root 2 canonical score} = 1.501 + (0.002 \times {}^{43}Ca) - (0.209 \times {}^{55}Mn\ log) + (0.004 \times {}^{66}Zn) - (0.154 \times {}^{85}Rb) - (0.432 \times {}^{88}Sr) + (0.115 \times {}^{137}Ba)$$

Table 2.6: Tributary stream water DFA classification matrix based on six isotopes (^{43}Ca, ^{55}Mn log, ^{66}Zn, ^{85}Rb, ^{88}Sr, ^{137}Ba). Rows are observed classifications and columns are predicted classifications. Total *N* = 28.

Group	Percent correct	(1)	(2)	(3)	(4)	(5)	(6)
Ngongotaha Stream (1)	100	4	0	0	0	0	0
Utuhina Stream (2)	100	0	4	0	0	0	0
Waiteti Stream (3)	100	0	0	4	0	0	0
Waingaehe Stream (4)	100	0	0	0	4	0	0
Te Toroa Stream (5)	100	0	0	0	0	4	0
Hauparu Stream (6)	100	0	0	0	0	0	4
Total	100	4	4	4	4	4	4

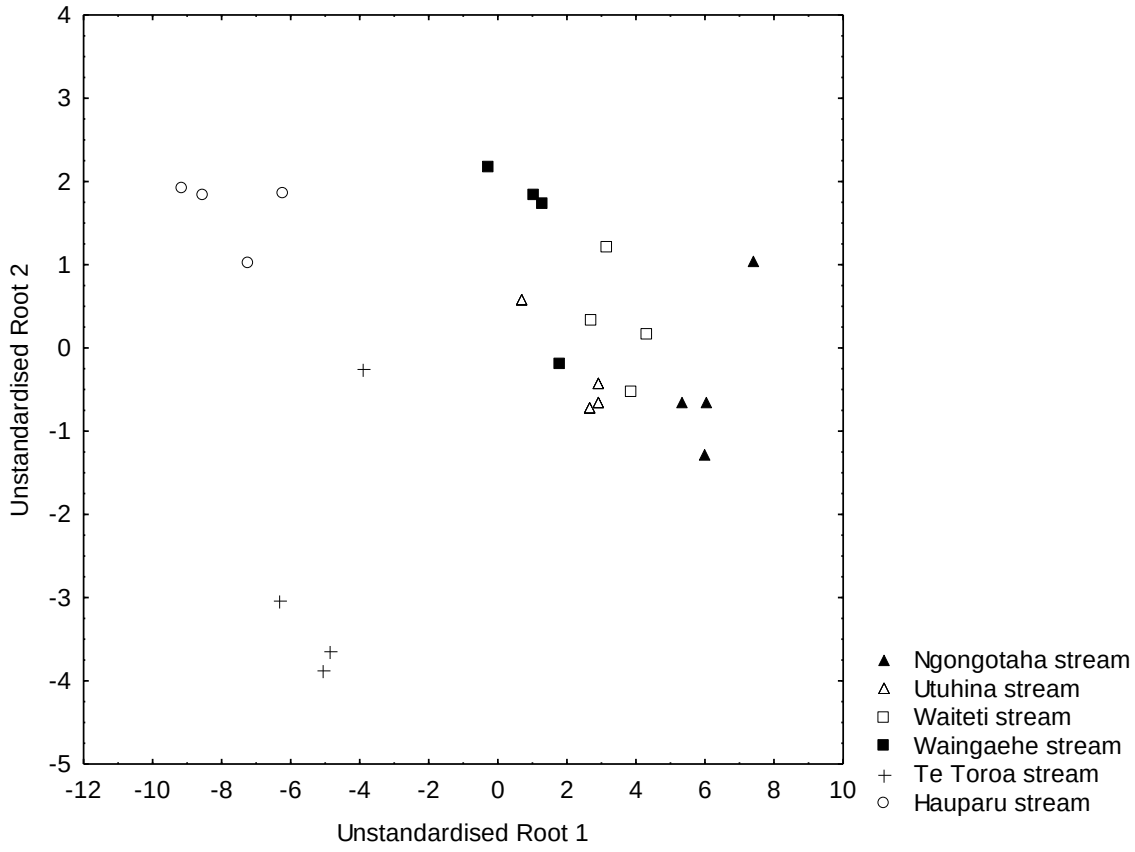

Figure 2.2: Scatter plot of tributary stream water sample canonical scores calculated from the unstandardised root 1 and unstandardised root 2 canonical coefficients (Equation 2.1) in stream DFA using six isotopic concentrations (^{43}Ca, ^{55}Mn log, ^{66}Zn, ^{85}Rb, ^{88}Sr, ^{137}Ba). Total *N* = 28.

3.2. Juvenile trout

A summary of the mean elemental concentrations at the nuclei of the juvenile rainbow trout collected from the spawning tributary streams is presented in Table 2.7. Waingaehe Stream stands out with high Ba and Sr concentrations and low Mn

concentration relative to Lake Rotorua tributaries. The lake Rotoiti tributary values are relatively similar; the concentration of Zn is greater than the Lake Rotorua tributaries.

Table 2.7: Summary of mean fork length and square-root transformed concentrations from the nucleus spots on juvenile rainbow trout otoliths.

Location	Fork length (mm)	Mn (ppm)	Zn (ppm)	Rb (ppm)	Sr (ppm)	Ba (ppm)
Lake Rotoiti						
Hauparu Stream	60	2.24	10.82	0.66	23.53	4.85
Te Toroa Stream	81	2.55	9.51	0.79	23.49	4.65
Means summary	71	2.40	10.17	0.73	23.51	4.75
Lake Rotorua						
Ngongotaha Stream	56	4.52	5.57	1.90	25.66	6.14
Utuhina Stream	37	5.53	5.55	1.22	23.73	4.59
Waingaehe Stream	47	3.51	8.71	1.31	26.50	7.45
Waiteti Stream	45	5.35	5.50	0.53	25.77	5.09
Means summary	46	4.73	6.33	1.24	25.42	5.82

The concentrations of Sr, Rb and Ba differed significantly at the nuclei of juvenile otoliths (P >0.001). The concentrations of Mn and Zn were analysed by ANCOVA removing the influence of fish fork length. The concentrations did not differ significantly between streams, Mn (P = 0.338) and Zn (P = 0.199). The results from post-hoc testing show that the square-root transformed Rb differed significantly between a range of streams. The concentration of square-root transformed Sr and Ba differed significantly between Waingaehe Stream and the other tributary streams (Table 2.8).

Table 2.8: Means comparison using Tukey unequal *N* HSD post-hoc test, illustrating the significant differences in otolith nucleus composition between the tributary streams sampled around Lake Rotorua and Lake Rotoiti. Bold, italicised values are significant at $P < 0.05$.

Rb sq root	Hauparu	Te Toroa	Ngongotaha	Utuhina	Waingaehe	Waiteti
Hauparu Stream		0.853	***< 0.001***	***< 0.001***	***< 0.001***	0.803
Te Toroa Stream	0.853		***< 0.001***	***0.004***	***< 0.001***	0.209
Ngongotaha Stream	***< 0.001***	***< 0.001***		***< 0.001***	***0.003***	***< 0.001***
Utuhina Stream	***< 0.001***	***0.004***	***< 0.001***		0.128	***< 0.001***
Waingaehe Stream	***< 0.001***	***< 0.001***	***0.003***	0.128		***< 0.001***
Waiteti Stream	0.803	0.209	***< 0.001***	***< 0.001***	***< 0.001***	

Sr sq root	Hauparu	Te Toroa	Ngongotaha	Utuhina	Waingaehe	Waiteti
Hauparu Stream		1.000	0.096	1.000	***0.007***	0.071
Te Toroa Stream	1.000		0.132	1.000	***0.013***	0.101
Ngongotaha Stream	0.096	0.132		0.162	0.890	1.000
Utuhina Stream	1.000	1.000	0.162		***0.013***	0.084
Waingaehe Stream	***0.007***	***0.013***	0.890	***0.013***		0.935
Waiteti Stream	0.071	0.101	1.000	0.084	0.935	

Ba sq root	Hauparu	Te Toroa	Ngongotaha	Utuhina	Waingaehe	Waiteti
Hauparu Stream		0.999	0.110	0.995	***< 0.001***	0.999
Te Toroa Stream	0.999		0.075	1.000	***< 0.001***	0.983
Ngongotaha Stream	0.110	0.075		***0.033***	0.256	0.213
Utuhina Stream	0.995	1.000	***0.033***		***< 0.001***	0.938
Waingaehe Stream	***< 0.001***	***< 0.001***	0.256	***< 0.001***		***0.001***
Waiteti Stream	0.999	0.983	0.213	0.938	***0.001***	

The Spearman's rank order correlation matrix (Table 2.9) calculated for the juvenile trout otoliths shows positive correlations between the elemental concentrations of Sr and Ba in the otolith and Ba and Rb at the otolith nucleus. A negative correlation between Mn and Zn elemental concentrations was observed.

Table 2.9: Spearman rank order correlation matrix of square-root transformed elemental correlation at the nuclei of juvenile rainbow trout otoliths analysed by LA-ICP-MS. Values in bold and italicised are significant at $P < 0.05$.

	Mn	Zn	Rb	Sr	Ba
Mn	1.00	***-0.66***	0.05	0.14	0.02
Zn	***-0.66***	1.00	-0.09	-0.11	0.08
Rb	0.05	-0.09	1.00	0.26	***0.39***
Sr	0.14	-0.11	0.26	1.00	***0.74***
Ba	0.02	0.08	***0.39***	***0.74***	1.00

The lake DFA correctly classified 98% of the juvenile trout overall (Table 2.10). The classification functions from juvenile trout DFA were used to create an

equation (Equation 2.2), which was used to classify adult rainbow trout to lake of origin.

Table 2.10: Juvenile trout classification matrix based on DFA using square-root transformed concentration of five (Mn, Zn, Rb, Sr and Ba) elements at the juvenile trout nuclei.

	Percent correct	Lake Rotoiti tributaries	Lake Rotorua tributaries
Lake Rotoiti tributaries	100	13	0
Lake Rotorua tributaries	97	1	29
Total	98	14	29

Equation 2.2: Classification function equation from juvenile trout DFA classifying individuals by lake of origin.

$$\textit{Factor Score 1 (Rotoiti)} = -201.399 + (8.338 \times \sqrt{Mn}) + (5.376 \times \sqrt{Zn}) + (18.867 \times \sqrt{Rb}) + (16.417 \times \sqrt{Sr}) - (15.523 \times \sqrt{Ba})$$

$$\textit{Factor Score 2 Rotorua} = -233.286 + (10.723 \times \sqrt{Mn}) + (4.560 \times \sqrt{Zn}) + (23.309 \times \sqrt{Rb}) + (17.363 \times \sqrt{Sr}) - (15.015 \times \sqrt{Ba})$$

A spatial representation of the classification functions illustrates the discrimination between the two populations of juvenile rainbow trout. The individuals have been graphed (Figure 2.3) on the basis of the classification functions calculated from Equation 2.1. Factor score 1 was significantly positively correlated with Sr (Pearson $r = 0.78$, $p < 0.001$) and factor score 2 was significantly positively correlated with Sr ($r = 0.78$, $p < 0.001$) and Mn ($r = 0.55$, $p = 0.003$).

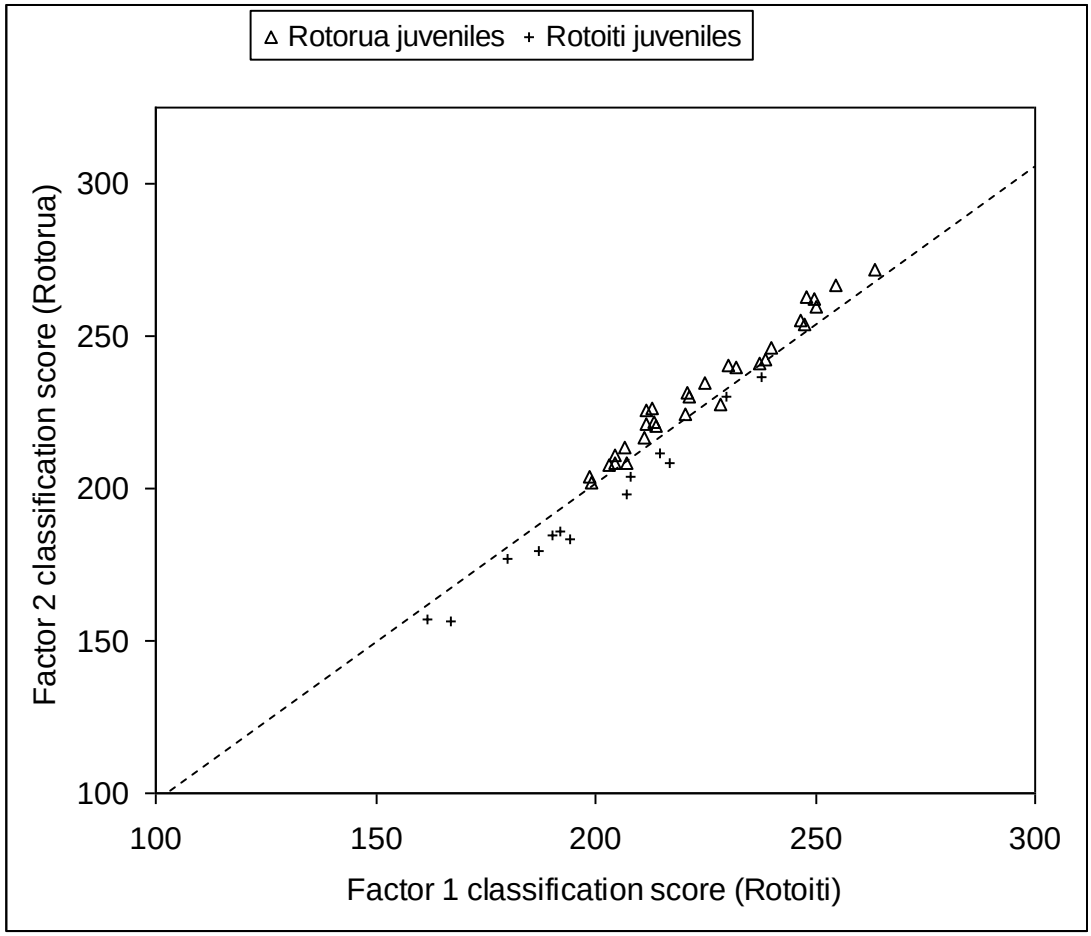

Figure 2.3: Scatterplot of juvenile rainbow trout otolith elemental signatures calculated from classification functions from juvenile trout lake group DFA (equation 2.1). Individuals grouped using five elements (Mn, Zn, Rb, Sr, and Ba). Dotted line distinguishes Rotorua fish (above the line) from Rotoiti fish (below the line). Note one misclassified Rotorua fish appears below the line.

The stream DFA classification matrix (Table 2.11) shows good discrimination between the tributary streams of both lakes with an overall correct classification of 91%. Three streams (Hauparu, Utuhina and Waiteti streams) classified 100% of juvenile otolith signatures correctly. The four fish that were incorrectly classified were classified to another tributary stream entering the same lake as the capture stream.

The juvenile rainbow trout were classified to tributary streams using the classification functions from the stream DFA. The classification functions were used

to create six equations relative to each spawning tributary and then the unknown rainbow trout elemental nucleus values were multiplied by each classification function (Equation 2.3).

Table 2.11: Juvenile rainbow trout classification matrix calculated from discriminant function analysis of five untransformed elemental otolith variables.

Group	Percent correct	Hauparu	Te Toroa	Ngongotaha	Utuhina	Waingaehe	Waiteti
Hauparu Stream	100	7	0	0	0	0	0
Te Toroa Stream	83	1	5	0	0	0	0
Ngongotaha Stream	71	0	0	5	1	1	0
Utuhina Stream	100	0	0	0	8	0	0
Waingaehe Stream	86	0	0	1	0	6	0
Waiteti Stream	100	0	0	0	0	0	8
Total	91	8	5	6	9	7	8

Equation 2.3: The classification function calculated for each stream in the juvenile rainbow trout DFA.

Hauparu stream classification $= -200.045 + (5.735 \times \sqrt{Mn}) + (5.481 \times \sqrt{Zn}) + (13.771 \times \sqrt{Rb}) + (15.831 \times \sqrt{Sr}) - (11.805 \times \sqrt{Ba})$

Te Toroa Stream classification $= -198.700 + (6.134 \times \sqrt{Mn}) + (5.123 \times \sqrt{Zn}) + (17.206 \times \sqrt{Rb}) + (15.799 \times \sqrt{Sr}) - (11.923 \times \sqrt{Ba})$

Ngongotaha Stream classification $= -251.177 + (9.012 \times \sqrt{Mn}) + (4.336 \times \sqrt{Zn}) + (51.231 \times \sqrt{Rb}) + (15.342 \times \sqrt{Sr}) - (9.351 \times \sqrt{Ba})$

Utuhina Stream classification $= -218.38 + (9.351 \times \sqrt{Mn}) + (4.156 \times \sqrt{Zn}) + (31.700 \times \sqrt{Rb}) + (15.792 \times \sqrt{Sr}) - (11.946 \times \sqrt{Ba})$

Waingaehe Stream classification $= -244.605 + (7.671 \times \sqrt{Mn}) + (5.229 \times \sqrt{Zn}) + (39.693 \times \sqrt{Rb}) + (15.581 \times \sqrt{Sr}) - (8.509 \times \sqrt{Ba})$

Waiteti Stream classification $= -232.122 + (8.660 \times \sqrt{Mn}) + (3.850 \times \sqrt{Zn}) + (9.154 \times \sqrt{Rb}) + (17.663 \times \sqrt{Sr}) - 13.481 \times \sqrt{Ba})$

To illustrate the spatial variation of the elemental values of the juvenile trout otoliths caught in different lake and spawning tributaries, canonical scores were calculated from the unstandardised canonical coefficients in the lake DFA (Equation 2.4) and the stream DFA (Equation 2.5). The canonical scores for each individual were plotted. A histogram shows the variability in canonical score by lake (Figure 2.4) and a scatterplot of the first two canonical scores illustrates the spatial variability in otolith concentrations between spawning tributaries (Figure 2.5).

Equation 2.4: The unstandardised root 1 canonical coefficients from the juvenile trout DFA grouping individuals by lake of origin using the square root transformed elemental concentrations of Mn, Zn, Rb, Sr and Ba at the otolith nucleus.

$$\textit{Unstandardised root 1canonical score} = 9.709 - (0.655 \times \sqrt{Mn}) + (0.200 \times \sqrt{Zn}) - (1.220 \times \sqrt{Rb}) - (0.260 \times \sqrt{Sr}) - (0.139 \times \sqrt{Ba})$$

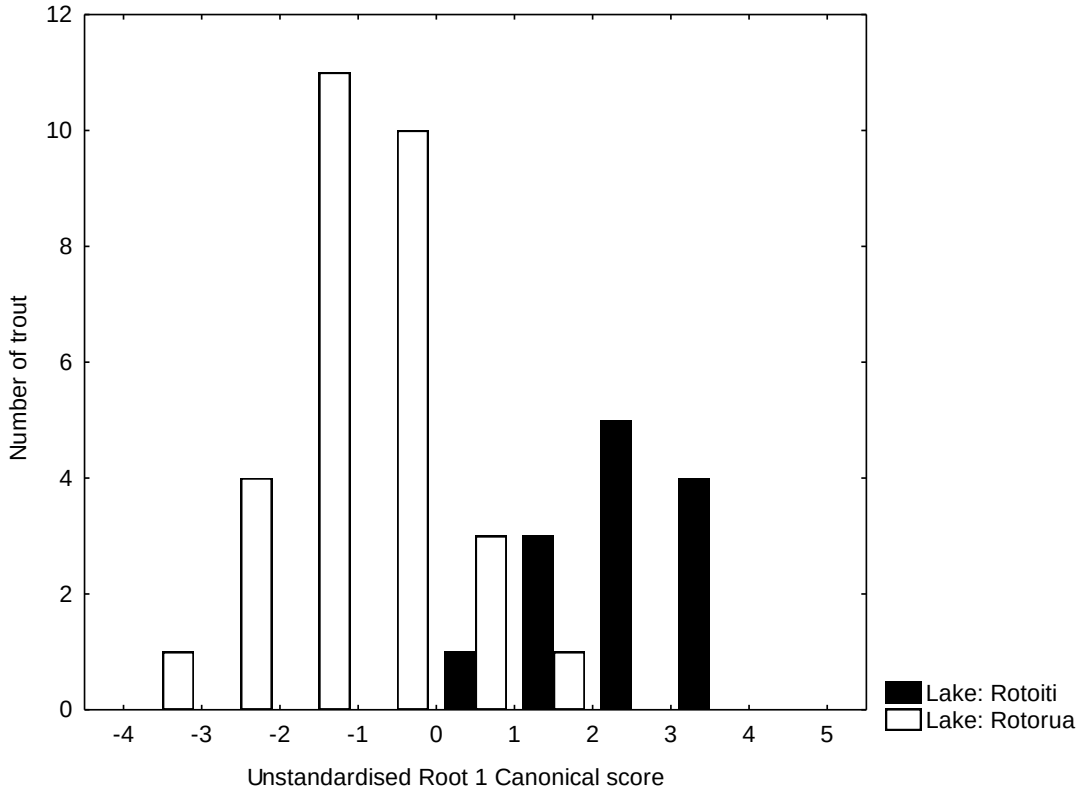

Figure 2.4: Histogram of the canonical scores calculated from equation 2.2 for the juvenile trout DFA grouping individuals by lake of capture using the square root transformed elemental concentrations of Mn, Zn, Rb, Sr, and Ba.

Equation 2.5: The unstandardised canonical root 1 and unstandardised canonical root 2 from the juvenile trout DFA grouping individuals by tributary stream using the square root transformed elemental concentrations of Mn, Zn, Rb, Sr and Ba at the otolith nucleus.

Unstandardised root 1canonical score = 4.895 – (0.257 x $\sqrt{Mn}$ *) + (0.022 x* $\sqrt{Zn}$ *) – (5.227 x* $\sqrt{Rb}$ *) + (0.178 x* $\sqrt{Sr}$ *) – (0.499 x* $\sqrt{Ba}$ *)*

Unstandardised root 2 canonical score = -3.744 + (0.656 x $\sqrt{Mn}$ *) – (0.345 x* $\sqrt{Zn}$ *) – (0.650 x* $\sqrt{Rb}$ *) + (0.281 x* $\sqrt{Sr}$ *) – (0.482 x* $\sqrt{Ba}$ *)*

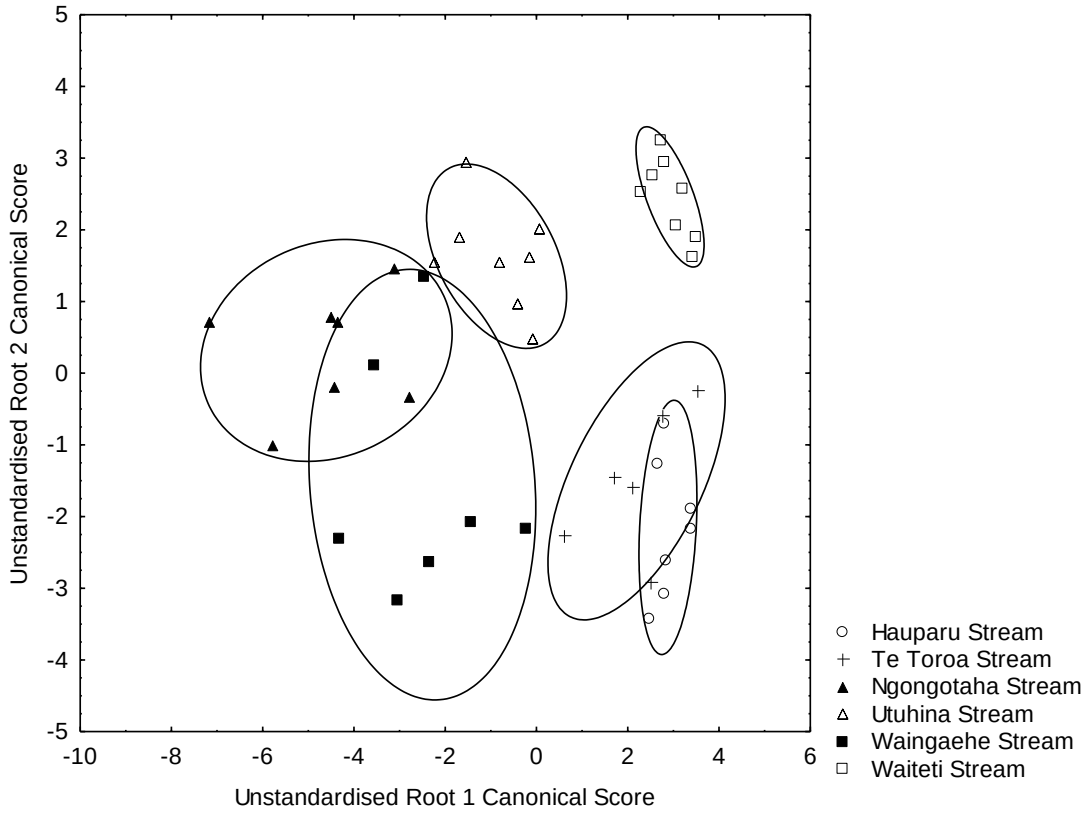

Figure 2.5: Canonical scores calculated from unstandardised root 1 and unstandardised root 2 equation 2.3 from juvenile rainbow trout nucleus DFA using five elemental concentrations (Mn, Zn, Rb, Sr, Ba). 63% confidence ellipses encompass individuals to illustrate stream differentiation pattern in otolith microchemical composition. Hauparu and Te Toroa are Rotoiti tributaries; other streams flow into L. Rotorua.

3.3. Adult trout

The elemental concentrations of Mn, Zn, Rb, Sr and Ba from adult rainbow trout nuclei were multiplied by the lake classification functions (Equation 2.2) from

the juvenile trout lake DFA. The two scores were then compared and the greater of the two classification scores indicated the lake of origin (Figure 2.6). A small proportion of individuals from Lake Rotoiti and Lake Rotorua appear to have origins in a Rotoiti tributary (Table 2.12).

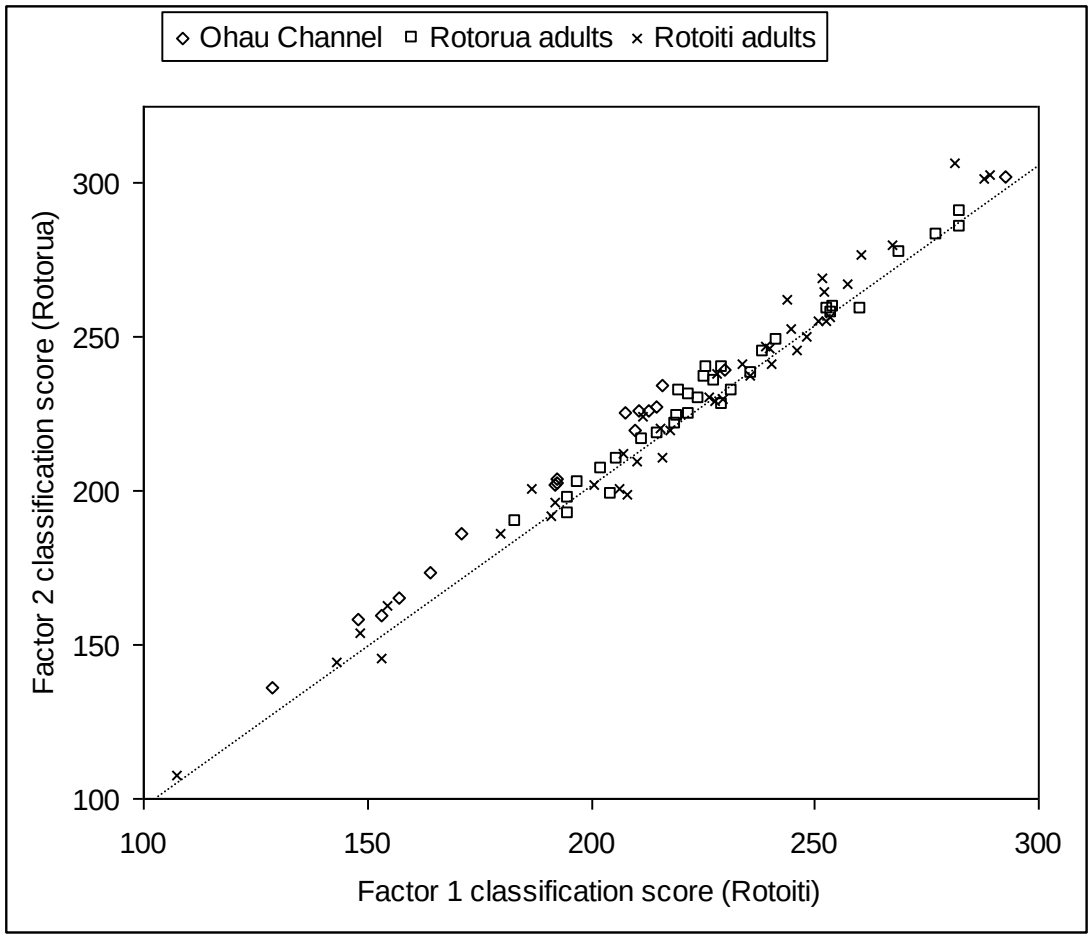

Figure 2.6: Classification function scores for wild adult rainbow trout of unknown natal origin calculated using juvenile trout raw classification function coefficients for Lake DFA. Individuals below the line classify as Lake Rotoiti natal origin, and individuals above the line classify as Lake Rotorua origin.

The calculated classification scores show that Lake Rotorua tributaries provided spawning habitat for 89% of the wild adult rainbow trout collected. The rainbow trout collected from the Ohau Channel classified 100% as a Lake Rotorua tributary.

Table 2.12: Classification of adult trout from lakes Rotoiti and Rotorua to lake of origin based on elemental concentrations of five elements (Mn, Zn, Rb, Sr and Ba) at the nucleus of each otolith. Classification scores were calculated from equation 2.2.

Capture location	Lake of origin (number)		
	Lake Rotorua	Lake Rotoiti	Total
Lake Rotorua	28	4	32
Lake Rotoiti	37	6	43
Ohau Channel	17	0	17
Total	82	10	92

Table 2.13: Percentage classification of adult trout from lakes Rotoiti and Rotorua to lake of origin based on elemental concentrations of five elements (Mn, Zn, Rb, Sr and Ba) at the nucleus of each otolith. Classification scores were calculated from equation 2.2

Capture location	Lake of origin (%)	
	Lake Rotorua	Lake Rotoiti
Lake Rotorua	88	13
Lake Rotoiti	86	14
Ohau Channel	100	0
Total	89	11

The natal tributary stream of each adult rainbow trout was investigated using the classification functions from the juvenile trout stream DFA (Equation 2.3) Waingaehe Stream contributed 50% of the adult rainbow trout to the Lake Rotorua capture population in this sample group. The other tributaries contributed to the Lake Rotorua population of wild rainbow trout except for Hauparu Stream. The wild rainbow trout captured in the Ohau Channel were from a range of the Lake Rotorua spawning tributaries, predominantly Utuhina Stream. The wild rainbow trout caught in Lake Rotoiti were mainly from Waiteti and Utuhina streams, a large contribution of 23% of the population were from the Lake Rotoiti tributary Te Toroa stream. Hauparu Stream, the second tributary of Lake Rotoiti sampled contributed only 2% of the wild rainbow trout population caught in Lake Rotoiti (Table 2.15).

Table 2.14: Numbers of adult rainbow trout classifying to tributary streams on the basis of classification score (equation 2.3)

Natal Stream	Number captured in each location			
	Lake Rotorua	Ohau Channel	Lake Rotoiti	Total
Lake Rotorua				
Ngongotaha Stream	9	4	2	15
Utuhina Stream	3	6	12	21
Waingaehe Stream	16	4	2	22
Waiteti Stream	1	3	15	19
Lake Rotoiti				
Hauparu Stream	0	0	2	2
Te Toroa Stream	3	0	10	13
Total	32	17	43	92

Table 2.15: Percentage of adult rainbow trout classifying to tributary streams on the basis of classification score (equation 2.3)

Natal Stream	Proportion captured in each location %			
	Lake Rotorua	Ohau Channel	Lake Rotoiti	Total
Lake Rotorua				
Ngongotaha Stream	28	24	5	16
Utuhina Stream	9	35	28	23
Waingaehe Stream	50	24	5	24
Waiteti Stream	3	18	35	21
Lake Rotoiti				
Hauparu Stream	0	0	5	2
Te Toroa Stream	9	0	23	14
Total	100	100	100	100

The trout were then grouped by natal origin lake and the specific differences between the samples were investigated. The mean concentrations of each group were calculated (Table 2.16). The concentrations of square root transformed Sr (P <0.001) and Ba (P <0.001) were significantly different between otolith nuclei of adult trout when grouped by lake of origin. The square root transformed concentrations of Mn and Zn were investigated using Kruskal-Wallis ANOVA by ranks non parametric test. The concentration of Mn (P = 0.001) and Zn (P < 0.001) were significantly different between lakes.

Table 2.16: Summary of the mean fork length and elemental concentrations of wild rainbow trout otoliths grouped by natal origin.

Natal origin	Fork length (mm)	*N*	Mn (ppm)	Zn (ppm)	Rb (ppm)	Sr (ppm)	Ba (ppm)
Lake Rotorua	460	82	4.24	5.48	1.26	26.33	6.29
Lake Rotoiti	480	10	2.56	9.53	1.07	23.29	3.92

Spearman's rank order correlation matrices were calculated for adult rainbow trout from Lake Rotorua (Table 2.17) and Lake Rotoiti (Table 2.18). The correlation matrices show similar relationships at the nuclei, the square-root transformed concentrations of Sr and Ba are significantly positively correlated and the concentrations of Rb and Mn are significantly negatively correlated.

Table 2.17: Spearman rank order correlation matrix of the elemental concentrations of Mn, Zn, Rb, Sr and Ba at the nucleus of rainbow trout otoliths classified to a Lake Rotorua natal stream.

	Mn	Zn	Rb	Sr	Ba
Mn	1.00	-0.08	***-0.27***	***-0.32***	-0.13
Zn	-0.08	1.00	0.01	0.07	0.09
Rb	***-0.27***	0.01	1.00	0.02	0.07
Sr	***-0.32***	0.07	0.02	1.00	***0.43***
Ba	-0.13	0.09	0.07	***0.43***	1.00

Table 2.18: Spearman rank order correlation matrix of the elemental concentrations of Mn, Zn, Rb, Sr and Ba at the nucleus of rainbow trout otoliths classified to a Lake Rotoiti natal stream.

	Mn	Zn	Rb	Sr	Ba
Mn	1.00	-0.32	***-0.84***	0.09	0.15
Zn	-0.32	1.00	0.14	0.20	0.36
Rb	***-0.84***	0.14	1.00	-0.02	-0.04
Sr	0.09	0.20	-0.02	1.00	***0.81***
Ba	0.15	0.36	-0.04	***0.81***	1.00

A similar relationship is observed when calculating the canonical scores for adult trout using the juvenile lake DFA. The histogram shows a large proportion of all adult trout sampled with values < 0. This was the observed pattern in the juvenile trout DFA, suggesting the majority of wild rainbow trout are showing a canonical score similar to the juvenile rainbow trout from Lake Rotorua tributaries.

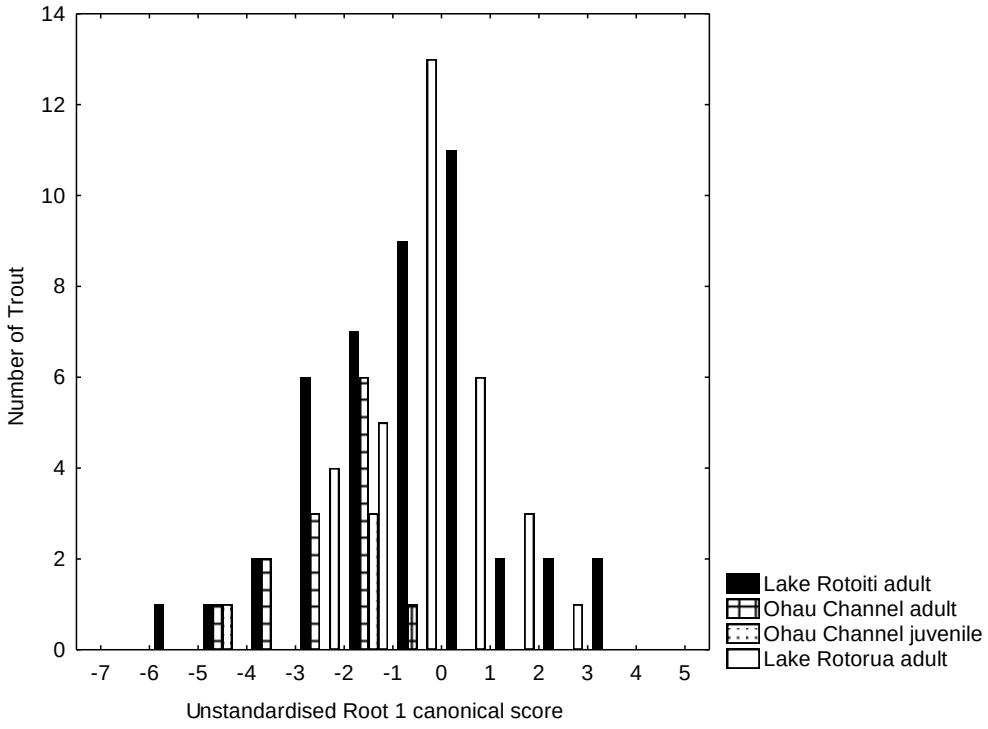

Figure 2.7: Histogram of the canonical scores for rainbow trout of unknown origin calculated using the juvenile trout unstandardised DFA coefficients. The canonical score is calculated from the elemental concentrations of Mn, Zn, Rb, Sr, and Ba at the nucleus of adult trout based on the training set of juvenile trout of known origin.

4. Discussion

4.1. Water samples

The isotopic concentration of the water samples collected from the different tributary streams was significantly different. The six isotopes (^{43}Ca, ^{55}Mn, ^{66}Zn, ^{85}Rb, ^{88}Sr and ^{137}Ba) used as predictor variables correctly classify 100% of the stream water samples to the tributary stream of collection. A range of factors can contribute to unique local water chemistry 'fingerprints'. Factors such as the stream substrate geology (Lucas and Baras, 2000; Wells et al., 2003), land use practice within the stream catchment and the vegetation at the margin of the stream may all influence the water chemistry. Unique water chemical fingerprints have been illustrated in a range of otolith microchemical studies (Wells et al., 2003; Munro et al., 2005; Clarke and Telmer, 2007) which suggest the use of otolith microchemistry to investigate natal origins and track migrations is feasible within a freshwater system.

The ionic composition of freshwater is generally regarded as poor compared with marine concentrations, which provides difficulty for otolith microchemical studies in a freshwater system (Wells et al., 2003). This is reflected by the limited number of otolith microchemistry studies conducted in freshwater systems to date. The 100% classification of the tributary stream water samples from this investigation suggests the tributary streams around lakes Rotorua and Rotoiti have unique elemental compositions and this may be reflected in the otolith. The otolith chemical concentration is not always proportionally related to the ambient water concentration. The otolith is influenced by the ambient water concentration although the interaction

between the otolith and the environmental concentration is not always well understood.

The Spearman's rank order correlation matrix shows a range of positive significant relationships in the isotopic values of the tributary stream water. The isotopic concentrations are therefore increasing proportionally in the water. A few correlations are worth discussing. The significant correlation between ^{88}Sr and ^{137}Ba is interesting as an inverse relationship between these elements has been observed in marine and freshwater systems. (Elsdon and Gillanders, 2005b) the concentrations in the tributary stream water all illustrate greater concentrations of ^{137}Ba relative to ^{88}Sr with the exception of Hauparu Stream.

4.2. Juvenile trout

Juvenile trout elemental data was collected from the otolith nucleus. The otolith nucleus is the first calcified tissue in a juvenile fish (Campana and Neilson, 1985), it is the area that is inside the first daily growth increment (Secor et al., 1991) and is assumed to represent the original chemical environment occupied by the juvenile fish (Swearer et al., 2003; Ruttenberg et al., 2005). Juvenile rainbow trout occupy the natal stream for approximately one year post hatch, after which the fish is likely to migrate downstream to the main lake basin (McDowall, 1978). The stream fidelity displayed by juvenile trout is important in the context of this study because the trout occupying the stream experience the local stream conditions including the ambient chemistry. The chemistry differences may be subsequently reflected in the otolith. The otolith is regarded as a natural tag that permanently stores environmental data chronologically (Campana, 1999; Campana and Thorrold, 2001; Swearer et al.,

2003) potentially showing the different chemical habitats the fish occupies. The otolith is not susceptible to metabolic reworking therefore the chemical concentration at the nucleus should be represent the chemistry of the original natal tributary stream.

The significant differences in water chemistry were reflected in the otoliths differences between streams on seven occasions. The difference in the isotopic concentration of ^{137}Ba in Utuhina and Ngongotaha streams in water the water samples was also represented by a significant difference in the elemental Ba of juvenile rainbow trout otoliths in these streams. The same difference in Ba was also observed in the water and otolith concentrations between Utuhina and Waingaehe streams, Waingaehe and Te Toroa streams and Waingaehe and Hauparu streams. The Ba concentration in freshwater systems appears to be well reflected in the otolith and was useful for determining the natal origins of fish (Elsdon and Gillanders, 2005b). Otolith isotopic concentrations of ^{88}Sr are streams and otoliths Sr concentrations were significantly different between Waingaehe and Te Toroa streams. The ^{85}Rb isotopic concentration and Rb otolith concentration were significantly different between Ngongotaha Stream and the two tributary streams of Lake Rotoiti.

The variation in otolith nucleus Mn concentrations was explained by the fork length of the individual juvenile trout, when the relationship was modeled using linear regression. Physiological factors have been suggested to influence the elemental concentration of the otolith (Fowler et al., 1995). Mn is an interesting element for otolith microchemical studies. The nucleus of an otolith has been reported to show an elevated Mn concentration or spike (Brophy et al., 2004; Ruttenberg et al. 2005). The elemental and visual observation of a Mn spike was used where possible to identify the successful ablation of the otolith nucleus.

The Spearman rank order correlation matrix showed some interesting correlations. The positive correlation between elemental Ba and Sr in the otolith nucleus may be related to the uptake of Sr. The Sr concentration of an otolith has been suggested to increase the relative proportion of otolith Ba by altering the crystal structure of the calcium carbonate (De Vries et al., 2005). The correlation matrix also showed significant positive correlation between Ba and Rb and negative correlation between Mn and Zn validating the inclusion in analysis. The positive correlation was observed in the water isotopic concentration but the negative Mn and Zn relationship was not significant.

The DFA analysis that grouped juvenile trout by tributary stream of collection correctly classified 91% using five elemental otolith values. Juvenile trout from Utuhina, Waiteti and Hauparu streams were classified with 100% accuracy. Any juveniles that misclassified did so into one of the tributaries flowing into the same lake. These results suggest the juvenile trout are demonstrating stream fidelity as expected to a relatively high degree. The otolith concentrations are stream specific and are suitable to provide values to classify the adult trout to natal location by otolith microchemistry. The differences between tributary water samples are reflected by unique otolith microchemistry fingerprints for each tributary stream.

4.3. Adult trout

The adult rainbow trout otoliths from the three capture locations were used as a training set to investigate the natal lake and stream origin of the fish. To investigate the lake of origin the classification functions from the juvenile trout DFA grouping individuals by lake were used.

The wild rainbow trout of unknown natal location were classified to lake of origin based on the square-root transformed elemental concentrations at the nucleus which were multiplied by the classification functions from the juvenile DFA. This compared the same otolith region. The relative classification functions are computed and then compared in each individual. The equation that returns the greatest relative classification value indicates the natal origin of the fish. Lake Rotorua contributes the greatest number of individuals to all capture locations, with 100% of adult and juvenile rainbow trout from the Ohau Channel classifying to Lake Rotorua tributaries, 88% of the adults caught in Lake Rotorua have Lake Rotorua tributary scores, and 86% of the adults caught in Lake Rotoiti have a classification score indicating origin in a Lake Rotorua natal tributary stream. The results from the otolith microchemical analysis indicate that populations of wild trout can be discriminated on the basis of the microchemical analysis of the otolith. The canonical score from the Lake DFA also shows that the majority of unknown rainbow trout are spawning in Lake Rotorua with the majority of observations on the Lake Rotorua side of the histogram.

The unknown otolith values of adult rainbow trout were then multiplied by the classification functions from the stream DFA to investigate the spawning stream origin. The 92 trout from unknown natal origin were classified to one of the six spawning streams. The majority of rainbow trout captured in Lake Rotorua were from Waingaehe Stream (50%), which is proportionally a small tributary. Ngongotaha stream, which is the largest tributary stream of Lake Rotorua contributed 28% of the adult wild trout captured in Lake Rotorua. Three of the other tributary streams contributed < 10% of fish to Lake Rotorua, including Te Toroa Stream, which is a tributary of Lake Rotoiti. This shows that migration from Lake Rotoiti tributaries to the main basin of Lake Rotorua is occurring.

The majority of rainbow trout captured in Lake Rotoiti were classified to two tributary streams of Lake Rotorua. Utuhina and Waiteti streams were natal streams for 35% and 28% of the adults collected respectively. All of the six tributaries contributed some individuals to the Lake Rotoiti wild adult rainbow trout population. Te Toroa Stream is the greatest contributor of the two natal streams sampled to Lake Rotoiti populations and this may be a reflection of the larger spawning tributary size.

The wild rainbow trout collected in the Ohau Channel were all classified to a Lake Rotorua tributary. Utuhina Stream was the natal stream of 35% of the adult trout. Ngongotaha and Waingaehe streams both contributed 24% each to the wild rainbow trout population of Lake Rotorua and Waiteti Stream contributed the final 18%. The timing of the Ohau adult capture and classification scores suggest these individuals were adults on a late spawning migration moving through the Ohau Channel and back to the relevant spawning tributary of Lake Rotorua.

The Spearman's rank order correlation matrix showed the same positive relationship between Ba and Sr in the otolith and also a unique significant correlation between Rb and Mn, which was not observed significantly in either the water or the juvenile trout correlation matrices.

The tributaries of Lake Rotorua are of greater magnitude and can provide spawning habitat for a larger amount of mature rainbow trout. A proportion of wild adult rainbow trout have natal origins in the spawning tributaries of Lake Rotoiti as well. Individuals captured in the Ohau channel classified 100% to a Lake Rotorua tributary. The sample size was smaller although this is still an interesting result. The four juvenile trout collected in the Ohau Channel were also included in the unknown training set for natal origin identification because the Ohau Channel was assumed to

not support spawning. The classification functions indicated these four individuals have an origin in a Lake Rotorua tributary.

The results suggest the Ohau Channel provides a link between lakes for the populations of wild rainbow trout in Lakes Rotorua and Rotoiti.

The results indicate otolith microchemistry is useful for discriminating trout populations and suggests that the Ohau Channel is an important migratory route for the rainbow trout, especially for wild rainbow trout recruiting into Lake Rotoiti from Lake Rotorua spawning tributaries.

Chapter 3. Smelt investigation

1. Smelt introduction

1.1. Species introduction

Common smelt, *Retropinna retropinna*, is one of the most widespread indigenous fishes in New Zealand. Common smelt exist as both lacustrine and diadromous populations in New Zealand (Ward et al., 2005). Lacustrine populations are present in areas such as Lake Rotorua, where they have been introduced and a self-recruiting population has been established.

Mature common smelt are silvery fish approximately 40-65 mm length at maturity, occupying the pelagic and littoral zones of lakes. They move to stream mouths or lake margins to spawn (Jolly, 1967). Smelt shoals release eggs at slow-moving margins near the entrance point of a tributary to a lake, or over shallow sandy substrates around the lake edge. Typically eggs incubate for 6-10 days then juveniles emerge at approximately 2-3 mm length (Jolly, 1967; McDowall, 1978). Smelt are an important species for trout fisheries; the fish were originally introduced as a forage species for rainbow and brown trout (Ward et al., 2005).

The aim of this study is to investigate whether the common smelt populations in each of the two lakes are resident or if they migrate between lakes Rotorua and Rotoiti. To investigate migration, the elemental composition of the otolith nucleus and edge was compared, which represents different fish life stages. A difference in microchemistry composition between spots in an individual otolith is assumed to be an indication that migration has occurred. The results will assist fishery management decisions regarding the smelt and rainbow trout populations of Lake Rotorua and

Lake Rotoiti, particularly in the context of the diversion wall construction (Chapter 2), which may interrupt fish movement between the lakes.

2. Methods

2.1. Water samples

The smelt investigation included an assessment of the spatial variability of the water chemistry at seven of the ten beach smelt collection sites. Water samples were collected on 19-5-2007, 20-7-2007, 16-10-2007, and 17-11-2007. The collection, preparation and analysis procedure for the water samples is outlined in Chapter two, 2.2.1.

2.2. Sample locations

Common smelt were collected from nine of the 10 sites sampled around the shores of Lake Rotorua and Lake Rotoiti. The locations sampled were Hannah's Bay, Pohue Bay, Mission Bay, Hamurana Stream and Ngongotaha Beach around Lake Rotorua, and Hinehopu Beach, Ruato Bay, Cherry Bay, Pikiao ski lane and Hotpools Beach around Lake Rotoiti (Figure 3.1)

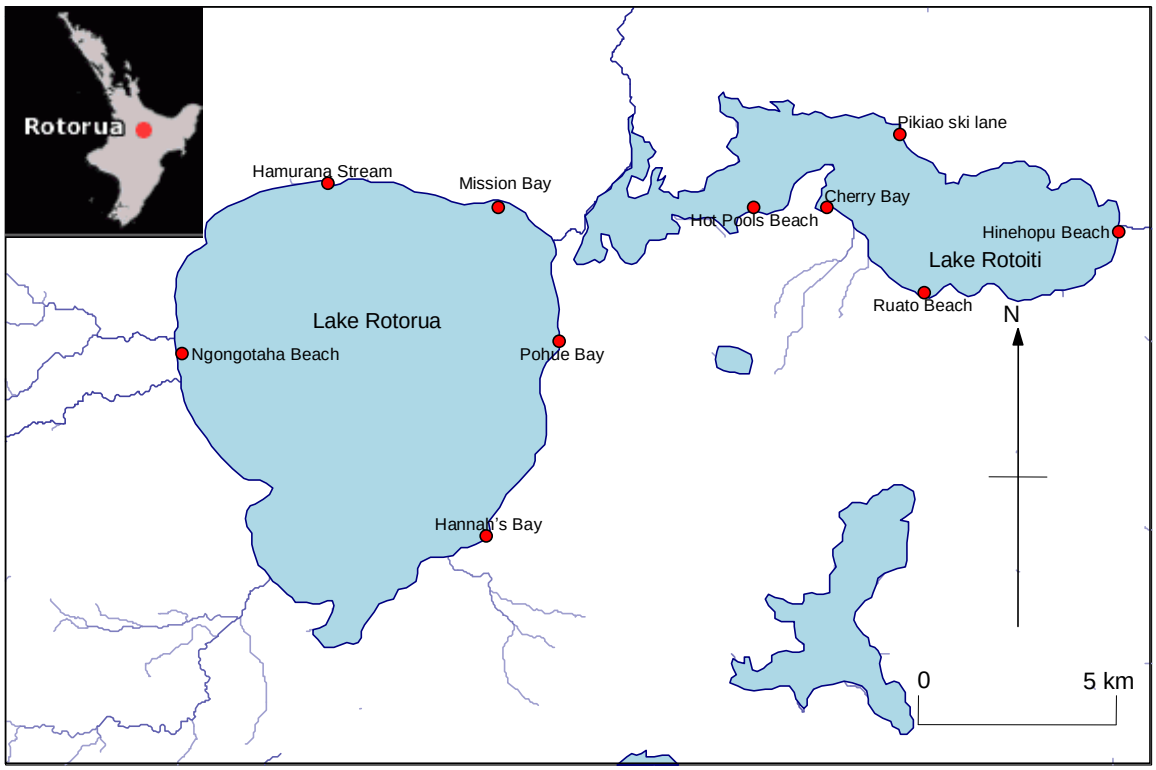

Figure 3.1: Map of beaches from which common smelt were collected around Lake Rotorua and Lake Rotoiti. Map constructed with Freshwater Fish Database Assistant (Ian Jowett, National Institute of Water and Atmospheric Research, 2007)

2.3. Sample collection

Common smelt were collected (range 15-40 individuals) using seine net at Hannah's Bay (38 mm-67 mm fork length (FL) range), Mission Bay (58 mm-68 mm FL), Pohue Bay (38 mm-63 mm FL) and Hamurana Stream (unsuccessful) on 12-12-2005. Hinehopu Beach (37 mm-66 mm), Ruato Bay (36 mm-51 mm FL) and Hamurana Stream (unsuccessful) were sampled on 21-12-2005. Cherry Bay (33 mm-50 mm FL), Pikiao ski lane (38 mm-48 mm FL) and Hotpools (33 mm-50 mm FL) were sampled on 23-2-2006. Hamurana Stream (51 -mm75 mm FL) and Ngongotaha Beach (unsuccessful) were sampled on 19-5-2007.

Common smelt are highly sensitive fish and often perish on capture. Smelt were sacrificed in the field by immersing the individuals in an overdose of anaesthetic

benzocaine, following the University of Waikato's standard operating procedure (SOP) for fish euthanasia. The fork length of the smelt was measured to the nearest millimetre, and then the fish were transferred to 500-ml sample containers containing 95% ethanol for preservation and transportation back to the laboratory.

2.4. Otolith extraction

The sagittal otoliths of the common smelt were removed using the same procedure as for juvenile rainbow trout; see Chapter two, 2.2.4.

2.5. Otolith preparation

The sagittal otoliths of smelt were prepared for LA-ICP-MS analysis using the same procedure used for juvenile rainbow trout otoliths, described in Chapter two, 2.2.5. The composite slides of smelt otoliths that were mounted on Ward's petrographic slides had a larger number of individual otoliths per slide, range 11-22 otoliths. This was because the common smelt sagittal otoliths were smaller than the juvenile rainbow trout otoliths.

2.6. LA-ICPMS protocol

The same LA-ICP-MS instruments at the University of Waikato's ICP suite were used for the analysis of smelt otoliths. The laser was warmed up and optimized as outlined in the trout analysis protocol. The smelt otolith analysis protocol differed in two ways. A smaller laser spot diameter (50 µm) was selected for smelt otolith analysis and two ablation spots were fired onto each otolith, one spot on the nucleus

of the otolith as in the trout samples and a second ablation spot was focused approximately 50 µm in from the otolith edge to investigate the elemental signature at the capture location. The external standard NIST 612 SRM was analysed twice prior to each run then after every five otoliths (corresponding to 10 otolith analyses). To correct for differential ablation yield and instrument drift, ^{43}Ca was analysed and used as an internal standard.

2.7. Statistical analysis

Beach water samples were analysed using parametric statistical tests with the exception of Spearman's rank order correlation. Seven (^{24}Mg, ^{43}Ca, ^{55}Mn, ^{66}Zn, ^{85}Rb, ^{88}Sr, ^{137}Ba) of 26 isotopes analysed by solution based ICP-MS were used to investigate the water samples. The otolith data from nucleus and edge spots did not satisfy the assumption of homogeneous variances; therefore nonparametric statistical tests were used. Five isotopic (^{55}Mn, ^{66}Zn, ^{85}Rb, ^{88}Sr, ^{137}Ba) counts were converted to elemental concentrations in GLITTER Laser Ablation ICP/MS data reduction software (Version 4.4.1, Macquarie Research Limited © 1991-2000) and the elemental concentrations were used for smelt otolith analysis.

Beach water samples satisfied the assumption of data normality (Shapiro-Wilks W = 0.553-0.959) and had homogenous variances (Brown & Forsythe test P = 0.057-0.790). One-way ANOVA analysis was used to investigate the difference in isotope concentration between samples. Multivariate DFA using six isotope concentrations (^{43}Ca, ^{55}Mn, ^{66}Zn, ^{85}Rb, ^{88}Sr and ^{137}Ba) as predictor variables was used to investigate the water samples. One DFA was calculated for the water samples grouped by lake, a second DFA was calculated for water samples grouped by beach.

Otolith elemental concentrations within two standard deviations of the mean for each collection location were included in analysis, values greater than two standard deviations were considered outliers and removed from analysis. The Kruskal-Wallis ANOVA test and multiple mean rank comparison post-hoc tests were used to investigate the nucleus and edge elemental values.

DFA was used to determine if smelt otolith nucleus spots or smelt edge spots from different beaches could be separated on the basis of otolith elemental concentration. Two DFA analyses were computed for nucleus spot and edge spot data, one which grouped smelt to lake of origin and the second which grouped smelt by beach of capture. Nonparametric Spearman's rank order correlation matrices were computed for stream water samples, smelt nucleus spot and smelt edge otolith spot samples separately. Wilcoxon matched pairs test was used to investigate the difference in otolith concentration between nucleus and edge spots on smelt otoliths. The influence of fork length on the resulting otolith elemental concentration was investigated using linear regression analysis.

3. Results

3.1. Water samples

A summary table of the mean elemental corrected concentrations of the beach water samples from the respective collection locations presented in Table 3.1. The water concentrations show a range of differences, the mean Mn, Zn and Ba concentrations are different between lakes.

Table.3.1: A summary of the mean elemental corrected concentrations of the water samples collected at beach locations around Lake Rotoiti and Lake Rotorua.

Site	Sample N	Mg (ppb)	Ca (ppb)	Mn (ppb)	Zn (ppb)	Rb (ppb)	Sr (ppb)	Ba (ppb)
Lake Rotorua								
Mission Bay	4	1991	1729630	0.88	38.46	27.26	28.92	206.64
Pohue Bay	4	2285	2487407	30.98	27.78	30.54	37.31	261.13
Hannah's Bay	4	2333	2105926	54.18	59.75	34.67	33.94	314.28
Ngongotaha Beach	4	1810	1789630	13.47	46.70	25.01	28.84	265.31
Hamurana Beach	4	1996	1582963	4.02	54.41	22.02	26.70	210.83
Means Summary	4	2083	1939111	20.71	45.42	27.90	31.14	251.64
Lake Rotoiti								
Hinehopu Beach	4	2541	1739259	0.80	27.46	27.67	27.63	162.30
Ruato Bay	4	2331	1867407	2.07	28.78	25.05	28.49	175.48
Means Summary	4	2436	1803333	1.44	28.12	26.36	28.06	168.89

Three isotope concentrations differed significantly between the beach water samples ^{43}Ca (P = 0.048), ^{85}Rb (P = 0.014) and ^{88}Sr (P = 0.023), and two isotope concentrations differed significantly between the lakes ^{55}Mn (P = 0.002) and ^{137}Ba (P = 0.002) when lake of origin of the water was treated as a group.

The specific differences between the beach locations were investigated using a multiple means comparison (Table 3.2).

Table.3.2: Means comparison Tukey HSD post-hoc test investigating the difference in isotopic concentration in water samples from beaches around Lake Rotorua and Lake Rotoiti. Significant values (*P < 0.05)* are in bold and italicised.

	(1)	(2)	(3)	(4)	(5)	(6)	(7)
^{43}Ca							
Mission Bay (1)		0.113	0.790	1.000	0.998	1.000	0.998
Pohue Bay (2)	0.113		0.780	0.171	***0.037***	0.121	0.279
Hannah's Bay (3)	0.790	0.780		0.892	0.466	0.809	0.970
Ngongotaha Beach (4)	1.000	0.171	0.892		0.985	1.000	1.000
Hamurana Stream (5)	0.998	***0.037***	0.466	0.985		0.997	0.931
Hinehopu Beach (6)	1.000	0.121	0.809	1.000	0.997		0.999
Ruato Bay (7)	0.998	0.279	0.970	1.000	0.931	0.999	
^{85}Rb							
Mission Bay (1)		0.933	0.253	0.990	0.635	1.000	0.991
Pohue Bay (2)	0.933		0.832	0.574	0.137	0.964	0.583
Hannah's Bay (3)	0.253	0.832		0.067	***0.009***	0.312	0.069
Ngongotaha Beach (4)	0.990	0.574	0.067		0.957	0.976	1.000
Hamurana Stream (5)	0.635	0.137	***0.009***	0.957		0.553	0.954
Hinehopu Beach (6)	1.000	0.964	0.312	0.976	0.553		0.978
Ruato Bay (7)	0.991	0.583	0.069	1.000	0.954	0.978	
^{88}Sr							
Mission Bay (1)		0.140	0.663	1.000	0.990	1.000	1.000
Pohue Bay (2)	0.140		0.923	0.135	***0.033***	0.062	0.108
Hannah's Bay (3)	0.663	0.923		0.652	0.266	0.414	0.579
Ngongotaha Beach (4)	1.000	0.135	0.652		0.991	1.000	1.000
Hamurana Stream (5)	0.990	***0.033***	0.266	0.991		1.000	0.997
Hinehopu Beach (6)	1.000	0.062	0.414	1.000	1.000		1.000
Ruato Bay (7)	1.000	0.108	0.579	1.000	0.997	1.000	

The Spearman rank order correlation matrix (Table 3.3) was used to investigate the correlation between isotopes in the beach sample water. The correlation matrices show significant positive correlations between a range of isotopes in the water samples such as ^{137}Ba and ^{88}Sr and ^{85}Rb and ^{137}Ba, which indicates the concentrations of isotopes increase proportionally. There is also a negative correlation between ^{66}Zn and ^{43}Ca shown.

Table 3.3: Spearman rank order correlation matrix of the relationships between elements in the water samples from beaches around Lake Rotorua and Lake Rotoiti. Significant correlation values ($P < 0.05$) are bold and italicised.

	^{24}Mg	^{43}Ca	^{55}Mn	^{66}Zn	^{85}Rb	^{88}Sr	^{137}Ba
^{24}Mg	1.00	***0.43***	0.21	-0.23	0.22	0.24	-0.21
^{43}Ca	***0.43***	1.00	0.30	***-0.39***	***0.41***	***0.65***	0.35
^{55}Mn	0.21	0.30	1.00	-0.07	***0.55***	***0.66***	***0.72***
^{66}Zn	-0.23	***-0.39***	-0.07	1.00	0.00	-0.30	0.07
^{85}Rb	0.22	***0.41***	***0.55***	0.00	1.00	***0.79***	***0.52***
^{88}Sr	0.24	***0.65***	***0.66***	-0.30	***0.79***	1.00	***0.71***
^{137}Ba	-0.21	0.35	***0.72***	0.07	***0.52***	***0.71***	1.00

Multivariate DFA was applied using six of the seven isotopes (^{43}Ca, ^{55}Mn, ^{66}Zn, ^{85}Rb, ^{88}Sr and ^{137}Ba) to investigate discrimination between beach locations and lake groups within the freshwater system. The beach water samples were classified with 64% accuracy (Table 3.4) and samples grouped by lake of origin were classified with 93% accuracy (Table 3.5).

Table 3.4: Classification matrix from DFA of beach water samples using six isotopic concentrations (^{43}Ca, ^{55}Mn, ^{66}Zn, ^{85}Rb, ^{88}Sr and ^{137}Ba). Rows indicate observed classifications, columns indicate predicted classifications.

Beach	Percent correct	(1)	(2)	(3)	(4)	(5)	(6)	(7)
Mission Bay (1)	75	3	0	0	0	1	0	0
Pohue Bay (2)	50	0	2	1	0	0	1	0
Hannah's Bay (3)	50	0	0	2	0	0	2	0
Ngongotaha Beach (4)	50	0	0	1	2	1	0	0
Hamurana Stream (5)	75	0	0	0	1	3	0	0
Hinehopu Beach (6)	100	0	0	0	0	0	4	0
Ruato Bay (7)	50	0	0	0	0	0	2	2
Total	64	3	2	4	3	5	9	2

Table 3.5: Classification matrix from DFA investigating lake water sample group separation using six isotopic concentrations (^{43}Ca, ^{55}Mn, ^{66}Zn, ^{85}Rb, ^{88}Sr and ^{137}Ba). Rows indicate observed classifications, columns indicate predicted classifications

Lake	Percent correct	Rotorua	Rotoiti
Rotorua	95	19	1
Rotoiti	88	1	7
Total	93	20	8

3.2. Common smelt edge

A summary of the mean elemental concentration at the nuclei of otoliths from each of the beach locations is presented in Table 3.6. The Hamurana Stream sample stands out with a greater Rb concentration at the edge of the smelt otolith. The Zn concentration also shows difference between lakes.

Table 3.6: Mean values of fork length and elemental composition (ppm) of five elements obtained from LA-ICP-MS spot analysis at the edge of smelt otoliths.

Location	N Smelt	Fork length (mm)	Mn (ppm)	Zn (ppm)	Rb (ppm)	Sr (ppm)	Ba (ppm)
Lake Rotoiti							
Cherry Bay	9	42	0.53	15.19	0.50	978	28.18
Hinehopu Beach	14	50	0.58	8.88	0.50	1028	27.69
Hot pools Beach	17	43	0.90	9.43	0.58	1097	33.51
Pikiao ski lane	17	41	1.31	19.23	0.46	1041	29.02
Ruato Bay	11	42	1.22	9.05	0.54	1135	32.58
Means summary	14	44	0.91	12.36	0.52	1056	30.20
Lake Rotorua							
Hamurana Beach	19	66	0.42	3.69	1.22	1105	25.69
Hannah's Bay	16	53	1.14	8.96	0.43	1077	29.89
Mission Bay	16	62	0.34	5.23	0.67	1022	19.04
Pohue Bay	15	60	0.89	9.85	0.42	1070	25.55
Means summary	17	60	0.70	6.93	0.69	1069	25.04

The common smelt edge results were analysed using non-parametric tests. The concentrations of Mn (P = 0.019), Zn (P = < 0.001), Rb (P = 0.015) and Ba (P = 0.001) differed significantly between lakes. The concentrations of Mn (P < 0.001), Zn (P = 0.002), Rb (P <0.001), Sr (P = 0.002) and Ba (P < 0.001) differed between beach location at the edge spot on smelt otoliths. Post-hoc testing of multiple mean ranks illustrates the separation between individual beach locations (Table 3.7).

Table 3.7: Multiple comparison of mean rank post hoc testing illustrating the beach specific differences in smelt otolith edge elemental composition. Significant ($P < 0.05$) values are in bold and italicised.

Mn	(1)	(2)	(3)	(4)	(5)	(6)	(7)	(8)	(9)
Cherry Bay (1)		1.000	1.000	1.000	0.423	1.000	1.000	1.000	1.000
Hinehopu Beach (2)	1.000		1.000	1.000	0.235	1.000	1.000	1.000	1.000
Hot pools Beach (3)	1.000	1.000		1.000	1.000	0.100	1.000	0.075	1.000
Pikiao ski lane (4)	1.000	1.000	1.000		0.543	1.000	1.000	1.000	1.000
Ruato Bay (5)	0.423	0.235	1.000	0.543		***0.001***	1.000	***0.001***	0.811
Hamurana Stream (6)	1.000	1.000	0.100	1.000	***0.001***		***0.017***	1.000	1.000
Hannah's Bay (7)	1.000	1.000	1.000	1.000	1.000	***0.017***		***0.013***	1.000
Mission Bay (8)	1.000	1.000	0.075	1.000	***0.001***	1.000	***0.013***		1.000
Pohue Bay (9)	1.000	1.000	1.000	1.000	0.811	1.000	1.000	1.000	

Zn	(1)	(2)	(3)	(4)	(5)	(6)	(7)	(8)	(9)
Cherry Bay (1)		1.000	1.000	1.000	1.000	0.054	1.000	1.000	1.000
Hinehopu Beach (2)	1.000		1.000	1.000	1.000	0.069	1.000	1.000	1.000
Hot pools Beach (3)	1.000	1.000		1.000	1.000	0.085	1.000	1.000	1.000
Pikiao ski lane (4)	1.000	1.000	1.000		1.000	***0.002***	1.000	0.227	1.000
Ruato Bay (5)	1.000	1.000	1.000	1.000		0.077	1.000	1.000	1.000
Hamurana Stream (6)	0.054	0.069	0.085	***0.002***	0.077		0.255	1.000	0.586
Hannah's Bay (7)	1.000	1.000	1.000	1.000	1.000	0.255		1.000	1.000
Mission Bay (8)	1.000	1.000	1.000	0.227	1.000	1.000	1.000		1.000
Pohue Bay (9)	1.000	1.000	1.000	1.000	1.000	0.586	1.000	1.000	

Rb	(1)	(2)	(3)	(4)	(5)	(6)	(7)	(8)	(9)
Cherry Bay (1)		1.000	1.000	1.000	1.000	***0.001***	1.000	0.513	1.000
Hinehopu Beach (2)	1.000		1.000	1.000	1.000	***0.001***	1.000	1.000	1.000
Hot pools Beach (3)	1.000	1.000		1.000	1.000	***0.001***	1.000	1.000	1.000
Pikiao ski lane (4)	1.000	1.000	1.000		1.000	***<0.001***	1.000	***0.003***	1.000
Ruato Bay (5)	1.000	1.000	1.000	1.000		***0.016***	1.000	1.000	1.000
Hamurana Stream (6)	***0.001***	***0.001***	***0.001***	***<0.001***	***0.016***		***<0.001***	1.000	***<0.001***
Hannah's Bay (7)	1.000	1.000	1.000	1.000	1.000	***<0.001***		***0.003***	1.000
Mission Bay (8)	0.513	1.000	1.000	***0.003***	1.000	1.000	***0.003***		***0.004***
Pohue Bay (9)	1.000	1.000	1.000	1.000	1.000	***<0.001***	1.000	***0.004***	

Sr	(1)	(2)	(3)	(4)	(5)	(6)	(7)	(8)	(9)
Cherry Bay (1)		1.000	0.224	1.000	***0.039***	0.053	0.227	1.000	0.790
Hinehopu Beach (2)	1.000		1.000	1.000	1.000	1.000	1.000	1.000	1.000
Hot pools Beach (3)	0.224	1.000		1.000	1.000	1.000	1.000	1.000	1.000
Pikiao ski lane (4)	1.000	1.000	1.000		1.000	1.000	1.000	1.000	1.000
Ruato Bay (5)	***0.039***	1.000	1.000	1.000		1.000	1.000	0.242	1.000
Hamurana Stream (6)	0.053	1.000	1.000	1.000	1.000		1.000	0.346	1.000
Hannah's Bay (7)	0.227	1.000	1.000	1.000	1.000	1.000		1.000	1.000
Mission Bay (8)	1.000	1.000	1.000	1.000	0.242	0.346	1.000		1.000
Pohue Bay (9)	0.790	1.000	1.000	1.000	1.000	1.000	1.000	1.000	

Ba	(1)	(2)	(3)	(4)	(5)	(6)	(7)	(8)	(9)
Cherry Bay (1)		1.000	1.000	1.000	1.000	1.000	1.000	0.289	1.000
Hinehopu Beach (2)	1.000		1.000	1.000	1.000	1.000	1.000	0.143	1.000
Hot pools Beach (3)	1.000	1.000		1.000	1.000	0.332	1.000	***<0.001***	0.522
Pikiao ski lane (4)	1.000	1.000	1.000		1.000	1.000	1.000	***0.019***	1.000
Ruato Bay (5)	1.000	1.000	1.000	1.000		1.000	1.000	***0.003***	1.000
Hamurana Stream (6)	1.000	1.000	0.332	1.000	1.000		1.000	1.000	1.000
Hannah's Bay (7)	1.000	1.000	1.000	1.000	1.000	1.000		***0.045***	1.000
Mission Bay (8)	0.289	0.143	***<0.001***	***0.019***	***0.003***	1.000	***0.045***		1.000
Pohue Bay (9)	1.000	1.000	0.522	1.000	1.000	1.000	1.000	1.000	

A range of significant correlations were observed in the smelt otolith edge data (Table 3.8). The significant positive correlations of Sr and Ba, Mn and Ba and Sr and Mn were observed in the beach water samples.

Table 3.8: Spearman rank order correlation matrix illustrating the relationships between the elemental compositions of smelt otolith edges analysed by LA-ICP-MS. Significant correlations ($P < 0.05$) are in bold and italicised.

	Mn	Zn	Rb	Sr	Ba
Mn	1.00	***0.50***	***-0.36***	***0.32***	***0.57***
Zn	***0.50***	1.00	***-0.44***	0.04	***0.35***
Rb	***-0.36***	***-0.44***	1.00	-0.03	***-0.26***
Sr	***0.32***	0.04	-0.03	1.00	***0.63***
Ba	***0.57***	***0.35***	***-0.26***	***0.63***	1.00

Multivariate DFA analysis classified 74% of the smelt edge elemental values to the correct lake of origin (Table 3.9) and 43% of the smelt to the original beach of capture (Table 3.10).

Table 3.9: Classification matrix from DFA analysis grouping common smelt to lake of origin using five elemental concentrations (Mn, Zn, Rb, Sr and Ba) from LA-ICP-MS analysis of the otolith edge. Rows represent observed classifications and columns represent predicted classifications.

	Percent correct	Rotoiti	Rotorua
Rotoiti	76	52	16
Rotorua	71	19	47
Total	74	71	63

Table 3.10: Classification matrix from DFA analysis grouping common smelt to beach of capture using five elemental concentrations (Mn, Zn, Rb, Sr and Ba) from otolith edge LA-ICP-MS analysis. Rows represent observed classifications and columns represent predicted classifications.

Group	Percent correct	(1)	(2)	(3)	(4)	(5)	(6)	(7)	(8)	(9)
Cherry Bay (1)	11	1	2	1	3	0	0	1	0	1
Hinehopu Beach (2)	43	2	6	3	0	2	0	1	0	0
Hot pools Beach (3)	59	0	0	10	3	0	0	2	1	1
Pikiao ski lane (4)	29	1	4	0	5	0	1	3	1	2
Ruato Bay (5)	27	0	0	3	1	3	0	2	2	0
Hamurana Stream (6)	72	0	0	0	0	1	13	0	4	0
Hannah's Bay (7)	24	0	1	5	2	0	0	4	4	1
Mission Bay (8)	81	0	1	2	0	0	0	0	13	0
Pohue Bay (9)	13	0	1	1	3	0	0	4	4	2
Total	43	4	15	25	17	6	14	17	29	7

The classification functions from the lake DFA were used to create an equation (Equation 3.1) which was used to classify the individual fish to lake of capture on the basis of the elemental signature at the edge of the otolith. The spatial variation between beach capture sites is illustrated using the factor 1 and factor 2 classification scores from the lake DFA Figure 3.2).

Equation 3.1: Classification equation developed from smelt edge spot DFA analysis using classification functions.

Factor 1 score (Rotoiti) = -64.526 – (1.591 x Mn) + (0.236 x Zn) + (3.947 x Rb) + (0.137 x Sr) – (0.684 x Ba)

Factor 2 score (Rotorua) = -69.964 – (1.580 x Mn) + (0.212 x Zn) + (4.876 x Rb) + 0.145 x Sr) – (0.801 x Ba)

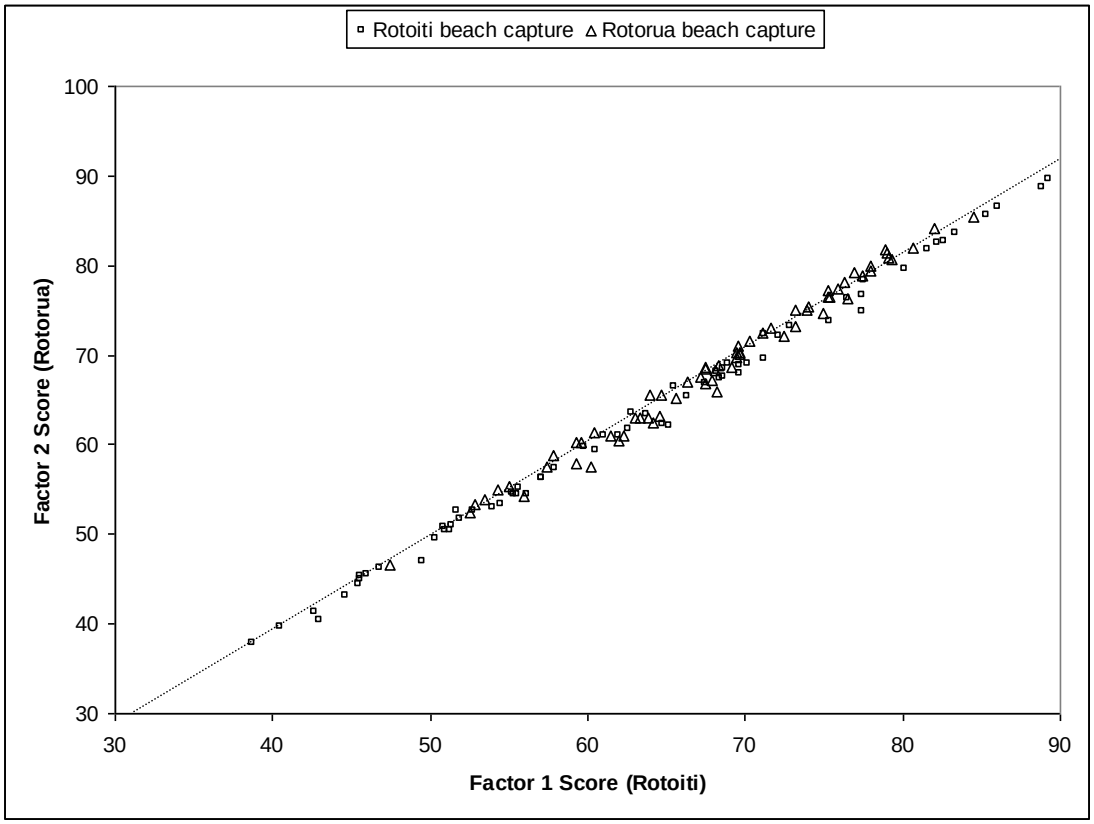

Figure 3.2: Scatterplot of the classification function scores of common smelt edge spots from LA-ICP-MS data calculated from a DFA using (Mn, Zn, Rb, Sr and Ba concentrations.

The canonical scores were calculated for lake DFA (Equation 3.2) and beach DFA (Equation 3.3). The spatial separation was illustrated in a histogram for the lake DFA (Figure 3.3) and a scatterplot for the stream DFA (Figure 3.4).

Equation Equation developed from smelt edge Lake DFA unstandardised coefficients to calculate canonical score.

Unstandardised root 1 = -5.139 + (0.011 x Mn) – (0.024 x Zn) + (1.312 x Rb) + (0.007 x Sr) – (0.111 x Ba)

Equation 3.3: Equation developed from smelt edge spot DFA analysis using unstandardised values to create canonical score 1 and canonical score 2 to separate individuals smelt to beach of capture.

Unstandardised root 1canonical score = -6.504 - (0.144 × Mn) + (0.001 × Zn) + (4.403 × Rb) + (0.005 × Sr) - (0.043 × Ba)

Unstandardised root 2canonical score = 1.831 – (0.001 ×Mn) + (0.030 × Zn) + (1.430 × Rb) – (0.006 × Sr) + (0.130 × Ba)

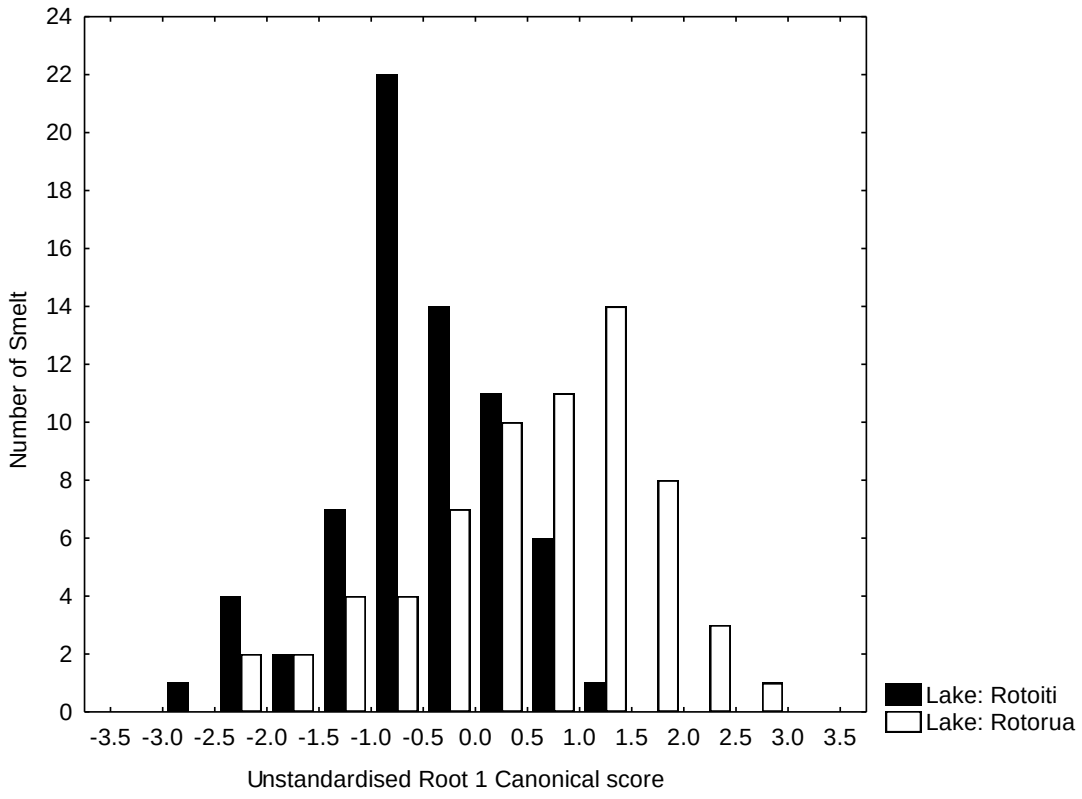

Figure 3.3: Canonical scores for smelt otolith edges. Values calculated using the unstandardised coefficients from the DFA using untransformed Mn, Zn, Rb, Sr and Ba elemental concentrations at the otolith edge.

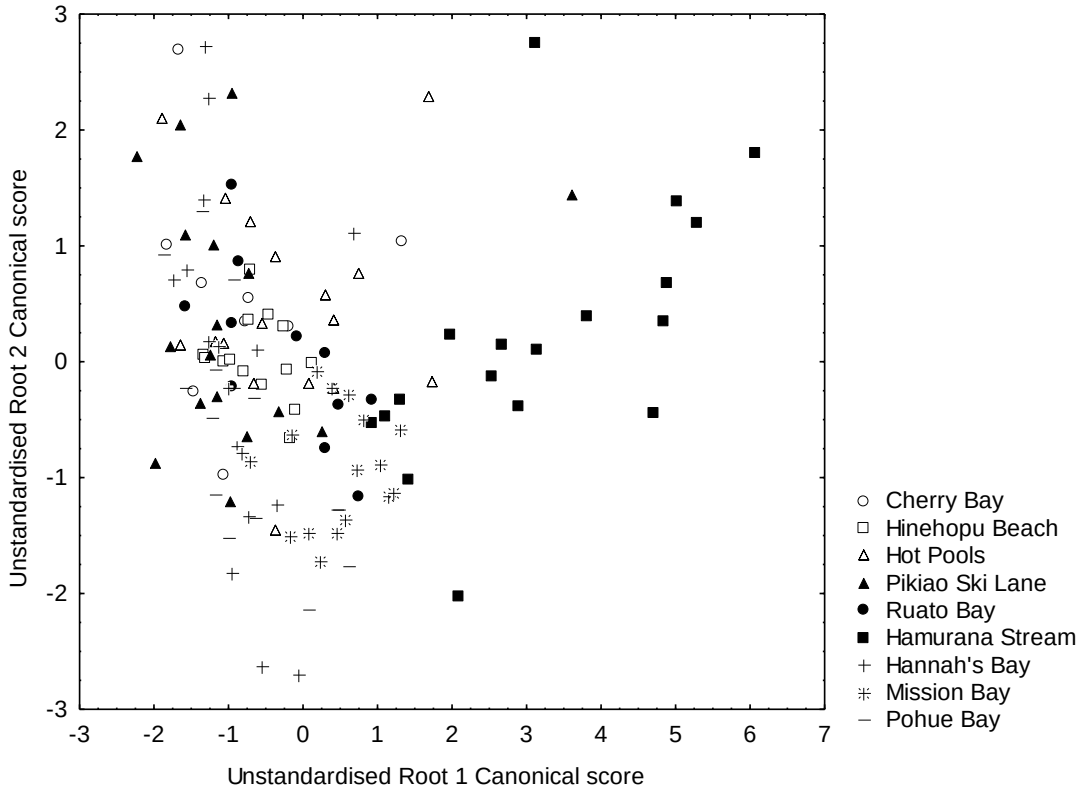

Figure 3.4: Scatterplot of unstandardised canonical root 1 and unstandardised root 2 for common smelt otolith edge values calculated using equation 3.2

The Wilcoxon paired test indicated the concentrations of Mn, Rb, Sr and Ba ($P < 0.001$) are significantly different between the nucleus and edge laser ablation spots on the smelt otoliths. The concentration of Zn was not significantly different ($P = 0.093$).

The concentrations of Mn, Zn, Rb and Ba were significantly correlated with fork length ($P = <0.001$). The concentration of Sr was not significantly correlated with fork length in linear regression ($P = 0.144$).

3.3. Common smelt nucleus

A summary of the mean elemental concentration at the nuclei of otoliths from each of the beach locations is presented in Table 3.11. Hamurana Beach and Mission Bay smelt stand out because of the greater elemental concentrations of Rb and Sr respectively.

Table 3.11: Summary of the mean fork length and elemental concentrations at smelt nucleus spots analysed by LA-ICP-MS.

Location	N Smelt	Fork length (mm)	Mn	Zn	Rb	Sr	Ba
Lake Rotoiti							
Cherry Bay	9	41	4.26	29.56	0.60	1142	46.28
Hinehopu Beach	18	51	3.09	6.67	0.61	1141	36.36
Hot pools Beach	17	43	4.03	7.00	0.77	1130	37.63
Pikiao ski lane	16	41	4.92	14.64	0.62	1127	39.48
Ruato Bay	12	42	4.74	5.71	0.45	1141	45.32
Means summary	14	44	4.21	12.72	0.61	1136	41.01
Lake Rotorua							
Hamurana Beach	16	68	3.19	4.98	1.65	1172	39.79
Hannah's Bay	17	50	4.63	10.24	0.50	1186	45.86
Mission Bay	17	62	2.83	9.35	0.66	1247	36.63
Pohue Bay	16	48	3.38	6.41	0.46	1114	39.30
Means summary	17	57	3.51	7.75	0.82	1180	40.40

The concentration of Sr ($P = 0.001$) was significantly different between lake groups. The concentrations of, Mn ($P = 0.037$), Rb ($P < 0.001$) and Sr ($P < 0.001$) differed significantly between beach groups. The Ba concentration ($P = 0.053$) is right on the threshold of significance. The specific site differences are illustrated in multiple comparison of mean rank post-hoc test (Table 3.12).

Table 3.12: Comparison of multiple mean rank post-hoc test illustrating the difference in smelt nucleus concentration of Rb and Sr from the different capture locations. Significant values ($P < 0.05$) are in bold and italicised.

Rb	(1)	(2)	(3)	(4)	(5)	(6)	(7)	(8)	(9)
Cherry Bay (1)		1.000	1.000	1.000	1.000	0.079	1.000	1.000	1.000
Hinehopu Beach (2)	1.000		1.000	1.000	1.000	***0.006***	0.572	1.000	1.000
Hot pools Beach (3)	1.000	1.000		1.000	***0.040***	0.787	***0.005***	1.000	***0.018***
Pikiao ski lane (4)	1.000	1.000	1.000		1.000	***0.022***	0.376	1.000	0.864
Ruato Bay (5)	1.000	1.000	***0.040***	1.000		***< 0.001***	1.000	0.518	1.000
Hamurana Stream (6)	0.079	***0.006***	0.787	***0.022***	***< 0.001***		***< 0.001***	0.055	***< 0.001***
Hannah's Bay (7)	1.000	0.572	***0.005***	0.376	1.000	***< 0.001***		0.126	1.000
Mission Bay (8)	1.000	1.000	1.000	1.000	0.518	0.055	0.126		0.331
Pohue Bay (9)	1.000	1.000	***0.018***	0.864	1.000	***< 0.001***	1.000	0.331	

Sr	(1)	(2)	(3)	(4)	(5)	(6)	(7)	(8)	(9)
Cherry Bay (1)		1.000	1.000	1.000	1.000	1.000	1.000	***0.125***	1.000
Hinehopu Beach (2)	1.000		1.000	1.000	1.000	1.000	1.000	***0.017***	1.000
Hot pools Beach (3)	1.000	1.000		1.000	1.000	1.000	1.000	***0.007***	1.000
Pikiao ski lane (4)	1.000	1.000	1.000		1.000	1.000	0.591	***0.002***	1.000
Ruato Bay (5)	1.000	1.000	1.000	1.000		1.000	1.000	***0.046***	1.000
Hamurana Stream (6)	1.000	1.000	1.000	1.000	1.000		1.000	1.000	0.648
Hannah's Bay (7)	1.000	1.000	1.000	0.591	1.000	1.000		1.000	0.170
Mission Bay (8)	0.125	***0.017***	***0.007***	***0.002***	***0.046***	1.000	1.000		***<0.001***
Pohue Bay (9)	1.000	1.000	1.000	1.000	1.000	0.648	0.170	***<0.001***	

The correlation matrix for smelt nucleus otolith concentrations (Table 3.13) show positive correlations for the elemental concentrations of Mn and Ba and, Sr and Ba. These positive correlations were observed at the otolith edge and in the water samples.

Table 3.13: Spearman rank order correlation matrix indicating the correlation between elements at the nucleus of common smelt otoliths collected in Lake Rotorua and Lake Rotoiti. Significant correlations ($P < 0.05$) are in bold and italicised.

	Mn	Zn	Rb	Sr	Ba
Mn	1.00	0.02	-0.02	0.13	***0.36***
Zn	0.02	1.00	-0.11	0.08	0.02
Rb	-0.02	-0.11	1.00	0.03	-0.08
Sr	0.13	0.08	0.03	1.00	***0.26***
Ba	***0.36***	0.02	-0.08	***0.26***	1.00

The elemental data obtained from the nuclei of common smelt was investigated using multivariate DFA. The smelt classified 70% correctly by lake (Table 3.14) and 38% correctly by beach of capture (Table 3.15).

Table 3.14: The classification matrix from DFA grouping individuals by lake. The concentration of five elements (Mn, Zn, Rb, Sr and Ba) was used to classify the nucleus of smelt otoliths. Rows represent observed classifications and columns represent predicted classifications.

	Percent correct	Rotoiti	Rotorua
Rotoiti	79	57	15
Rotorua	59	27	39
Total	70	84	54

Table 3.15: The classification matrix from DFA grouping individuals by beach. The concentration of five elements (Mn, Zn, Rb, Sr and Ba) was used to classify the nucleus of smelt otoliths. Rows represent observed classification and columns represent predicted classifications.

	Percent correct	(1)	(2)	(3)	(4)	(5)	(6)	(7)	(8)	(9)
Cherry Bay (1)	11	1	3	0	1	0	0	2	0	2
Hinehoopu Beach (2)	44	0	8	0	3	0	0	2	3	2
Hot pools Beach (3)	24	0	4	4	4	1	1	0	2	1
Pikiao ski lane (4)	38	1	1	3	6	0	0	3	0	2
Ruato Bay (5)	8	0	1	0	3	1	0	3	0	4
Hamurana Stream (6)	69	0	0	0	0	0	11	0	4	1
Hannah's Bay (7)	24	0	2	0	2	2	1	4	3	3
Mission Bay (8)	71	0	3	1	0	0	0	1	12	0
Pohue Bay (9)	31	0	5	0	0	3	0	2	1	5
Total	38	2	27	8	19	7	13	17	25	20

The classification functions from the lake DFA were used to produce Equation 3.3 which was used to calculate two lake classification scores, based on the five elemental concentrations at the nucleus of the otolith. The classification function gives an indication of the lake each individual classifies as, based on the otolith elemental signature at the nucleus (Figure 3.4).

Equation 3.3: Classification functions from smelt nucleus DFA grouping individuals by lake of capture.

Factor Score 1 (Rotoiti) = -116.449 + (0.340 x Mn) + (0.007 x Zn) + (5.299 x Rb) + (0.201 x Sr) – (0.041 x Ba)

Factor Score 2 (Rotorua) = -126.774 + (0.194 x Mn) – (0.002 x Zn) + (6.258 x Rb) + (0.210 x Sr) – (0.043 x Ba)

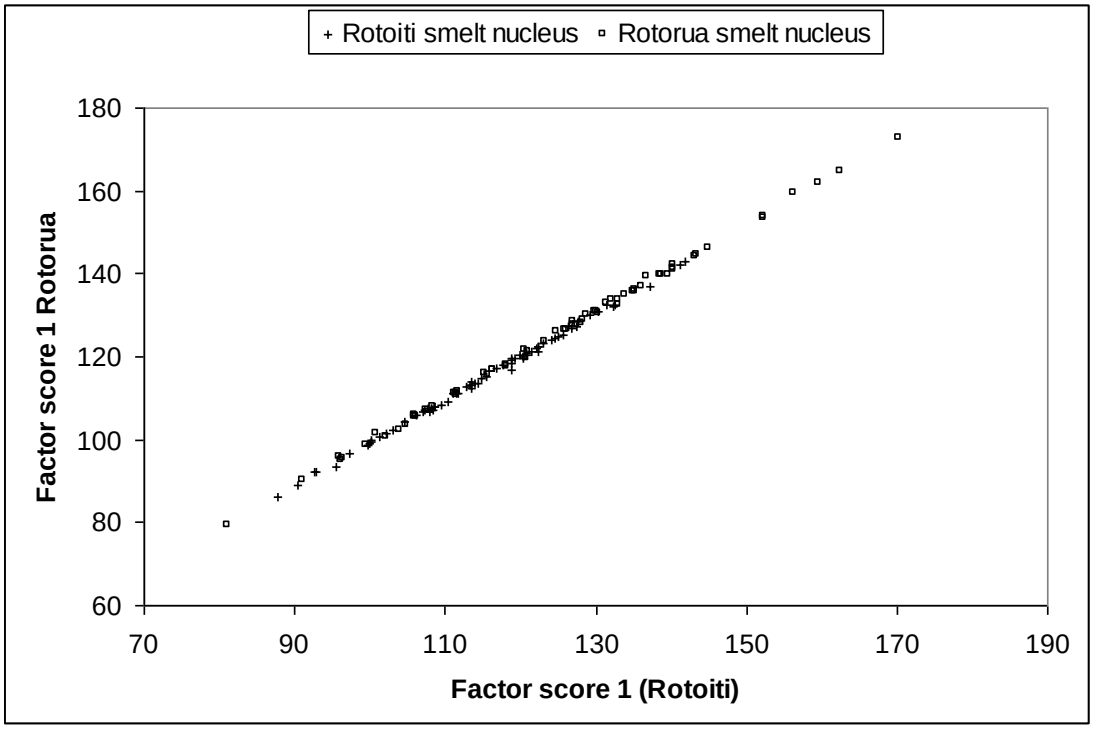

Figure 3.5: Classification scores of common smelt nucleus calculated from equation 3.3 classifying individuals to lake of origin

The unstandardised canonical coefficients from the lake DFA were used to create equation 3.4 which calculates the canonical score for each individual fish and gives an indication of the separation between the lakes. (Figure 3.6)

Equation 3.4: The unstandardised coefficients from the DFA grouping smelt nucleus elemental concentrations (Mn, Zn, Rb, Sr and Ba) to Lake.

Unstandardised root 1 = -12.136 – (0.173 x Mn) – (0.011 x Zn) + 1.139 x Rb) + (0.011x Sr) – (0.002 x Ba)

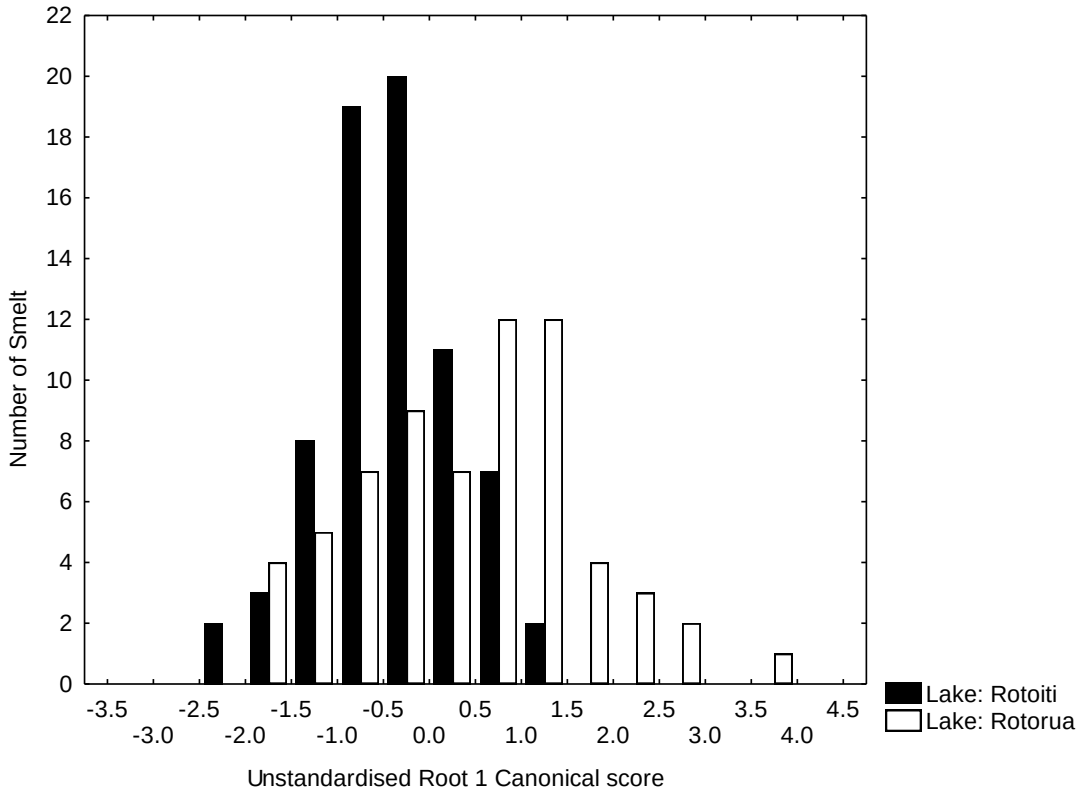

Figure 3.6: Histogram of common smelt canonical score calculated using unstandardised root 1 and the concentration of Mn, Zn, Rb Sr and Ba at the nucleus of each otolith indicating the lake of origin.

. To investigate the population dynamics regarding resident and migratory smelt the nucleus smelt values were compared with the edge laser ablation spots (Table 3.16). The nucleus spot was also compared with the known location of

capture (Table 3.17) to investigate the relative percentages of resident fish defined as occupying the same lake, and migratory fish, defined as individuals with a classification score from each of the lakes at either the nucleus or edge spot.

Table 3.16: Classification of migratory and resident classes of common smelt in Lake Rotorua and Lake Rotoiti based on the classification cases from DFA for lakes at otolith nucleus and edge spot.

Otolith nucleus signal	Otolith edge signal	Classification	*N* individuals	Percent classification
Rotorua	Rotoiti	Migratory	16	14
Rotoiti	Rotorua	Migratory	15	13
Rotorua	Rotorua	Resident	33	29
Rotoiti	Rotoiti	Resident	49	43
Total			113	100

Table 3.17: Classification of migratory and resident classes of common smelt in Lake Rotorua and Lake Rotoiti based on the classification cases from DFA for lakes at otolith nucleus and edge spot.

Otolith nucelus signal	Known edge location	Classification	*N* individuals	Percent classification
Rotorua	Rotoiti	Migratory	16	14
Rotoiti	Rotorua	Migratory	20	18
Rotorua	Rotorua	Resident	36	32
Rotoiti	Rotoiti	Resident	41	36
Total			113	100

4. Discussion

4.1. Water samples

The isotopic concentration of the water samples grouped by lake and by beach differed significantly. The significant differences suggest the movement of smelt within lakes and between lakes may be reflected in the chemistry of the otoliths.

DFA was used to classify lake water samples with 93% accuracy and beach water samples with 64% accuracy. These results suggest there are differences in the isotopic composition unique to the water at beach sites around Lake Rotorua and Lake Rotoiti and between the lakes. The ambient water concentration has a major influence on the otolith chemical composition, and the differences illustrated in the water samples suggest that the differences may also be illustrated in the otolith chemical composition.

The spearman rank order correlation matrix for water samples showed significant correlations between the concentrations of isotopes in the beach water samples. The ^{88}Sr concentration is positively correlated with the ^{43}Ca concentration in the water. Calcium is a major constituent of the otolith matrix (Campana, 1999). The positive correlation between ^{88}Sr and ^{43}Ca indicates a linear relationship between the isotopes. The incorporation of Sr into the otolith is as a substitute for Ca in the otolith matrix (Arai and Hirata, 2006). If the values of Sr and Ca increase proportionally in the water there is presumably less chance for substitution unless the internal free calcium concentration is modified physiologically.

The differentiation between the beach water samples is not as definitive as the values for tributary streams. The water analysis has indicated some differences between lakes and between beaches. The microchemistry of smelt otolith may show

local migration within each of the lakes or migration between the two lakes, relative to the chemical differences in the water.

4.2. Smelt edge

The laser ablation spot at the edge of the otolith is assumed to represent the chemical environment occupied directly prior to the capture of the individual (Chittaro et al., 2006). DFA analysis was used to classify the smelt edge concentrations to beach of capture with 43% accuracy and lake of capture with 74% accuracy. The discrimination between beach locations is not very accurate and this may be a reflection of similar chemical conditions experienced by the common smelt. The ambient water concentration is not represented proportionally in the concentration of the otolith. Physiological factors may modify the concentration of trace elements in the otolith. The fork length of the smelt influenced the elemental composition of the otolith edge spot.

The laser spot diameter of 50 µm may have influenced the LA-ICP-MS results. The 50 µm spot size was selected to maximise isotopic counts during analysis, but it may have liberated otolith material from the matrix over a time period greater than the period the smelt had occupied the beach. This may have influenced the accuracy of the investigation.

The Wilcoxon matched pairs test shows significant differences between the concentrations at the otolith nucleus and otolith edge from the same common smelt. This result suggests one of two things. The first is that the smelt has migrated or occupied water bodies that have differed significantly in chemical concentration, or there are differences in the chemistry of the nucleus and edge of the otolith, related to physiological or ontogenetic factors. When investigating the migration of fishes the

individuals can be classified as either migrants or residents (Elsdon and Gillanders, 2006). A significant difference between a spot at the otolith nucleus, and a spot at the otolith edge, analysed by LA-ICP-MS suggests that the external chemical concentration has influenced the endolymph and the otolith subsequently reflects the chemical change. The potential influence of ontogenetic factors is also important to consider as elevated levels of Mn, Mg and Ba have been observed at the nucleus of the otolith relative to the external concentrations (Ruttenberg et al., 2005). The significant difference between Mn and Ba nucleus and edge values was observed in the smelt otoliths. Additionally, the elemental concentrations of Rb and Sr differ between the core and edge values of the otoliths. These concentrations were influenced by smelt fork length, which was included to represent otolith size.

Two different classes of resident and migratory fish were represented in the data. This may suggest that the difference in otolith chemistry is an indication of migration. There are otoliths that have different nucleus classifications from edge classifications which represents a migrating fish. The majority of the smelt have a classification from the same lake at the otolith nucleus and edge. To investigate the influence of ontogenetic factors on the chemistry of smelt otoliths the study of a lake locked population of smelt may offer information about the change in otolith chemistry relative to life stage. The lake locked population of common smelt would presumably experience the same conditions so any differences between the nucleus and edge would suggest the physiology of this influencing the otolith microchemistry.

The investigation comparing the different otolith spots suggests that some smelt are using the Ohau Channel for migration and the majority are not. To investigate the migration of the smelt a line transect or series of spots is likely to give

better information specific to daily time scales as compared with a two spot comparison (Sanborn and Telmer, 2003).

4.3. Smelt nucleus

The otolith nucleus is the first calcified tissue in a fish (Secor et al., 1991). The otolith is regarded as a natural tag and indicator of nursery chemical habitat because of the potential for elements from the nursery area to be retained at the core of the nucleus.

The elemental concentration of Sr from smelt otolith nuclei differed significantly between lakes. The beach capture locations differed significantly in the levels of Mn, Rb, Sr and Ba. Post-hoc analysis indicated significant differences between the concentration of Rb at Hamurana Stream, which differed significantly with the other beach locations and in the concentration of Sr at Mission Bay where the concentrations at differed significantly with a range of other beach locations. The relationship between fork length and otolith elemental concentration was investigated using linear regression.

Elements at the nucleus of common smelt otoliths showed some similar correlation relationships to the water chemistry. The correlation between Sr and Ba concentration is significant at the otolith nuclei spot for common smelt. A proposed reason for the positive correlation between the Sr and Ba concentrations is that the incorporation of Sr into the aragonite calcium carbonate of the otolith facilitates the uptake of the Ba. The Sr uptake is suggested to alter the configuration of the aragonite in the otolith facilitating a larger uptake of Ba from the environment provided it is available to crystallise onto the otolith if it is present in the endolymph

fluid (De Vries et al., 2005). The water samples have positive Ba and Sr isotopic correlation. The correlation between Ba and Mn is also significant in the nuclei of smelt from both lakes. The significant correlation may be related physiological processes in the otolith. The elevated levels of Mn, that have been used as a chemical indication that the nucleus of the otolith has been sampled by laser ablation, been observed at the nucleus of other species of fish otoliths have been accompanied by an elevated level of Ba (Ruttenberg et al., 2005).

DFA classified common smelt to lake of origin with 68% accuracy and beach of origin with 38% accuracy. This shows a large number of misclassifications based on the elemental otolith values at the nuclei of smelt. The discrimination between the water samples grouped by lake is not perfectly reflected in the otolith nucleus data. The smelt populations may be discriminated by the chemical concentration of the five elements (Mn, Zn, Rb, Sr and Ba) between lakes. The lack of differentiation between smelt nuclei at a beach level may be an indication of the smelt populations from the two lakes not having discrete spawning fidelity or the spawning habitats not having unique water 'fingerprints' although the water samples indicated some separation at beach level..

The water samples had ^{24}Mg an extra isotope to distinguish between groups. The concentration of Mg at the otolith has not increased the resolution power of the DFA. The incorporation of Mg, as with other elements to the otolith may be regulated physiologically; hence the difference in the water chemistry is not always mirrored in the microchemistry of the otolith. The relationship between the otolith and the ambient chemistry suggests the otolith is influenced by external chemistry but the relationship is not proportional and may be altered by a range of factors in the otolith. The isotopic concentration of ^{43}Ca was also a good distinguishing variable in

the water. The concentration of Ca is not included to discriminate the otoliths because the otolith is composed of a large percentage of Calcium and it was used as the internal standard to quantify the concentrations of the other elements at the otolith nucleus.

Common smelt nucleus elemental concentration values classified smelt to the beach of capture with 38% accuracy. The two beach locations with the greatest percent correct classification are Hamurana Stream (69% correct) and Mission Bay (71% correct), which demonstrated significant differences in otolith chemistry of Rb and Sr respectively. The apparent factor driving this discrimination is not a local factor influencing the water and otoliths but seems to be size-related, as the concentrations of Rb and Sr increased proportionally with fork length.

Common smelt are both lacustrine and migratory fish; there is the potential for common smelt to migrate between lakes Rotorua and Rotoiti through the Ohau Channel. The relative lack of differentiation between the otolith nuclei may be a reflection of the lack of water chemistry differences although DFA does classify the lakes with reasonable accuracy. The lack of classification accuracy at the smelt nucleus means the results need to be interpreted with caution. The nucleus values are used to classify the lake of origin of the common smelt, the degree of classification between the two lakes is not as great as hoped. The use of a smaller LA-ICP-MS spot may increase the resolution of the nucleus signal, provided sufficient accuracy of ICP-MS counts can be obtained.

The classification cases calculated from smelt otolith nucleus and edge data suggest four different classes of smelt live in Lake Rotoiti and Lake Rotorua. The groups are; individuals that have migrated from Lake Rotorua to Lake Rotoiti, individuals that have migrated from Lake Rotoiti to Lake Rotorua, individuals that

have stayed in Lake Rotoiti and individuals that have stayed in Lake Rotorua. The nucleus values and edge values were compared to classify the fish into one of the four categories. The fish were again classified using the nucleus classification as the Lake of origin and this was compared with the known capture location. The percentages between the two samples reported similar results with approximately 30% of individuals migrating between lakes while the remaining 70% of common smelt appear to be resident fish. The Ohau Channel appears to be a migration link for approximately 30% of the common smelt. The Ohau Channel diversion wall may impede the movement of these fish between lakes Rotorua and Rotoiti.

Chapter 4 General Conclusion

1. Conclusion

The water samples collected from the tributary stream and beach locations of lakes Rotoiti and Rotorua differed significantly in the concentration of a range of isotopes. The ambient water chemical concentration influences the otolith chemical composition; therefore the different isotopic concentrations observed in the water samples suggest good differentiation between the tributary stream waters and between the lake groups. The differences in water chemistry were reflected by different compositions of the otolith. The relationship between water and otolith is not proportional but the otolith signatures illustrate unique elemental signatures for the different spawning sites.

The results from this study show that juvenile rainbow trout otolith signatures are unique to each lake and tributary stream sampled. The square-root transformed elemental concentrations (Mn, Zn, Rb, Sr and Ba) collected from the juvenile trout otolith nuclei; using LA-ICP-MS analysis classified the juvenile rainbow trout to lake with 98% accuracy and to tributary stream with 91% accuracy. The classification functions from the juvenile trout analysis were used to investigate the natal lake and tributary stream of wild adult rainbow trout. This study shows approximately 89% of adult wild rainbow trout collected from Lake Rotorua, Lake Rotoiti and the Ohau Channel spawned in a Lake Rotorua tributary stream. The relative contribution of the spawning stream to each of the three collection sites differed. Waingaehe Stream was

the major spawning stream for adults collected in Lake Rotorua with 50% of adults originating there. Waiteti Stream (35%) was the major spawning tributary for adult rainbow trout collected in Lake Rotoiti, and some spawning occurred in the Lake Rotoiti tributary Te Toroa Stream (23%). Utuhina Stream (35%) was the greatest contributor to the adult trout collected in the Ohau Channel; all trout of unknown origin collected in the Ohau Channel were classified to a Lake Rotorua tributary. The Ohau Channel is likely to provide passage for rainbow trout migration between lakes Rotorua and Rotoiti. The Ohau Channel is the major outflow of Lake Rotorua and the major inflow of Lake Rotoiti, linking the two lakes. The diversion wall being built at the Rotoiti end of the Ohau Channel is likely to impede the movement of the rainbow trout stocks between the two lakes.

The results from the common smelt otolith signatures at the core and edge indicate differences between the nucleus spot, representative of hatching and edge spot which is representative of capture location. The classification of water samples and otolith signatures was not as powerful as for the juvenile rainbow trout DFA. Some relationships have been identified by using the common smelt otoliths. The significant difference in the concentrations of elemental Mn, Rb, Sr and Ba between the core and edge of 113 smelt indicate that smelt populations are both migratory and resident in broad terms of fish movement. The larger proportion, approximately 70% of smelt appear to be resident in either of the lakes, and 30% of smelt appear to be migrating between lakes. The result was similar when edge values were calculated using the classification functions from smelt edge spot DFA grouping individuals by lake was compared with the actual location of capture. The results need to be interpreted with caution as the discrimination between lakes at the nucleus of common smelt accurately classified 70% of smelt. There is the potential for the

physiology of the fish to influence the otolith chemistry data. The signatures compared are from two different life stages, which may correspond to different otolith chemistries inherently. The elemental concentrations at the nucleus and edge appear to be influenced by fish size indicated by fork length. The effect of life history stage on the smelt otolith may be assessed in a closed lake where smelt are unable to migrate between different water masses. These data suggest that common smelt from Lake Rotorua and Lake Rotoiti also use the Ohau Channel as a migratory link between the two lakes. The populations appear to be mixed and the Ohau diversion wall is likely to impede the migration of approximately 30% of the common smelt populations of Lake Rotorua and Lake Rotoiti.

Reference List

Arai T, Hirata T 2006. Determination of trace elements in otoliths of chum salmon *Oncorhynchus keta* by laser ablation-ICP-mass spectrometry. Fisheries Science 72: 977-984.

Bath GE, Thorrold SR, Jones CM, Campana SE, McLaren JW, Lam JWH 2000. Strontium and Barium uptake in aragonitic otoliths of marine fish. Geochimica et Cosmochimica Acta. 64(10): 1705-1714.

Begg GA, Campana SE, Fowler AJ, Suthers IM 2005. Otolith research and application: current directions in innovation and implementation. Marine and Freshwater Research 56: 477-483.

Borelli G, Mayer-Gostan N, De Pontual H, Boeuf G, Payan P 2001. Biochemical Relationships Between Endolymph and Otolith Matrix in the Trout (*Oncorhynchus mykiss*) and Turbot (*Psetta maxima*). Calcified Tissue International 69: 356-364.

Borelli G, Mayer-Gostan N, Merle PL, De Pontual H, Boeuf G, Allemand D, Payan P 2003. Composition of Biomineral Organic Matrices with Special Emphasis on Turbot (*Pseyya maxima)* Otolith and Endolymph. Calcified Tissue International 72: 717-725.

Brophy D, Danilowicz BS, Jeffries TE 2003. The detection of elements in larval otoliths from Atlantic herring using laser ablation ICP-MS. Journal of Fish Biology 63: 990-1007.

Brophy D, Jeffries TE, Danilowicz BS 2004. Elevated manganese concentrations at the core of clupeid otoliths: possible environmental, physiological, or structural origins. Marine Biology 144: 779-786.

Buckel JA, Sharack BL, Zdanowicz VS 2004. Effect of diet on otolith composition in *Pomatomus saltatrix*, an estuarine pscivore. Journal of Fish Biology 64: 1469-1484.

Burns N, McIntosh J, Scholes P 2005. Strategies for Managing the Lakes f the Rotorua District, New Zealand. Lake and Reservoir Management 21(1): 61-72.

Campana SE 1999. Chemistry and composition of fish otoliths: pathways, mechanisms and applications. Marine Ecology Progress Series 188: 263-297.

Campana SE, Neilson JD 1985. Microstructure of Fish Otoliths. Canadian Journal of Fisheries and Aquatic Sciences 42: 1014-1032.

Campana SE, Thorrold SR 2001. Otoliths, increments, and elements: keys to a comprehensive understanding of fish populations? Canadian Journal of Fisheries and Aquatic Sciences 58: 30-38.

Chen LS, Yan HY 2002. The Relative Distribution of Otoliths as a Means of Larval Fish identification. Zoological Studies 41(2): 144-152.

Chen Z 1999. Inter-element fractionation and correction in laser ablation inductively coupled plasma mass spectrometry. Journal of Analytical Atomic Spectrometry 14: 1823-1828.

Chittaro PM, Fryer BJ, Sale PF 2004. Discrimination of French grunts (*Haemulon flavolineatum*, Desmarest, 1823) from mangrove and coral reef habitats using otolith microchemistry. Journal of Experimental Marine Biology and Ecology 308: 169-183.

Chittaro PM, Gagnon J, Fryer BJ 2006. The differentiation of *Stegastes partitus* populations using lapillar and sagittal otolith chemistry. Journal of Fish Biology 68: 1909-1917.

Clarke AD, Telmer KH, Mark Shrimpton J 2007. Elemental analysis of otoliths, fin rays and scales: a comparison of bony structures to provide population and life-history information for the Artic grayling (*Thymallus articus*). Ecology of Freshwater Fish: 1-8.

Clarke LM, Friedland KD 2004. Influence of growth and temperature on strontium deposition in the otoliths of Atlantic Salmon. Journal of Fish Biology 64: 744-759.

Crook DA, MacDonald JI, O'Connor JP, Barry B 2006. Use of otolith chemistry to examine patterns of diadromy in the threatened Australian grayling *Prototroctes maraena*. Journal of Fish Biology 69: 1330-1344.

De Vries MC, Gillanders BM, Elsdon TS 2005. Facilitation of barium uptake into fish otoliths: Influence of strontium concentration and salinity. Geochimica et Cosmochimica Acta. 69(16): 4061-4072.

Elsdon TS, Gillanders BM 2002. Interactive effects of temperature and salinity on otolith chemistry: challenges for determining environmental histories of fish. Canadian Journal of Fisheries and Aquatic Sciences 59: 1796-1808.

Elsdon TS, Gillanders BM 2004. Fish otolith chemistry influenced by exposure to multiple environmental variables. Journal of Experimental Marine Biology and Ecology 313: 269-284.

Elsdon TS, Gillanders BM 2005a. Consistency of patterns between laboratory experiments and field collected fish in otolith chemistry: an example and applications for salinity reconstructions. Marine and Freshwater Research 56: 609-617.

Elsdon TS, Gillanders BM 2005b. Alternative life-history patterns of estuarine fish: barium in otoliths elucidates freshwater residency. Canadian Journal of Fisheries and Aquatic Sciences 62: 1143-1152.

Elsdon TS, Gillanders BM 2006. Identifying migratory contingents of fish by combining otolith Sr:Ca with temporal collections of ambient Sr:Ca concentrations. Journal of Fish Biology 69: 643-657.

Farrell J, Campana SE 1996. Regulation of calcium and strontium deposition on the otoliths of juvenile tilapia, *Oreochromis niloticus*. Comparative Biochemistry and Physiology Part A: Physiology 115(2): 103-109.

Fowler AJ, Campana SE, Jones CM, Thorrold SR 1995. Experimental assessment of the effect of temperature and salinity on the elemental composition of otoliths using solution-based ICPMS. Canadian Journal of Fisheries and Aquatic Sciences 52: 1421-1430.

Gall GAE, Crandell PA 1992. The rainbow trout. Aquaculture 100: 1-10.

Gallahar NK, Kingsford MJ 1996. Elements in otoliths may elucidate the contribution of estuarine recruitment to sustaining coastal reef populations of a temperate reef fish. Marine Ecology Progress Series 141: 13-20.

Gemperline PJ, Rulifson RA, Paramore L 2002. Multi-way analysis of trace elements in fish otoliths to track migratory patterns. Chemometrices and Intelligent Laboratory Systems 60: 135-146.

Guido P, Omori M, Katayama S, Kimura K 2004. Classification of juvenile rockfish, *Sebastes inermis*, to *Zostera* and *Sargassum* beds, using the macrostructure and chemistry of otoliths. Marine Biology 145: 1243-1255.

Hamer PA, Jenkins GP, Coutin P 2006. Barium variation in *Pagrus auratus* (Sparidae) otoliths: A potential indicator of migration between an embayment

and ocean waters in south-eastern Australia. Estuarine, Coastal and Shelf Science 68: 686-702.

Hoff GR, Fuiman LA 1995. Environmentally induced variation in elemental composition of red drum (*Sciaenops ocellatus*) otoliths. Bulletin of Marine Science 56: 578-591.

Jolly VH 1967. Observations on the smelt *Retropinna lacustris* Stokell. New Zealand Journal of Science 10: 330-355.

Kalish JM 1989. Otolith microchemistry: validation of the effects of physiology, age and environment on otolith composition. Journal of Experimental Marine Biology and Ecology 132: 151-178.

Kraus RT, Secor DH 2004. Incorporation of strontium into otoliths of an estuarine fish. Journal of Experimental Marine Biology and Ecology 302: 85-106.

Lamson HM, Shiao J-C, Iizuka Y, Tzeng W-N, Cairns DK 2006. Movement patterns of American eels (*Anguilla rostrata*) between salt- and freshwater in a coastal watershed, based on otolith microchemistry. Marine Biology 149: 1567-1576.

Limburg KE 1995. Otolith strontium traces environmental history of subyearling American shad *Alosa sapidissima*. Marine Ecology Progress Series 119: 25-35.

Lo-Yat A, Meekan M, Munksgaard N, Parry D, Serge P, Wolter M, Carleton J 2005. Small-scale spatial variation in the elemental composition of otoliths of *Stegastes nigricans* (Pomacentridae) in French Polynesia. Coral Reefs 24: 646-653.

Lucas MC, Baras E 2000. Methods for studying spatial behaviours of freshwater fishes in the natural environment. Fish and Fisheries 1: 283-316.

May TW, Wiedmeyer RH 1998. A Table of Polyatomic Interferences in ICP-MS. Atomic Spectroscopy 19(5): 150-155.

McDowall B 1984. Trout in New Zealand Waters. Wellington, New Zealand, The wetland press. 120 p.

McDowall RM 1978. New Zealand freshwater fishes. A natural history and guide. Auckland, New Zealand, Octopus Publishing Group (NZ) Ltd. 553 p.

Miller MB, Clough AM, Batson JN, Vachet RW 2006. Transition metal binding to cod otolith proteins. Journal of Experimental Marine Biology and Ecology 329: 135-143.

Milton DA, Chenery SR 2001. Sources and uptake of trace metals in otoliths of juvenile barramundi (*Lates calcarifer*). Journal of Experimental Marine Biology and Ecology 264: 47-65.

Milton DA, Chenery SR, Farmer MJ, Blaber SJM 1997. Identifying the spawning estuaries of the tropical shad, terubok *Tenualosa toli*, using otolith microchemistry. Marine Ecology Progress Series 153: 283-291.

Morris Jr. JA, Rulifson RA, Toburen LH 2003. Life history strategies of striped bass, *Morone saxatilis*, populations inferred from otolith microchemistry. Fisheries Research 62: 53-63.

Munro AR, McMahon TE, Ruzycki JR 2005. Natural chemical markers identify source and date of introduction of an exotic species: lake trout (*Salvelinus namaycush*) in Yellowstone Lake. Canadian Journal of Fisheries and Aquatic Sciences 62: 79-87.

Payan P, Edeyer A, De Pontual H, Borelli G, Boeuf G, Mayer-Gostan N 1999. Chemical composition of saccular endolymph and otolith in fish inner ear:

lack of spatial uniformity. American Journal of Physiology-Regulatory Integrative and Comparative Physiology 277(1): R123-R131.

Payan P, Borelli G, Priouzeau F, De Pontual H, Boeuf G, Mayer-Gostan N 2002. Otolith growth in trout *Oncorhynchus mykiss*: supply of Ca2+ and Sr2+ to the saccular endolymph. The Journal of Experimental Biology 205: 2687-2695.

Pearce NJGP, W.T., Westgate JA, Gorton MP, Jackson SE, Neal CR, Chenery SP 1997. A compilation of new and published major and trace element data for NIST SRM 610 and NIST SRM 612 glass reference materials. Geostandards and Geoanalytical Reserch 21(1): 115-144.

Popper AN, Ramcharitar J, Campana SE 2005. Why otoliths? Insights from inner ear physiology and fisheries biology. Marine and Freshwater Research 56: 497-504.

Ruttenberg BI, Hamilton SL, Hickford MJH, Paradis GL, Sheehy MS, Standish JD, Ben-Tzvi O, Warner RR 2005. Elevated levels of trace elements in cores of otoliths and their potential for use as natural tags. 297: 273-281.

Sanborn M, Telmer K 2003. The spatial resolution of LA-ICP-MS line scans across heterogeneous materials such as fish otoliths and zoned minerals. Journal of Analytical Atomic Spectrometry 18: 1231-1237.

Sanchez-Jerez P, Gillanders BM, Kingsford MJ 2002. Spatial variability of trace elements in fish otoliths: comparison with dietary items and habitat constituents in seagrass meadows. Journal of Fish Biology 61: 801-821.

Scott D, Poynter M 1991. Upper temperature limits for trout in New Zealand and climate change. Hydrobiologia 222: 147-151.

Secor DH, Dean JM, Laban EH 1991. Manual for Otolith Removal and Preparation for Microstructural Examination. 1-84 p.

Secor DH, Rooker JR, Zlokovitz E, Zdanowicz VS 2001. Identification of riverine, estuarine, and costal contingents of Hudson River striped bass based upon otolith elemental fingerprints. Marine Ecology Progress Series 211: 245-253.

Shiao JC, Lozys L, Iizuka Y, Tzeng WN 2006. Migratory patterns and contribution of stocking to the population of European eel in Lithuanian waters as indicated by otolith Sr:Ca ratios. Journal of Fish Biology 69: 749-769.

Smith DCW 1959. The biology of the rainbow trout (*Salmo gairdnerii*) in the lakes of the Rotorua district, North Island. New Zealand Journal of Science 2(3): 275-312.

Swearer SE, Forrester GE, Steele MA, Brooks AJ, Lea DW 2003. Spatio-temporal and interspecific variation in otolith trace-elemental fingerprints in a temperate estuarine fish assemblage. Estuarine, Coastal and Shelf Science 56: 1111-1123.

Thorrold SR, Jones CM, Campana SE 1997. Response of otolith microchemistry to environmental variations experienced by larval and juvenile Atlantic croaker (*Micropogonias undulatus*). Limnology and Oceanography 42(1): 102-111.

Tomas J, Geffen AJ 2003. Morphometry and composition of aragonite and vaterite otoliths of deformed laboratory reared juvenile herring from two populations. Journal of Fish Biology 63: 1383-1401.

Ward FJ, Northcote TG, Boubee JAT 2005. The New Zealand common smelt: biology and ecology. Journal of Fish Biology 66: 1-32.

Watson RC 1959 Smelt: an important trout food. Ammohouse bulletin: 10.

Wells BK, Rieman BE, Clayton JL, Horan DL, Jones CM 2003. Relationships between Water, Otolith and Scale Chemistries of Westlope Cutthroat Trout from the Coeur d'Alene River, Idaho: The Potential Application of Hard-Part

Chemistry to Describe Movements in Freshwater. Transactions of the American Fisheries Society 132: 409-424.

Appendix

Appendix Table 1: Isotope concentrations (ppb) in the water samples collected from tributary streams around Lake Rotorua and Lake Rotoiti. Total *N* = 24.

Site	Sample date	^{24}Mg	^{43}Ca	^{55}Mn	^{66}Zn	^{85}Rb	^{88}Sr	^{137}Ba
Lake Rotorua								
Ngongotaha Stream	19-May-07	1158	1493	1.00	69.82	9.18	18.44	29.28
Ngongotaha Stream	20-Jul-07	1381	2686	1.91	14.63	15.96	26.52	60.30
Ngongotaha Stream	16-Oct-07	1194	1672	7.60	6.55	9.69	19.81	34.01
Ngongotaha Stream	17-Nov-07	1164	1476	7.37	3.06	9.76	19.02	29.99
Utuhina Stream	19-May-07	1200	1428	0.77	7.59	8.09	15.01	17.62
Utuhina Stream	20-Jul-07	776	1538	0.75	15.78	7.29	12.72	16.60
Utuhina Stream	16-Oct-07	1214	1608	9.77	4.92	8.70	15.42	19.81
Utuhina Stream	17-Nov-07	1067	1423	8.20	4.30	7.99	14.42	16.88
Waiteti Stream	19-May-07	1442	1852	0.83	64.69	6.51	23.75	45.20
Waiteti Stream	20-Jul-07	1197	2383	0.93	7.35	14.85	16.28	28.12
Waiteti Stream	16-Oct-07	1690	2315	4.77	6.71	8.25	24.66	45.12
Waiteti Stream	17-Nov-07	1498	2032	2.16	7.10	7.39	25.73	46.12
Waingaehe Stream	19-May-07	3073	2701	6.09	14.18	11.55	19.63	35.62
Waingaehe Stream	20-Jul-07	2540	2775	7.84	8.29	11.56	17.80	30.24
Waingaehe Stream	16-Oct-07	3355	3005	21.72	9.48	12.94	21.32	37.03
Waingaehe Stream	17-Nov-07	2985	3285	16.35	3.11	13.17	26.68	34.88
Lake Rotoiti								
Te Toroa Stream	19-May-07	2800	4329	2.18	6.31	6.88	38.46	17.72
Te Toroa Stream	20-Jul-07	1596	2778	3.58	2.96	6.04	20.85	13.03
Te Toroa Stream	16-Oct-07	3299	5062	45.45	5.26	7.75	41.34	20.71
Te Toroa Stream	17-Nov-07	2770	4724	29.15	3.97	7.15	41.31	19.64
Hauparu Stream	19-May-07	1708	3442	0.04	12.51	6.84	18.29	7.37
Hauparu Stream	20-Jul-07	1186	2793	0.49	7.96	7.24	14.31	7.25
Hauparu Stream	16-Oct-07	1825	3746	0.95	2.60	8.40	19.40	7.99
Hauparu Stream	17-Nov-07	1570	3376	0.65	3.69	7.50	19.44	7.49

Appendix Table 2: Isotope concentrations (ppb) in beach water samples from collection locations around Lake Rotorua and Lake Rotoiti. Total *N = 28.*

Site	Date	^{24}Mg	^{43}Ca	^{55}Mn	^{66}Zn	^{85}Rb	^{88}Sr	^{137}Ba
Lake Rotorua								
Mission Bay	19-May-07	1550	1997	0.37	28.83	21.78	22.75	22.00
Mission Bay	20-Jul-07	1499	2780	0.40	4.68	20.75	25.02	24.26
Mission Bay	16-Oct-07	1755	2294	0.55	2.73	14.29	22.31	20.45
Mission Bay	17-Nov-07	1489	2267	2.19	6.67	21.84	25.45	26.12
Pohue Bay	19-May-07	1720	2690	103.98	18.30	25.18	29.40	40.94
Pohue Bay	20-Jul-07	1410	2631	0.62	6.02	20.38	23.45	23.01
Pohue Bay	16-Oct-07	2101	4199	4.94	3.55	20.35	34.34	27.74
Pohue Bay	17-Nov-07	1988	3915	14.38	3.14	22.26	36.05	25.63
Hannah Bay	19-May-07	1597	2130	39.67	44.01	23.88	23.35	26.47
Hannah Bay	20-Jul-07	1546	2773	0.97	5.24	23.60	26.09	25.27
Hannah Bay	16-Oct-07	2655	4102	121.19	14.66	29.74	36.39	60.33
Hannah Bay	17-Nov-07	1576	2367	54.89	2.78	22.85	26.30	29.13
Ngongotaha Beach	19-May-07	1506	2334	0.33	18.54	19.31	22.98	25.45
Ngongotaha Beach	20-Jul-07	1133	2149	0.68	23.01	12.53	19.06	22.80
Ngongotaha Beach	16-Oct-07	1700	2973	37.66	5.62	22.82	27.22	35.53
Ngongotaha Beach	17-Nov-07	1381	2208	15.21	4.96	17.53	26.07	35.42
Hamurana Beach	19-May-07	1532	2000	0.29	40.93	17.03	22.10	22.20
Hamurana Beach	20-Jul-07	1546	2155	0.59	5.77	13.04	19.61	19.64
Hamurana Beach	16-Oct-07	1679	2450	10.97	6.08	20.44	25.51	30.84
Hamurana Beach	17-Nov-07	1552	1943	4.22	7.94	13.06	20.98	22.06
Lake Rotoiti								
Hinehopu Beach	19-May-07	1889	2155	0.38	6.65	19.14	22.37	18.29
Hinehopu Beach	20-Jul-07	1759	2507	0.17	6.97	19.69	22.58	19.17
Hinehopu Beach	16-Oct-07	2621	2520	0.79	4.42	19.06	21.74	17.23
Hinehopu Beach	17-Nov-07	1759	2210	1.86	12.60	21.98	24.58	18.24
Ruato Bay	19-May-07	1919	2535	2.07	11.66	15.89	23.05	20.14
Ruato Bay	20-Jul-07	1697	2750	0.30	12.31	15.05	21.85	20.14
Ruato Bay	16-Oct-07	1995	2533	5.74	5.40	20.88	24.95	20.99
Ruato Bay	17-Nov-07	1754	2266	0.17	2.76	20.50	24.24	17.58

Appendix Table 3: Elemental concentrations (ppm) in juvenile trout otoliths nuclei analysed by LA-ICP-MS. Total *N* = 43.

Otolith	Fork length	Stream	Mn	Zn	Rb	Sr	Ba
Lake Rotoiti							
HPS006-1L	53	Hauparu	8.09	78.02	0.40	729	37.44
HPS013-R	42	Hauparu	11.45	114.09	0.44	577	24.05
HPS002-1	47	Hauparu	4.85	98.34	0.29	577	28.41
HPS014-L	39	Hauparu	3.15	97.97	0.32	560	25.77
HPS004-1	94	Hauparu	3.61	142.85	0.57	525	16.00
HPS001-1	63	Hauparu	2.86	138.49	0.50	458	22.38
HPS007-1	80	Hauparu	3.67	160.42	0.55	471	14.30
tts001-1	95	Te Toroa	5.38	122.12	1.12	715	40.14
tts006-1	55	Te Toroa	10.10	88.89	0.44	537	32.58
tts004-1	149	Te Toroa	7.35	71.90	0.56	548	13.75
tts003-1	63	Te Toroa	9.23	72.15	0.61	454	21.63
tts009-1	45	Te Toroa	6.56	53.44	0.38	510	11.09
tts002-1	81	Te Toroa	2.18	150.83	0.71	562	17.51
Lake Rotorua							
ngs004-R	52	Ngongataha	8.88	0.65	6.05	709	41.26
NGS011-L	unknown	Ngongataha	20.49	29.72	3.61	735	38.68
NGS007-L	51	Ngongataha	44.35	58.89	2.54	620	26.21
NGS015-L	unknown	Ngongataha	20.72	55.90	4.09	653	53.51
NGS014-L	unknown	Ngongataha	17.46	19.09	3.94	615	24.38
NGS013-L	unknown	Ngongataha	16.54	32.62	3.54	616	35.81
NGS009-L	65	Ngongataha	22.09	56.40	2.20	667	49.15
uts015-L	36	Utuhina	59.22	21.46	1.34	560	30.28
uts013-L	38	Utuhina	37.02	32.41	1.81	600	24.63
uts022-R	39	Utuhina	33.78	46.45	2.36	610	19.03
uts021-L	36	Utuhina	28.53	19.55	1.10	571	21.89
uts016-L	37	Utuhina	32.91	37.27	1.47	528	17.87
uts020-L	37	Utuhina	28.51	32.40	1.28	529	15.62
uts018-L	43	Utuhina	12.57	17.41	1.57	594	21.08
uts017-L	29	Utuhina	21.66	46.66	1.21	517	19.74
WNG002-l	37	Waingaehe	42.42	45.99	1.69	779	63.74
WNG012-l	unknown	Waingaehe	13.24	32.30	3.34	658	28.67
WNG013-l	unknown	Waingaehe	16.29	122.03	3.19	692	56.94
WNG004-l	54	Waingaehe	10.08	95.62	1.82	705	75.26
WNG011-l	unknown	Waingaehe	10.36	151.13	2.48	717	61.89
WNG006-l	52	Waingaehe	5.37	71.72	1.83	673	48.34
WNG005-l	46	Waingaehe	4.11	96.58	1.51	696	38.48
Was009-1	37	Waiteti	48.05	21.74	0.18	613	29.45
Was005-2	44	Waiteti	19.82	24.83	0.25	859	46.88
Was004-2	42	Waiteti	35.55	49.69	0.24	754	28.26
Was014-L	unknown	Waiteti	40.86	26.20	0.28	549	20.23
Was002-2	63	Waiteti	24.33	27.54	0.59	685	17.43
Was011-L	35	Waiteti	37.09	19.58	0.28	524	14.95
Was006-1	58	Waiteti	21.85	40.09	0.26	679	21.31
Was012-L	34	Waiteti	19.54	33.29	0.22	681	28.60

Appendix Table 4: Elemental concentrations (ppm) in Lake Rotorua adult trout otolith nuclei, analysed by LA-ICP-MS analysis. Total *N* = 32.

Otolith	Fork length	Capture Location	Mn	Zn	Rb	Sr	Ba
RRUA001-L	440	Rotorua	8.45	73.83	2.68	765	41.22
rrua002-L	385	Rotorua	18.48	67.59	2.94	733	30.90
rrua003-L	495	Rotorua	3.82	78.17	2.96	884	46.26
rrua005-L	460	Rotorua	35.74	50.39	3.77	556	27.25
rrua006-L	380	Rotorua	6.95	84.32	1.91	786	22.41
rrua007-L	440	Rotorua	9.17	60.54	2.60	689	22.35
rrua008-L	445	Rotorua	3.44	92.87	3.77	810	87.81
rrua010-L	390	Rotorua	7.26	71.12	1.27	526	19.70
rrua011-L	525	Rotorua	8.60	83.28	1.64	657	30.34
RRUA012-L	410	Rotorua	14.60	40.66	0.84	596	31.79
rrua013-L	550	Rotorua	6.74	61.90	2.63	718	76.58
rrua014-L	425	Rotorua	23.41	51.46	1.89	571	52.49
rrua015-L	460	Rotorua	13.54	126.64	2.94	744	56.99
rrua016-L	530	Rotorua	3.62	79.10	2.74	440	4.61
rrua017-L	460	Rotorua	10.61	72.29	2.38	604	27.91
rrua018-L	470	Rotorua	5.38	90.47	3.92	825	77.21
rrua020-L	485	Rotorua	10.34	68.47	1.81	690	60.59
rrua021-L	485	Rotorua	27.40	65.28	3.04	605	41.75
rrua022-L	525	Rotorua	9.56	45.88	4.94	671	41.81
rrua023-L	425	Rotorua	5.96	82.67	3.35	692	72.27
rrua025-L	430	Rotorua	1.79	88.59	1.51	766	24.96
RRUA028-L	630	Rotorua	7.71	38.69	1.84	650	26.94
RRUA029-L	450	Rotorua	22.98	94.51	3.93	572	28.01
RRUA030-L	420	Rotorua	27.61	56.07	4.90	604	43.57
RRUA033-L	420	Rotorua	4.27	89.22	4.45	504	8.55
rrua034-L	460	Rotorua	5.64	64.23	2.87	655	25.02
rrua035-L	435	Rotorua	14.81	55.16	2.02	595	28.66
rrua037-L	520	Rotorua	6.86	73.18	1.52	800	84.46
rrua038-L	495	Rotorua	8.01	44.16	3.78	610	26.91
rrua039-L	435	Rotorua	11.02	50.35	4.03	775	24.66
RRUA040-L	515	Rotorua	26.83	47.97	2.75	777	83.60
RRUA041-L	495	Rotorua	8.46	0.43	1.23	925	66.63

Appendix Table 5: Elemental concentrations (ppm) in Lake Rotoiti adult trout otolith nuclei analysed by LA-ICP-MS. Total *N* = 43

Otolith	Fork length	Capture Location	Mn	Zn	Rb	Sr	Ba
riti001-1	470	Rotoiti	9.03	35.07	0.92	748	47.48
riti002-1	575	Rotoiti	38.01	29.32	0.88	635	28.15
riti003-1	380	Rotoiti	17.74	66.03	0.51	708	23.39
riti004-1	440	Rotoiti	12.95	73.93	0.41	653	15.02
riti005-1	450	Rotoiti	8.04	62.01	0.31	738	34.88
riti006-1	485	Rotoiti	5.74	62.17	0.50	804	52.36
riti008-1	435	Rotoiti	28.83	70.87	0.28	691	26.05
riti009-1	575	Rotoiti	13.55	30.67	0.52	517	43.86
riti011-1	470	Rotoiti	8.05	122.62	0.46	548	21.88
riti012-1	590	Rotoiti	36.56	69.60	2.15	748	57.98
riti013-1	565	Rotoiti	6.66	133.91	0.71	461	7.67
riti014-1	500	Rotoiti	105.90	59.56	0.43	652	46.62
riti016-1	410	Rotoiti	25.33	78.13	0.59	655	20.08
riti017-1	515	Rotoiti	118.37	48.72	0.69	532	15.33
riti017-1	515	Rotoiti	24.04	39.89	0.22	547	17.90
riti018-1	550	Rotoiti	20.42	45.29	0.26	949	70.51
riti019-1	370	Rotoiti	7.40	135.27	0.54	594	27.88
RITI020-1	565	Rotoiti	16.94	34.27	0.55	683	27.16
riti021-1	535	Rotoiti	30.56	89.52	1.42	620	31.35
RITI023-1	510	Rotoiti	25.60	42.17	0.71	544	28.09
RITI024-1	560	Rotoiti	7.99	50.87	0.59	668	48.76
RITI025-1	590	Rotoiti	9.07	49.49	0.38	373	5.66
RITI026-1	600	Rotoiti	8.35	84.10	1.07	616	32.62
riti028-1	535	Rotoiti	22.72	33.62	1.02	714	32.17
RITI029-1	435	Rotoiti	20.78	50.37	0.28	646	18.44
RITI030-1	575	Rotoiti	17.81	34.32	0.73	770	44.35
RITI031-1	460	Rotoiti	11.13	82.52	0.57	718	51.75
riti032-1	410	Rotoiti	71.14	79.35	0.52	760	37.59
riti034-1	430	Rotoiti	65.50	75.13	0.40	661	75.80
riti035-1	510	Rotoiti	8.03	82.44	0.57	818	47.11
RITI037-1	575	Rotoiti	39.44	52.36	0.73	649	26.34
riti038-1	435	Rotoiti	11.28	57.39	1.99	667	50.95
riti039-1	610	Rotoiti	73.68	75.48	0.46	676	32.89
riti040-1	595	Rotoiti	10.89	99.27	1.38	659	28.65
RITI045-L	420	Rotoiti	2.99	104.55	4.02	349	11.26
RITI046-L	395	Rotoiti	10.70	91.32	1.48	623	46.90
RITI047-L	410	Rotoiti	14.10	120.44	1.26	569	17.84
RITI049-L	425	Rotoiti	10.23	111.29	1.61	543	31.02
RITI051-L	400	Rotoiti	68.26	106.02	2.42	859	42.51
RITI052-L	550	Rotoiti	31.97	63.28	1.50	884	54.98
RITI053-L	unknown	Rotoiti	40.75	74.69	3.07	508	21.31
RITI056-L	unknown	Rotoiti	12.26	62.98	1.56	990	28.38
RITI058-L	unknown	Rotoiti	5.16	120.93	1.41	1057	6.70

Appendix Table 6: Elemental concentration (ppm) in Ohau Channel adult trout otolith nuclei collected by LA-ICP-MS. Total *N* = 17

Otolith	Fork length	Capture Location	Mn	Zn	Rb	Sr	Ba
ohc001-2	unknown	Ohau Channel	4.47	140.61	2.72	882	8.83
ohc002-1	unknown	Ohau Channel	12.68	88.52	0.84	809	30.89
ohc003-2	unknown	Ohau Channel	25.38	54.89	1.62	886	81.65
ohc004-1	unknown	Ohau Channel	6.37	125.38	2.17	822	69.38
OHC005-1	unknown	Ohau Channel	30.60	67.31	0.79	744	48.76
OHC006-1	unknown	Ohau Channel	9.82	74.46	1.93	744	35.01
ohc007-1	unknown	Ohau Channel	5.62	122.06	1.54	650	76.80
OHC008-1	unknown	Ohau Channel	8.91	428.96	0.81	663	59.15
ohc010-1	unknown	Ohau Channel	8.46	90.08	1.54	718	65.11
OHC012-1	unknown	Ohau Channel	31.60	59.60	2.17	631	56.58
ohc013-1	unknown	Ohau Channel	15.90	50.09	2.26	758	42.77
OHC051-2	unknown	Ohau Channel	12.94	44.38	2.59	657	34.12
OHC054-1	unknown	Ohau Channel	18.72	49.36	1.94	843	71.29
OHCJ001-R	150	Ohau channel	32.79	29.07	4.14	663	44.06
OHCJ002-L	126	Ohau channel	18.53	55.32	0.92	640	63.58
OHCJ003-L	74	Ohau channel	35.73	11.49	0.78	557	16.93
OHCJ005-L	89	Ohau channel	27.37	24.25	1.40	485	22.09

Appendix Table 7: Elemental concentration (ppm) in Lake Rotoiti and Lake Rotorua common smelt otolith nuclei collected by LA-ICP-MS. Total *N* = 138

Otolith	Fork length	Beach	Mn	Zn	Rb	Sr	Ba
Lake Rotoiti							
chb002-2	47	Cherry Bay	1.87	19.80	0.52	1087	59.93
chb003-2	46	Cherry Bay	2.93	4.74	0.85	1152	31.40
chb004-2	43	Cherry Bay	9.21	3.13	0.72	1216	65.67
chb006-2	43	Cherry Bay	3.18	11.34	0.55	1105	28.12
chb008-2	38	Cherry Bay	2.08	1.81	0.50	1088	25.59
chb009-2	40	Cherry Bay	3.87	218.88	0.78	1147	55.07
chb013-1	33	Cherry Bay	2.81	0.76	0.32	1148	52.13
chb014-1	40	Cherry Bay	6.60	2.46	0.63	1169	62.96
chb015-1	42	Cherry Bay	5.83	3.08	0.49	1162	35.68
hib001-2	52	Hinehopu Beach	9.15	5.45	0.98	1096	44.89
hib002-2	51	Hinehopu Beach	0.82	2.02	0.72	1026	28.12
hib005-1	50	Hinehopu Beach	1.71	5.42	0.93	1093	28.29
hib006-2	48	Hinehopu Beach	1.01	1.75	0.70	1049	30.05
hib007-1	53	Hinehopu Beach	1.59	4.94	0.36	1159	29.64
hib009-1	53	Hinehopu Beach	2.73	6.35	0.72	1209	51.93
hib010-1	47	Hinehopu Beach	3.45	2.25	0.37	1275	44.64
hib011-1	51	Hinehopu Beach	3.24	3.27	0.58	1071	39.52
hib012-1	51	Hinehopu Beach	1.30	5.69	0.88	1150	25.89
hib013-1	51	Hinehopu Beach	1.17	1.97	0.37	1209	33.23
hib014-1	55	Hinehopu Beach	1.86	3.45	0.51	1122	32.76
hib015-1	52	Hinehopu Beach	3.32	3.86	0.56	1068	48.53
hib016-1	44	Hinehopu Beach	2.74	2.82	0.64	1214	41.19
hib018-1	45	Hinehopu Beach	2.07	3.63	0.52	1182	37.93
hib019-1	53	Hinehopu Beach	8.73	3.49	0.54	1123	36.08
hib020-1	47	Hinehopu Beach	4.32	51.85	0.33	1193	27.28
hib021-L	55	Hinehopu Beach	3.68	6.11	0.53	1176	50.16
hib022-L	53	Hinehopu Beach	2.72	5.79	0.70	1124	24.38
htp001-2	41	Hot Pools	7.12	0.60	0.85	1186	38.33
Htp002-L	46	Hot Pools	9.48	6.93	0.61	1030	37.29
htp003-2	50	Hot Pools	4.83	7.64	0.73	994	25.22
htp005-2	48	Hot Pools	3.62	5.57	1.03	1145	38.89
Htp007-L	44	Hot Pools	4.54	3.14	1.35	1173	43.54
htp009-2	45	Hot Pools	2.13	8.37	1.15	1114	23.46
htp012-1	40	Hot Pools	1.25	4.19	1.09	1018	36.64
htp013-1	44	Hot Pools	2.43	16.26	0.59	1272	35.93
htp014-1	44	Hot Pools	1.61	8.02	0.78	1162	45.15
htp016-1	41	Hot Pools	8.86	6.47	0.45	1098	38.78
htp017-1	40	Hot Pools	2.37	6.69	0.56	1122	34.54
htp018-1	39	Hot Pools	2.36	5.54	0.86	1214	37.82
htp019-1	41	Hot Pools	1.86	10.62	0.40	1180	29.64
htp020-1	41	Hot Pools	1.94	1.65	0.69	1095	48.00
Htp021-L	44	Hot Pools	9.41	9.20	0.95	1207	43.43
Htp023-L	39	Hot Pools	2.83	9.90	0.50	1128	55.31
Htp024-L	46	Hot Pools	1.93	8.20	0.47	1078	27.71
psl003-2	42	Pikiao Ski Lane	4.87	0.51	0.63	1176	61.87
psl005-2	39	Pikiao Ski Lane	5.21	18.10	0.72	1190	38.68
psl006-2	38	Pikiao Ski Lane	1.48	4.61	0.47	1130	25.49
psl007-1	45	Pikiao Ski Lane	2.66	16.30	0.85	1092	28.16

Otolith	Fork length	Beach	Mn	Zn	Rb	Sr	Ba
psl007-2	45	Pikiao Ski Lane	4.47	2.99	0.82	1091	41.29
psl008-2	48	Pikiao Ski Lane	6.69	4.68	0.61	1151	39.80
psl011-1	40	Pikiao Ski Lane	2.23	50.08	0.40	1064	21.32
psl013-1	38	Pikiao Ski Lane	2.03	68.03	0.81	1099	40.80
psl014-1	41	Pikiao Ski Lane	5.69	21.35	0.38	1137	43.16
psl016-1	38	Pikiao Ski Lane	5.38	4.11	0.42	1188	45.57
psl017-1	43	Pikiao Ski Lane	2.18	12.41	0.48	1018	31.95
psl018-1	38	Pikiao Ski Lane	9.61	6.37	0.91	1087	42.66
psl019-1	40	Pikiao Ski Lane	4.20	2.55	0.47	1135	38.61
psl020-1	43	Pikiao Ski Lane	7.73	14.75	0.76	1178	50.55
psl020-2	43	Pikiao Ski Lane	8.42	4.69	0.67	1154	39.56
psl022-r	37	Pikiao Ski Lane	5.87	2.70	0.49	1140	42.19
rub007-1	49	Ruato Bay	1.84	3.10	0.72	1146	35.86
rub009-1	45	Ruato Bay	3.96	2.14	0.47	1067	47.59
rub010-1	41	Ruato Bay	4.32	2.49	0.41	1190	53.62
rub012-1	40	Ruato Bay	4.06	7.15	0.42	1108	45.01
rub013-1	37	Ruato Bay	7.84	4.80	0.35	1249	50.30
rub014-1	42	Ruato Bay	3.19	3.64	0.40	1112	43.58
rub017-1	41	Ruato Bay	8.39	4.76	0.47	1104	34.50
RUB018-1	42	Ruato Bay	4.59	1.91	0.54	1168	48.10
rub019-1	43	Ruato Bay	6.45	3.49	0.53	1164	41.62
rub020-1	43	Ruato Bay	0.92	2.87	0.40	1075	47.27
RUB022-L	41	Ruato Bay	9.44	13.56	0.28	1171	37.12
RUB023-L	39	Ruato Bay	1.93	18.59	0.39	1142	59.29
Lake Rotorua							
hamb0.0-l	51	Hamurana Stream	0.64	0.67	2.17	1212	54.87
hamb001-R	74	Hamurana Stream	2.15	0.08	1.63	1017	35.38
hamb002-l	61	Hamurana Stream	7.34	7.84	3.50	986	49.68
Hamb003-l	74	Hamurana Stream	2.05	0.44	1.66	1169	26.78
HAMB004-L	70	Hamurana Stream	6.41	2.18	1.07	1260	35.30
Hamb005-l	70	Hamurana Stream	2.75	0.21	1.46	1115	27.73
hamb006-l	68	Hamurana Stream	1.79	10.68	1.08	1202	40.82
HAMB007-L	62	Hamurana Stream	2.77	5.19	2.48	1297	49.13
HAMB011-L	68	Hamurana Stream	3.57	10.75	2.15	1222	39.97
HAMB012-L	75	Hamurana Stream	4.96	3.03	2.19	1177	45.84
hamb013-l	71	Hamurana Stream	2.84	3.58	1.59	1161	34.78
Hamb015-L	69	Hamurana Stream	3.98	4.67	0.65	1322	41.12
Hamb016-l	75	Hamurana Stream	2.70	3.24	1.79	1133	30.43
Hamb017-l	60	Hamurana Stream	2.74	6.01	0.59	1046	39.22
hamb018-l	65	Hamurana Stream	1.22	8.85	0.61	1236	42.32
hamb020-l	70	Hamurana Stream	3.09	12.31	1.81	1192	43.21
hab025-1	42	Hannah's Bay	5.05	7.14	0.69	1265	72.16
hab026-1	45	Hannah's Bay	9.76	3.43	0.35	1163	44.54
hab029-1	43	Hannah's Bay	2.54	4.45	0.41	1263	46.79
hab030-1	46	Hannah's Bay	3.61	41.57	0.35	1222	53.74
hab033-1	59	Hannah's Bay	4.64	1.78	0.65	1235	38.75
hab034-1	44	Hannah's Bay	0.94	10.34	0.41	1130	50.36
hab035-1	39	Hannah's Bay	4.10	11.14	1.85	1172	40.57
hab0024-1	40	Hannah's Bay	4.93	13.22	0.27	1210	47.35
Hab005-2	58	Hannah's Bay	4.70	13.47	0.41	1156	39.32

Otolith	Fork length	Beach	Mn	Zn	Rb	Sr	Ba
Hab012-1	63	Hannah's Bay	3.00	2.21	0.40	1292	37.31
hab014-1	63	Hannah's Bay	3.46	4.62	0.39	1197	32.46
hab015-1	42	Hannah's Bay	3.20	27.60	0.35	1127	40.78
Hab017-L	45	Hannah's Bay	5.65	7.01	0.35	1159	51.86
Hab018-L	61	Hannah's Bay	6.94	5.56	0.24	1095	59.87
Hab019-L	44	Hannah's Bay	3.44	2.79	0.32	1109	42.95
hab023-1	49	Hannah's Bay	8.99	10.64	0.57	1220	47.00
hab028-1	67	Hannah's Bay	3.69	7.06	0.46	1143	33.76
mib003-2	64	Mission Bay	4.49	5.18	1.16	1161	31.01
mib004-2	63	Mission Bay	1.34	10.04	0.51	1147	19.72
Mib005-1	62	Mission Bay	3.39	9.80	0.70	1239	33.20
mib006-1	68	Mission Bay	1.30	1.93	0.64	1092	23.33
mib008-2	61	Mission Bay	3.95	10.64	1.07	1241	35.74
mib009-1	59	Mission Bay	3.98	8.51	0.90	1406	52.04
mib010-1	58	Mission Bay	4.00	4.88	0.58	1200	46.49
Mib011-1	59	Mission Bay	3.82	4.98	0.46	1281	35.40
mib012-1	65	Mission Bay	2.21	3.14	0.44	1380	38.01
mib013-1	65	Mission Bay	3.36	31.38	0.57	1324	46.12
mib014-1	62	Mission Bay	3.25	3.07	0.73	1198	26.15
mib015-1	64	Mission Bay	2.82	7.91	0.45	1240	29.72
mib016-1	61	Mission Bay	2.58	8.77	0.56	1213	29.52
mib017-2	59	Mission Bay	1.30	3.96	0.67	1201	49.48
mib018-1	59	Mission Bay	0.99	11.10	0.34	1372	45.43
mib020-1	63	Mission Bay	3.30	3.20	0.55	1241	42.30
mib021-L	67	Mission Bay	1.95	30.38	0.88	1258	39.12
Pob001-1	53	Pohue Bay	2.47	9.83	0.40	1233	36.02
Pob002-1	43	Pohue Bay	0.85	4.95	0.37	1029	36.61
Pob004-1	58	Pohue Bay	2.48	8.00	0.37	1049	28.82
pob005-1	59	Pohue Bay	2.60	4.49	0.43	1064	26.05
pob007-1	56	Pohue Bay	2.42	2.05	0.70	1141	27.48
Pob007-1	56	Pohue Bay	4.94	4.10	0.94	1097	57.40
pob008-1	40	Pohue Bay	7.29	1.26	0.41	1083	48.96
Pob009-1	44	Pohue Bay	1.52	3.15	0.36	976	29.59
Pob010-1	43	Pohue Bay	2.17	6.14	0.53	1126	39.59
Pob012-1	45	Pohue Bay	7.74	3.51	0.39	1263	62.35
Pob013-1	53	Pohue Bay	2.22	4.22	0.51	1124	35.98
Pob014-2	41	Pohue Bay	5.31	17.87	0.29	1080	47.74
Pob016-1	43	Pohue Bay	3.18	13.46	0.49	1095	33.90
pob018-1	42	Pohue Bay	3.70	6.04	0.39	1097	31.53
Pob020-1	44	Pohue Bay	2.27	6.75	0.43	1201	50.84
Pob021-1	46	Pohue Bay	2.89	6.68	0.41	1173	35.91

Appendix Table 8: Elemental concentration (ppm) in Lake Rotoiti and Lake Rotorua common smelt edge otolith spots collected by LA-ICP-MS. Total *N* = 134.

Otolith	Fork length	Beach	Mn	Zn	Rb	Sr	Ba
Lake Rotoiti							
chb002-2	47	Cherry Bay	0.14	4.61	0.46	904	28.18
chb004-2	43	Cherry Bay	0.71	16.81	0.54	915	22.42
chb006-2	43	Cherry Bay	0.63	8.41	0.69	886	21.03
chb007-2	39	Cherry Bay	0.82	5.16	0.31	1075	40.49
chb008-2	38	Cherry Bay	0.69	14.06	0.53	985	28.02
chb009-2	40	Cherry Bay	0.39	3.41	0.97	1042	32.25
chb012-1	47	Cherry Bay	0.41	9.69	0.32	995	25.71
chb014-1	40	Cherry Bay	0.87	63.79	0.36	1019	36.43
chb015-1	42	Cherry Bay	0.11	10.78	0.35	985	19.12
hib001-2	52	Hinehopu Beach	0.32	1.46	0.61	850	22.28
hib002-2	51	Hinehopu Beach	0.53	4.29	0.56	940	22.07
hib006-2	48	Hinehopu Beach	0.39	12.41	0.60	933	24.12
hib007-1	53	Hinehopu Beach	0.31	8.67	0.51	832	18.03
hib008-1	48	Hinehopu Beach	1.05	17.73	0.48	1119	36.09
hib009-1	53	Hinehopu Beach	0.13	3.47	0.66	878	19.30
hib011-1	51	Hinehopu Beach	0.50	9.09	0.44	1217	32.03
hib012-1	51	Hinehopu Beach	0.51	6.52	0.51	939	23.04
hib014-1	55	Hinehopu Beach	0.38	10.40	0.53	1227	36.21
hib015-1	52	Hinehopu Beach	0.31	10.94	0.43	882	21.28
hib016-1	44	Hinehopu Beach	0.88	13.16	0.46	1237	33.66
hib017-1	45	Hinehopu Beach	0.74	4.39	0.30	1158	37.21
hib018-1	45	Hinehopu Beach	1.53	13.98	0.52	1189	36.04
hib019-1	53	Hinehopu Beach	0.48	7.85	0.45	985	26.30
htp001-2	41	Hot Pools	0.83	3.71	0.60	1111	30.14
Htp002-L	46	Hot Pools	1.86	17.83	0.56	1069	36.02
htp003-2	50	Hot Pools	0.67	9.18	0.40	1129	22.15
htp005-2	48	Hot Pools	0.16	15.34	0.97	986	17.47
Htp007-L	44	Hot Pools	0.69	1.37	1.12	1076	42.37
htp008-2	43	Hot Pools	0.27	4.88	0.64	1130	30.02
htp012-1	40	Hot Pools	0.49	4.14	0.88	960	27.05
htp013-1	44	Hot Pools	0.39	2.19	0.56	1344	47.95
htp014-1	44	Hot Pools	1.29	2.40	0.71	1132	34.39
htp015-1	39	Hot Pools	0.94	15.88	0.43	960	24.68
htp016-1	41	Hot Pools	0.46	4.17	0.46	1069	29.51
htp017-1	40	Hot Pools	1.90	14.15	0.40	1039	44.10
htp018-1	39	Hot Pools	0.33	13.41	0.58	1058	33.93
htp019-1	41	Hot Pools	1.16	17.92	0.38	1090	30.82
htp020-1	41	Hot Pools	1.32	5.11	0.33	1031	31.52
Htp021-L	44	Hot Pools	0.67	10.25	0.42	1237	40.53
Htp023-L	39	Hot Pools	1.94	18.38	0.41	1235	46.97
psl002-2	42	Pikiao Ski Lane	0.82	34.93	0.29	1097	35.33
psl003-2	42	Pikiao Ski Lane	0.49	20.05	0.32	924	35.48
psl005-2	39	Pikiao Ski Lane	0.45	36.53	0.45	1057	28.88
psl006-2	38	Pikiao Ski Lane	0.37	11.28	0.36	1102	34.45
psl007-1	45	Pikiao Ski Lane	0.27	2.31	0.45	896	20.96
psl007-2	45	Pikiao Ski Lane	1.75	5.57	1.56	934	23.20
psl008-2	48	Pikiao Ski Lane	0.50	10.61	0.60	895	16.24
psl011-1	40	Pikiao Ski Lane	0.42	7.77	0.19	972	21.73

Otolith	Fork length	Beach	Mn	Zn	Rb	Sr	Ba
psl012-1	38	Pikiao Ski Lane	0.72	1.28	0.25	1232	32.45
psl014-1	41	Pikiao Ski Lane	0.17	26.48	0.49	1200	27.02
psl016-1	38	Pikiao Ski Lane	2.08	17.48	0.31	1203	36.37
psl017-1	43	Pikiao Ski Lane	0.68	4.00	0.40	910	21.34
psl018-1	38	Pikiao Ski Lane	0.14	3.31	0.50	941	32.46
psl019-1	40	Pikiao Ski Lane	0.57	39.57	0.34	1072	39.90
psl020-1	43	Pikiao Ski Lane	1.17	80.70	0.44	1048	30.07
psl020-2	43	Pikiao Ski Lane	0.09	2.18	0.48	941	20.09
psl022-r	37	Pikiao Ski Lane	11.50	22.85	0.43	1267	37.40
rub007-1	49	Ruato Bay	1.18	17.61	0.44	1190	45.53
rub009-1	45	Ruato Bay	1.42	6.05	0.60	1129	33.60
rub010-1	41	Ruato Bay	1.09	6.25	0.59	1261	35.31
RUB011-1	38	Ruato Bay	0.50	9.25	0.62	1329	37.87
rub012-1	40	Ruato Bay	1.03	5.57	0.44	1090	34.48
rub014-1	42	Ruato Bay	0.87	7.52	0.44	1007	25.74
rub015-1	43	Ruato Bay	0.99	4.12	0.70	1074	19.60
RUB016-1	39	Ruato Bay	2.15	16.52	0.38	1001	29.33
rub017-1	41	Ruato Bay	1.60	4.72	0.68	1025	20.57
RUB018-1	42	Ruato Bay	0.98	7.67	0.59	1235	37.16
rub019-1	43	Ruato Bay	1.64	14.28	0.46	1149	39.14
Lake Rotorua							
hamb0.0-l	51	Hamurana Stream	0.49	5.25	1.93	1147	32.06
HAMB001-R	74	Hamurana Stream	0.41	0.71	1.61	1114	23.97
hamb002-l	61	Hamurana Stream	0.40	3.94	1.75	1113	28.13
Hamb003-L	74	Hamurana Stream	0.27	5.87	1.37	1139	26.86
HAMB004-L	70	Hamurana Stream	0.40	7.88	1.11	916	17.46
Hamb005-l	70	Hamurana Stream	0.65	2.90	1.77	1020	25.14
hamb006-l	68	Hamurana Stream	0.02	0.98	0.81	981	19.62
HAMB007-L	62	Hamurana Stream	0.30	2.91	1.34	1234	50.64
HAMB009-L	74	Hamurana Stream	0.13	3.36	1.17	1073	20.59
HAMB011-L	68	Hamurana Stream	0.53	0.66	1.54	1102	18.09
HAMB012-L	75	Hamurana Stream	0.51	4.23	0.90	1077	10.88
hamb013-l	71	Hamurana Stream	0.36	0.03	1.23	1133	27.27
hamb014-l	58	Hamurana Stream	0.28	1.28	1.60	1176	29.46
Hamb015-l	69	Hamurana Stream	0.23	2.19	1.10	1107	25.21
Hamb017-l	60	Hamurana Stream	0.21	2.42	0.71	1230	32.68
hamb018-l	65	Hamurana Stream	0.13	15.58	0.83	1010	13.50
hamb019-l	66	Hamurana Stream	0.38	0.16	0.85	1090	26.07
hamb020-l	70	Hamurana Stream	0.67	4.38	1.11	1181	30.21
hab0024-1	40	Hannah's Bay	1.66	5.31	0.36	1157	30.29
Hab005-2	58	Hannah's Bay	0.15	0.53	0.41	1077	11.96
Hab012-1	63	Hannah's Bay	0.18	0.57	0.44	939	15.46
hab014-1	63	Hannah's Bay	0.18	2.45	0.35	1016	9.76
hab015-1	42	Hannah's Bay	1.57	15.01	0.37	1110	32.38
Hab017-L	45	Hannah's Bay	2.72	27.70	0.39	1041	26.18
Hab018-L	61	Hannah's Bay	2.31	18.41	0.38	1134	29.87
Hab019-L	44	Hannah's Bay	2.51	13.01	0.35	1137	39.45
hab023-1	49	Hannah's Bay	1.16	6.11	0.31	1091	38.69
hab025-1	42	Hannah's Bay	0.92	5.32	0.81	1119	37.84
hab026-1	45	Hannah's Bay	1.21	15.90	0.48	1147	52.68

Otolith	Fork length	Beach	Mn	Zn	Rb	Sr	Ba
hab027-1	46	Hannah's Bay	0.86	5.34	0.46	1137	34.68
hab028-1	67	Hannah's Bay	0.48	6.86	0.30	1051	17.22
hab029-1	43	Hannah's Bay	1.02	4.28	0.39	1169	47.30
hab030-1	46	Hannah's Bay	2.02	11.23	0.44	1236	55.05
hab031-1	69	Hannah's Bay	0.38	6.86	0.55	891	11.33
hab033-1	59	Hannah's Bay	0.60	3.70	0.47	934	18.40
mib003-2	64	Mission Bay	0.43	2.52	0.77	1069	18.95
mib004-2	63	Mission Bay	0.82	8.80	0.52	993	14.00
Mib005-1	62	Mission Bay	0.19	4.00	0.65	1044	27.06
mib006-1	68	Mission Bay	0.57	6.76	0.76	1038	21.64
Mib007-1	58	Mission Bay	0.38	1.22	0.85	1054	22.08
mib008-2	61	Mission Bay	0.18	7.05	0.65	1087	27.28
mib009-1	59	Mission Bay	0.17	2.76	0.83	939	14.15
mib010-1	58	Mission Bay	0.03	4.38	0.45	969	19.58
Mib011-1	59	Mission Bay	0.21	1.85	0.64	1059	18.51
mib014-1	62	Mission Bay	0.34	1.34	0.59	957	13.40
mib015-1	64	Mission Bay	0.19	4.20	0.79	927	18.36
mib017-2	59	Mission Bay	0.29	3.74	0.75	968	15.82
mib018-1	59	Mission Bay	0.06	2.50	0.62	1023	15.98
Mib019-1	63	Mission Bay	0.50	15.20	0.53	1053	13.52
mib020-1	63	Mission Bay	0.68	11.95	0.54	1045	22.25
mib021-L	67	Mission Bay	0.37	5.36	0.74	1136	22.05
Pob001-1	53	Pohue Bay	0.08	3.84	0.60	1092	20.72
Pob002-1	43	Pohue Bay	1.81	4.36	0.36	1080	28.75
Pob003-2	61	Pohue Bay	0.06	2.08	0.59	1109	18.31
Pob004-1	58	Pohue Bay	0.02	1.18	0.45	1112	17.27
pob005-1	59	Pohue Bay	0.22	1.50	0.30	1070	21.69
Pob006-1	63	Pohue Bay	0.17	10.12	0.38	1048	19.01
Pob007-1	56	Pohue Bay	0.68	4.04	0.60	1115	21.81
Pob010-1	43	Pohue Bay	2.74	27.08	0.34	1011	31.19
Pob012-1	45	Pohue Bay	0.68	6.36	0.39	1188	34.51
Pob013-1	53	Pohue Bay	0.29	10.08	0.35	898	20.92
Pob014-2	41	Pohue Bay	1.62	3.94	0.31	1097	25.10
Pob016-1	43	Pohue Bay	0.73	6.57	0.42	1044	27.93
pob018-1	42	Pohue Bay	1.75	10.82	0.41	1127	42.71
Pob021-1	46	Pohue Bay	1.64	18.25	0.36	1085	28.97
Pob022-1	43	Pohue Bay	0.90	37.58	0.46	981	24.39